This document was too large to scan as a single document. It has been divided into smaller sections.

Section 2 of 4

Document Information			
Document #	**RPP-10098**	**Revision**	**1**
Title	FIELD INVESTIGATION REPORT FOR WASTE MGMT AREA B-BX-BY [VOL 1 MAIN TEST & APPENEDICES A-C]		
Date	**1/6/2003**		
Originator	**KNEPP AJ**	**Originator Co.**	**CH2M**
Recipient		**Recipient Co.**	
References	**EDT-630527**		
Keywords			
Projects	**TFARM**		
Other Information			

APPENDIX C

NON-WORK PLAN ACTIVITIES AND RESULTS

This page intentionally left blank.

CONTENTS

FIGURES

TABLES

LIST OF TERMS

AT	advanced tensiometer
bgs	below ground surface
CAW	current acid wastes
CERCLA	*Comprehensive Environmental Restoration, Compensation, and Liability Act*
CH2M HILL	CH2M HILL Hanford Group, Inc.
HEDTA	hydroxethyl-ethylenediamine-triacetic acid
Kd	distribution coefficient
ITS	in-tank solidification
MTU	metric ton of uranium
PAW	PUREX current acid wastes from aluminum-clad fuel
PSN	PUREX supernatant
PSS	PUREX sludge supernatant
PUREX	plutonium-uranium extraction
RCRA	*Resource Conservation and Recovery Act*
REDOX	reduction-oxidation
RSN	REDOX supernatant
SST	single-shell tank
WIDS	Waste Information Data System
WMA	waste management area
ZAW	PUREX current acid wastes from zirconium-clad fuel

C.1.0 INTRODUCTION

The work plan addendum associated with waste management area (WMA) B-BX-BY was developed for the primary purpose of directing field work (Rogers and Knepp 2000). During the course of conducting the identified field work, other activities were identified that would either complement or supplement that field work.

Some 'projects of opportunity' that fit within the general scope of the Tank Farm Vadose Zone Project were undertaken. Included in this category were sampling and geological interpretation associated with *Resource Conservation and Recovery Act of 1976* (RCRA) groundwater monitoring wells that were drilled to enhance or maintain the WMA B-BX-BY groundwater monitoring program, and supplemental analysis of samples from nearby holes drilled by the 200 Area Remediation Project (Appendix B, Sections B.2.0 and B.5.0). Efforts to fully document the history of B, BX, and BY tank farm activities continued even though the majority of the information had been garnered for the subsurface conditions description report (Wood et al. 2000).

As noted in Jones et al. (1998), determination of the contaminant inventory that was lost to the vadose zone is the most pressing need. This inventory was estimated using historical data and then revised based on the data gathered during the drilling of the characterization boreholes called out in the work plan addendum.

An effort to characterize the distribution of moisture in the eastern portion of the BX tank farm was undertaken in an attempt to determine if pressurized water lines in that portion of the farm were a possible source of recharge. Those measurements added to the drive to eliminate unnecessary pressurized water lines leading to the tank farms. These measurements also added to the database used by the Science and Technology Program modeling effort reported in Appendix D.

Geochemical characterization of sediments collected from cores during construction of the RCRA groundwater monitoring wells provides a basis against which to judge the impact of tank wastes lost to the environment.

Finally, groundwater data and interpretation provide additional insight into the overall conceptual model of contaminant flow and transport through the vadose zone and into the unconfined aquifer.

C.2.0 CONSTRUCTION

Construction of the tank farms is an integral element in the conceptual model of waste distribution in the adjacent and underlying vadose zone. Because the primary focus of the subsurface investigation is the 241-BX tank farm, this discussion focuses on that tank farm. Construction practices and specifications applied at B and BY tank farms are not significantly different than those applied at BX farm, thereby allowing this review to be applied, by analogy, to those facilities. This discussion is based on analysis of construction photographs and construction specifications.

The BX tank farm was constructed from 1946 to 1948 under the direction of the General Electric Company. Planning for the farm was initiated in October 1946 and field construction started in February 1947. The goal was to have the farm on line and ready to receive waste by December 1, 1947. Tank space available elsewhere on site was expected to be exhausted by January 1, 1948. The original plans were amended in July 1947 and a revised completion date of May 1, 1948 was established. The first tank to be started was BX-110 and the last to be completed was BX-103.

BX tank farm was built so that gravity flow could be used to cascade waste fluids from the southernmost tier of tanks toward the northern tiers. In addition, the capability to further cascade those fluids from the BX farm to the BY farm was constructed although the BY farm was not yet approved. The tanks and their intakes are lower by approximately 0.3 m (1 ft) from the preceding row. Photographs of the farm during its construction show no evidence that this lowering of the construction surface was stepwise.

Figure C.1. Grading the BX Tank Farm Base

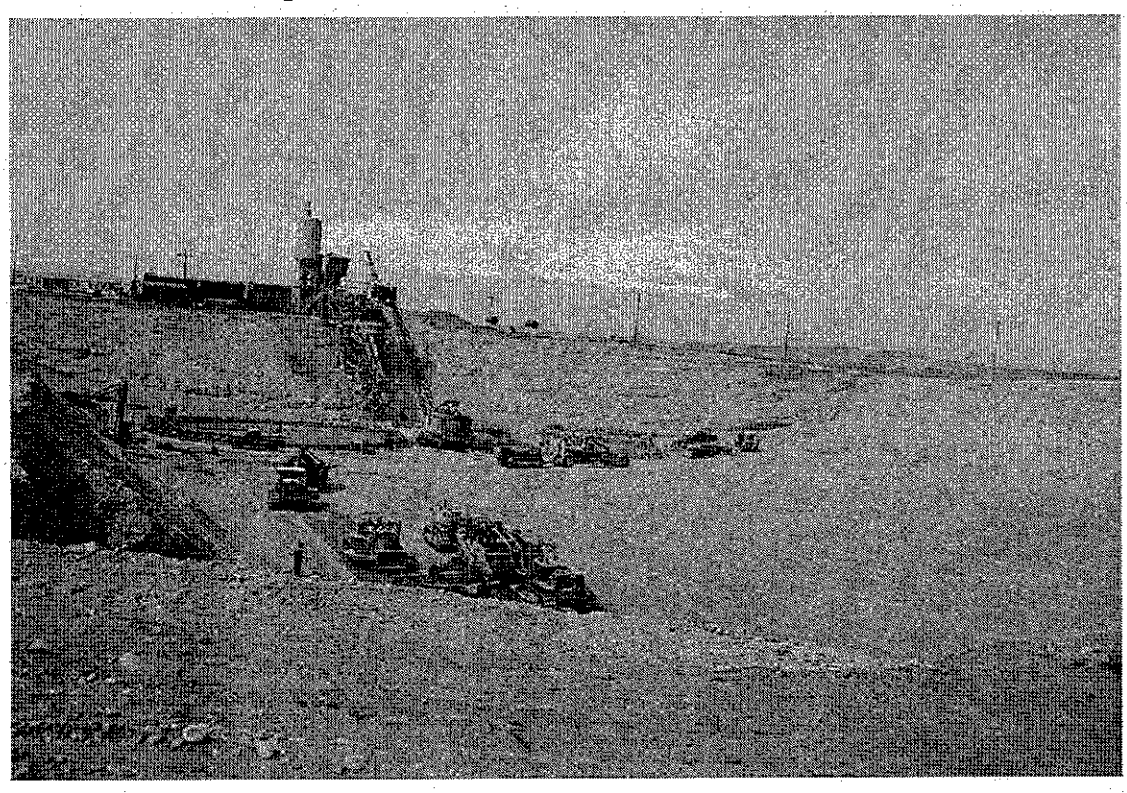

This leads to the hypothesis that the excavation was sloped from south to north with only the tank bases level. Entrances to and exits from the excavation were from the northeast and northwest corners of the farm (adjacent to what are now tanks BX-103 and BX-112). Contrary to earlier tank farms, it appears that all of the excavation, including final grading, was performed mechanically. The sides of the excavation were steeply sloped at an angle that appears to be consistent with the design of 1.5:1.

Construction traffic was routed between the tanks, resulting in a hard-packed surface.

Figure C.2. Hard Packed Surface Caused By Construction Traffic

A project-specific concrete batch plant was located along the western edge of the farm between tanks BX-110 and BX-111. From this plant, trip-buckets were transported by flatbed truck to the individual tank construction sites, where cranes were used to position the trip-buckets to deposit the concrete mixture within the forms. This batch plant was used throughout the construction effort. Construction of the tank bases included forming of the initial compound curvature leading from the tank base to vertical wall to a height of what appears to be about one foot. Once the individual concrete tank bases had been finished and cured, they were coated with the specified asphaltic mix and steel work initiated.

Figure C.3. Asphalt Placement on Concrete Base

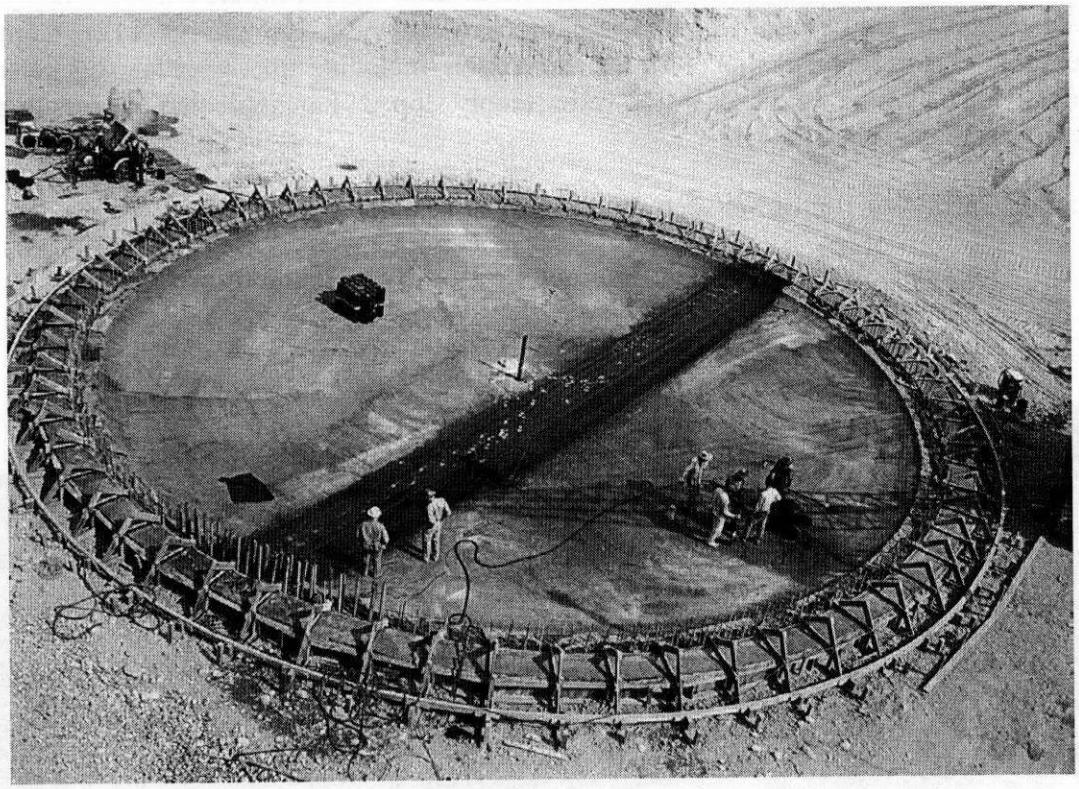

Figure C.4. Pouring the Concrete Base for Tank BX-110

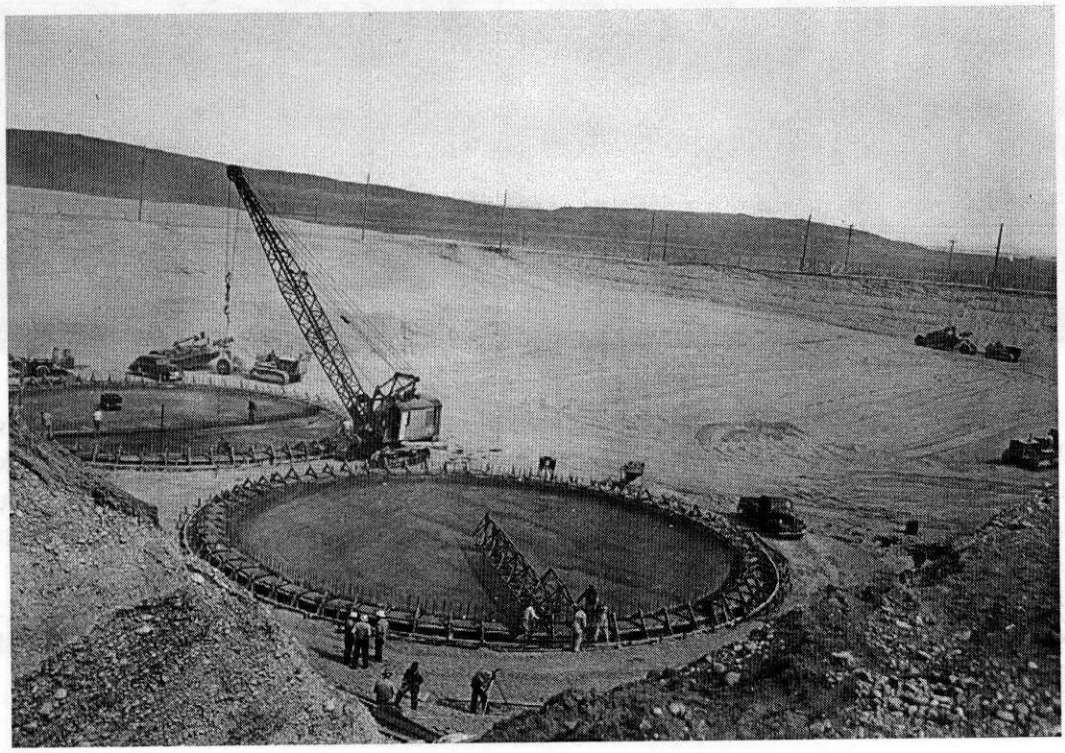

Precut and formed and numbered steel sections were delivered to the construction site and positioned on the concrete bases with the construction cranes. Once in place, these sections were welded together. The curved sections (knuckles) leading from the base to the vertical walls were then brought in, placed on supports, aligned, and welded into position. These curved pieces were a nominal 4.5 ft wide. To these pieces, side panels were fitted and welded. Curvature for these pieces was obtained by working the piece from one end to the other; flexibility of the steel was sufficient to allow the ends to be drawn in. Photos show retainer pieces along both horizontal and vertical edges of these sections. The vertical pieces are three rows high. Welding was apparently done from both the inside and outside of these pieces.

Figure C.5. Placing the Asphalt Seal

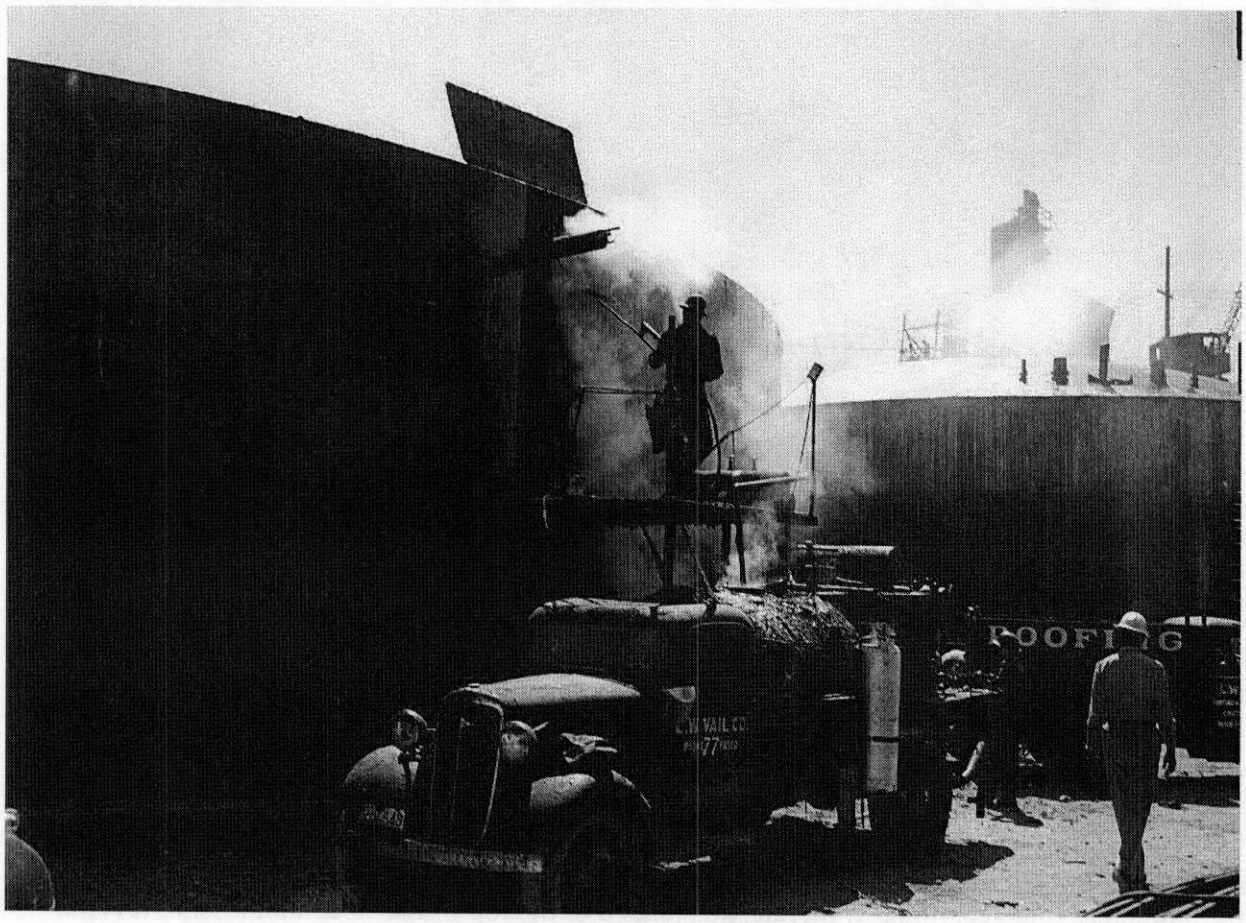

Figure C.6. Fitting the Steel Shell

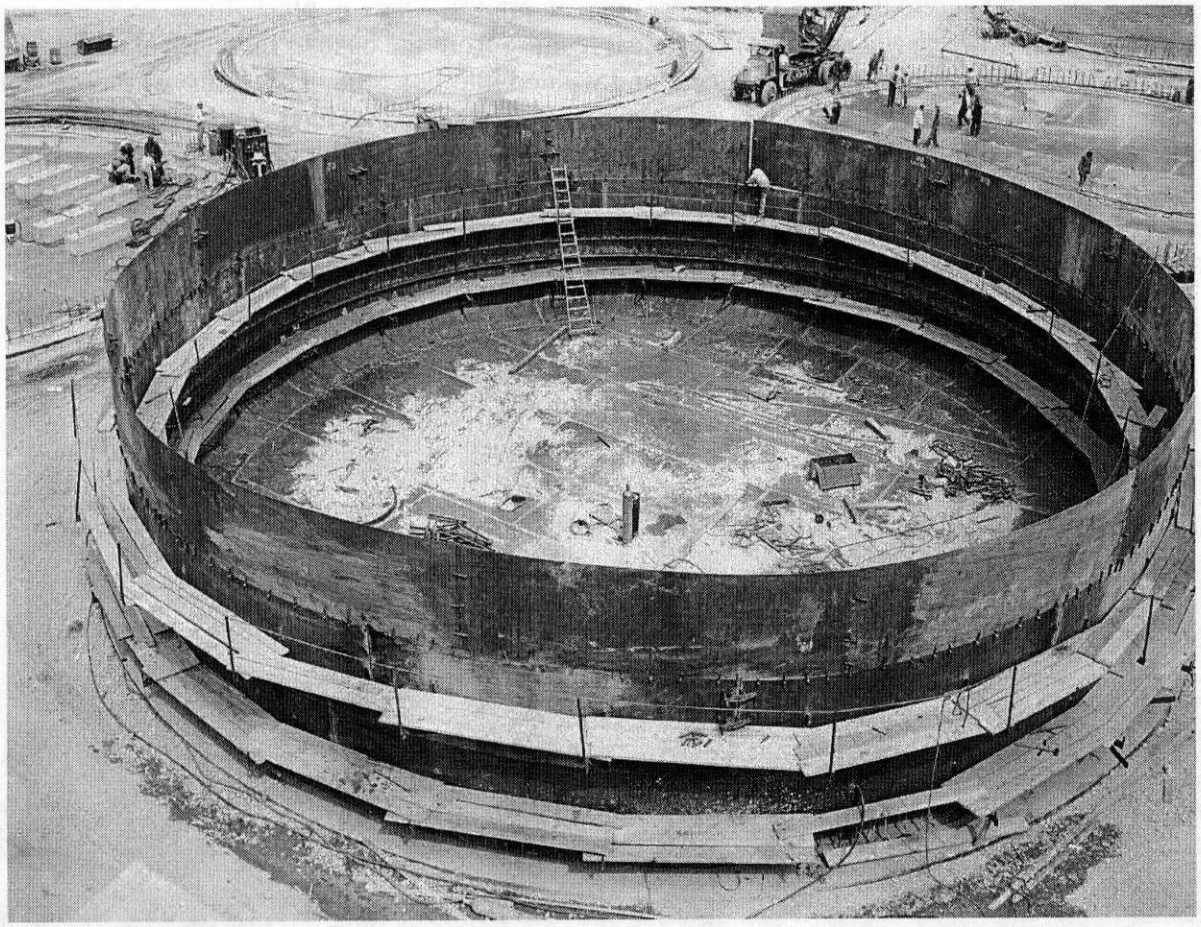

The vertical and curved portions of the steel walls were then coated with asphaltic material. This material was applied manually by swabbing or rolling it onto the surfaces. This manner of application helps to explain the black vertical stains seen in many of the in-tank photos. These empty steel tanks were subsequently filled with water to provide protection against collapse while the outer concrete was poured, and to keep the bases from floating as the curved bases were backfilled with concrete. Reinforcing rod meshes were constructed to support and provide strength to the concrete. Curved forms were set around the tanks, keying into the underlying footings and concrete was emplaced. These concrete forms appear from photos to be approximately four feet high. Concrete was placed to the top of the steel tank liners. It is not readily apparent from the photographs that the water was left in the tanks during placement of the vertical concrete walls. No water is evident in the tanks once the concrete was cured. Wooden supports for dome construction were then erected inside the tank liners. Forms for the inside of the dome appear to be constructed as blocks that rested on the interior wooden supports. Designed entrances to the tank were placed (e.g., man-holes, access ports, etc.); these entrances were in the northeast and southwest quadrants of the tanks. Reinforcing rod meshes were then put together to cover the dome and were attached to tie rods protruding from the vertical structure. Another level of vertical radial concrete forms was attached and the dome structure poured.

Figure C.7. Dome Rebar Placement

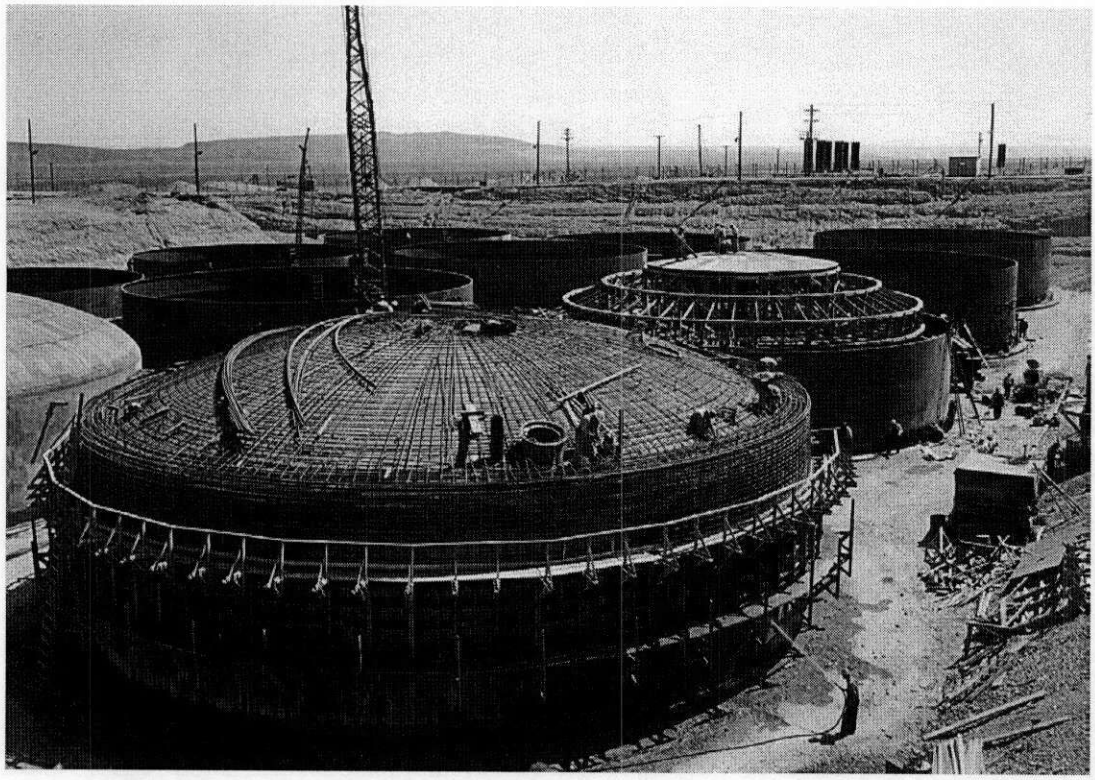

Figure C.8. Tank BX-153 with Feed Lines in Place

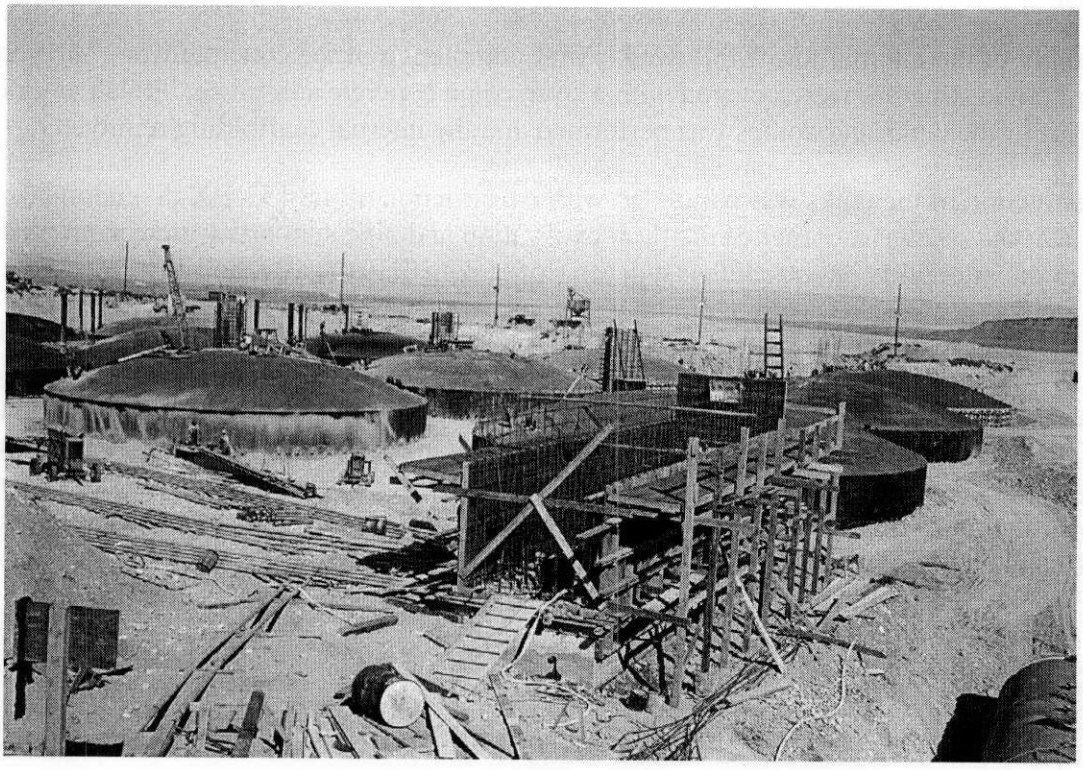

Figure C.9. Spraying Gunnite on Side Walls

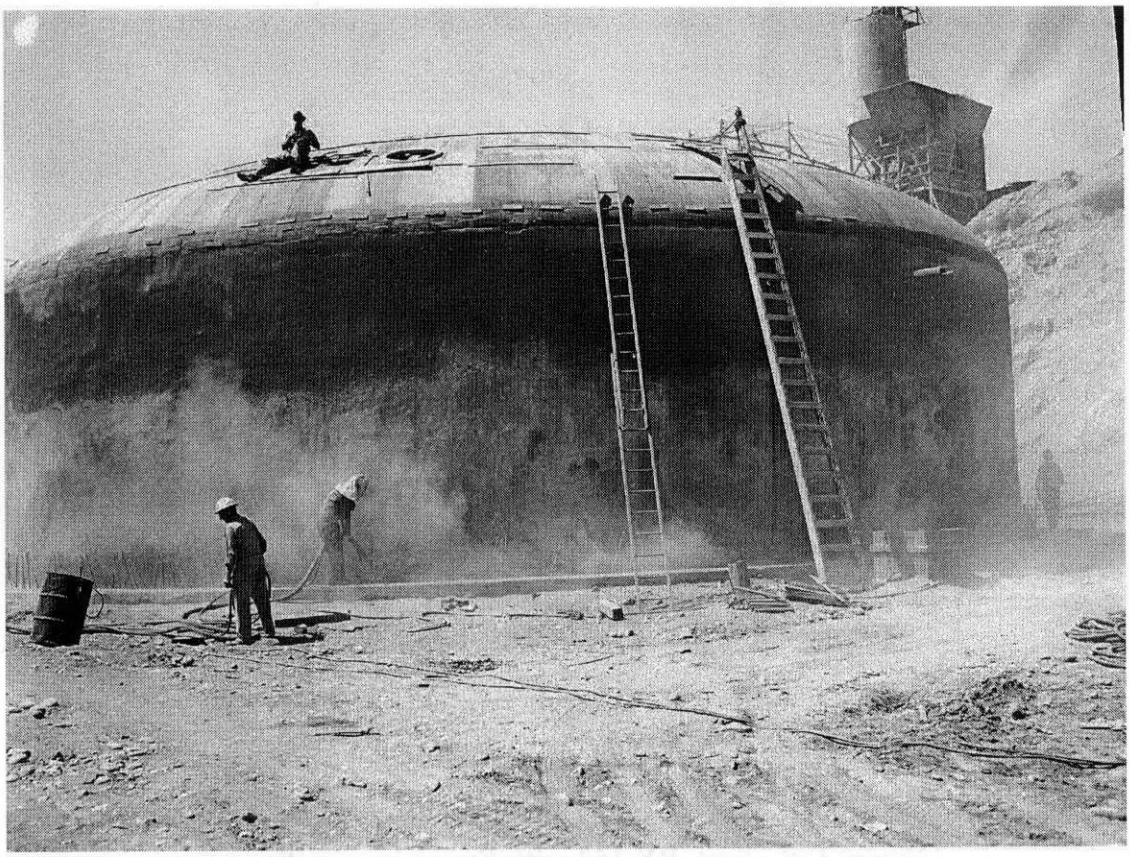

Disassembly of the internal forms followed. After completion of the concrete work, the vertical walls and dome structure were covered with a sprayed on concrete substance. Finish work on the interior of the tanks and domes was performed and the internal scaffolding removed.

The construction of the tanks was paralleled with construction of the 153-BX diversion box located near the southeast corner of the farm excavation and pipe supports were constructed leading to the inlet ports on the southeast quarter of tanks 101, 104, 107, and 110. After the excavation was partially backfilled, piping was constructed as parallel groups of four pipes leading to each row of tanks.

Cascade lines were installed at the 12 o'clock (exit) and 6 o'clock (inlet) positions on each tank. Shut-off valves were placed on the lines downstream of tanks 103, 106, 109, and 112. These lines were extended north to the edge of the excavation, apparently in anticipation of BY tank farm construction. The farm was backfilled from west to east and from south to north using "belly dump" earth-moving equipment.

Figure C.10. Cascade Line with Valve Leading to Future BY Tank Farm

Figure C.11. Belly-Dumper During Backfill of BX Tank Farm

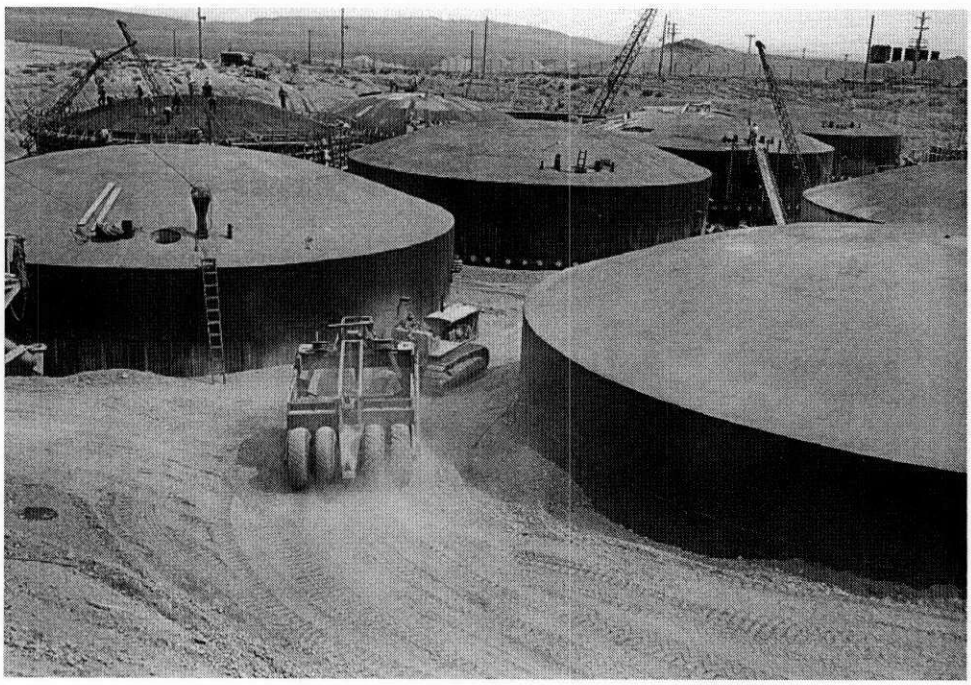

The method and approach to construction of the farms is postulated to play a role in how contamination from tanks or pipelines moved through the excavated area into the surrounding portions of the vadose zone:

- Gross excavation was conducted by heavy machinery. This resulted in the zones directly beneath the tanks being less disturbed, but sealed by the concrete of the tank bases.

- A significant amount of vehicular traffic moved over the excavated surface between rows of tanks. This is particularly true of the east-west row north of tanks 101, 104, 107, and 110 because of the location of the cement batch plant. This resulted in a hardened layer that inhibits downward migration of fluids.

- Placement of the asphaltic material on the steel walls and spraying of the concrete final layer on the tank resulted in some sealing of the excavation surface due to spills and overspray. This resulted in further decreasing the vertical hydraulic conductivity of the tank farm base.

- The general configuration of the tanks with cascade flow from south to north, combined with the impact of filling and compacting from west to east, creates a propensity for fluid movement in those same directions (i.e., north and east).

C.3.0 PROCESS CHEMISTRY AND KRIGING ESTIMATES

C.3.1 HANFORD CHEMICAL PROCESSING OPERATIONS IMPACTS TO THE WMA B-BX-BY VADOSE ZONE

The tanks in WMA B-BX-BY received a wide variety of high-level wastes coming from essentially all major chemical processing plants at the Hanford Site from 1945 through the late 1970s. The nature of chemicals and radionuclides lost or intentionally discharged to the soil column in or near this WMA are directly related to the process chemistries associated with their production. Extensive discussions of the Hanford chemical processing plant operations and associated waste stream compositions are available in Agnew (1997), Anderson (1990), Kupfer et al. (1999), and Gasper (1989). In addition, extremely detailed process technical manuals are available for each of the major Hanford chemical processing plants. Less contaminated process waste streams were routed to cribs, specific retention trenches, and surface impoundments, many near WMA B-BX-BY. An understanding of the impacts of waste discharges on the WMA vadose zone requires an assessment of chemical processes generation on the waste streams. Preliminary inventory estimates have been developed for tank farm releases (Jones et al. 2001) and discharges to cribs and trenches (Simpson et al. 2001) in and around this WMA. However, recent field and laboratory investigations have supplied information that requires changes to the previous inventory estimates. Development of this information is presented in this appendix.

C.3.1.1 Relevant Process Chemistry

Initially, tanks within WMA B-BX-BY were used in support of plutonium (Pu) production in the B Plant from 1945 through 1952 using the bismuth phosphate process. Certain tanks in this WMA were used to support the metal waste recovery program from 1952 through 1958. After the plutonium-uranium extraction (PUREX) process came online in 1956, some tanks were used for PUREX low-level wastes. As the isotope recovery programs began to develop in Hot-Semiworks, PUREX, and B Plant in the late 1950s, additional waste streams were transferred to tanks in this WMA. An abbreviated list of waste types processed through the B-BX-BY farm tanks is provided in Table C.1. The WMA B-BX-BY tanks were an integral component of the integrated isotope recovery/waste solidification program that was begun in the late 1960s. Three different tanks in the BY farm had heaters installed to support saltcake production in what was called the in-tank solidification (ITS) process. Tens of millions of gallons of tank waste supernatant were moved among the various tanks during ITS operations. As planned, the available tank space in this WMA became receiver tanks for saltcake produced in the ITS process. The extensive movement of wastes among the tanks in this WMA led to many near surface leaks, particularly in the BY farm.

Table C.1. 200 Area Chemical Process History and Waste Streams

B Plant - Bismuth Phosphate Process (1945 – 1952)

Primary Waste Streams-

- Metal waste
- First cycle (included Aluminum-cladding wastes)
- Second cycle
- 224 wastes

B Evaporator (1952 - 1956)

Primary Waste Streams-

- Evaporator bottoms
- Evaporator condensates (went to cribs)

Hot Semi-Works (1948 – 1968)

Primary Waste Streams-

- Believed to have gone initially to C farm tanks.

Uranium Recovery from E Area Tanks (1952 – 1958)

Primary Waste Streams-

- Fe-CN-scavenged uranium recovery sludges
- Fe-CN-scavenged uranium recovery supernatant (most went to the soil column).

PUREX (1956 – 1972)

Primary Waste Streams going to tanks-

- Aluminum-cladding wastes
- Zirconium-cladding wastes
- Neutralized fission-product wastes to boiling waste tanks
- Organic wash wastes
- Inorganic wash wastes
- Current acid wastes transferred to B Plant for isotope recovery

B Plant Isotope Recovery Program (1960 – 1978)

Primary Waste Types Processed at B Plant-

- Aged PUREX supernatant (from A and AX farms)
- Aged PUREX sludges (from A and AX farms)
- Current acid wastes from PUREX
- Current acid waste from REDOX
- Aged REDOX supernatants

Primary B Plant Waste Streams going to tanks-

- Waste streams from initial current acid wastes processing (went to boiling waste tanks)
- Cesium-recovery (ion exchange) wastes from PUREX PAW and zirconium acid wastes
- Cesium-recovery (ion exchange) wastes from aged PUREX supernatant
- Cesium-recovery (ion exchange) wastes from aged PUREX-sludge supernatant
- Cesium-recovery (ion exchange) wastes from aged REDOX supernatant
- Strontium-recovery (extraction) wastes from PUREX acidified sludges
- Strontium-recovery (extraction) wastes from PUREX acid wastes
- Strontium-recovery (extraction) wastes from PUREX zirconium acid wastes

In-Tank Solidification Process (1965 – 1974) (in-tank heaters were placed in 3 BY farm tanks)

Primary Waste Types Processed-

All tank supernatants having acceptable levels of heat-generating radionuclides such as cesium-137 and strontium-90. Available tank space in the B-BX-BY tanks was eventually filled with saltcake from the ITS Process.

Fe-CN = ferrocyanide
PUREX = plutonium-uranium extraction
REDOX = reduction-oxidation

Many of the contamination plumes in and around WMA B-BX-BY appear to be associated with the B Plant isotope recovery program conducted in the 1960s and 1970s in support of waste solidification program. The isotope recoveries were accomplished with plant-scale solvent extraction, ion exchange, and precipitation processes (Buckingham 1967). Although some earlier pilot-plant isotope recovery operations were completed in PUREX, Hot-Semi Works, and the B Plant, the major isotope recovery program began in late 1967 (Larson 1967, 1968; Buckingham 1967). Initially, the chemical separations processes followed the flowsheets reported by Larson (1967, 1968). However, in practice, the separations efficiencies were not as good as expected (Gasper 1989). Thus, there was a continuing series of process changes improvements that appear to have been ongoing throughout the life of this program. Thus, it becomes important to identify the timing of the waste loss events so as to better define leak inventories. In addition, it appears that effluent waste streams going back to the tanks had higher activity levels than are suggested by process flowsheet data. The chemical compositions of waste streams returning to the tanks would reflect both the feedstock going into the process and the particular flowsheet being applied.

C.3.1.2 Tank Farm Operational History

The B farm tanks (constructed in 1943 to 1944) began receiving bismuth phosphate waste streams from B Plant in 1945. The first 3-tank cascade (i.e., tanks B-101 through B-103) received waste designated as metal waste. The other three 3-tank cascades received first cycle and second cycle bismuth phosphate wastes. The four 55,000-gallon (200-series) tanks received 224 wastes. The 224 wastes were a relatively low fission product level waste stream coming from the final plutonium purification steps completed in the 224-B facility. (Similar wastes were generated in the 224-T facility in the 200 West Area and discharged to the T farm 200-series tanks.) Solids in the 224 waste stream were allowed to settle in the 200 series tanks and supernatants were transferred to cribs. During the early years of operating the bismuth phosphate process, over 10,000 gallons of aqueous waste were produced per metric ton of irradiated uranium metal (MTU) processed. Approximately 2,100 gal of the 10,000 gal total would have been metal waste, i.e., the high-fission product waste stream containing essentially all of the uranium and soluble fission products. In contrast, the PUREX process produced approximately 300 gallons of aqueous high-fission product wastes per MTU processed.

In the late 1940s, the BX and BY tank farms were constructed to support continuing plutonium production in the B Plant bismuth phosphate operations (Appendix C.2.0). It appears the tank space in the B, BX, and BY tank farms (as well as the tanks in the C tank farm) was completely utilized supporting the B Plant bismuth phosphate operations. In 1951, the B Evaporator came online to reduce the volume of first cycle bismuth phosphate being stored in 200 East Area tanks. In addition, a major effort was undertaken to retrieve the stored metal waste for transfer to the U Plant in the 200 West Area for uranium recovery. The B Plant bismuth phosphate process was placed on standby in 1952 and was not reactivated as a bismuth phosphate plant. After 1952, some B, BX, and BY tanks became receiver tanks for evaporator bottoms in support of B Evaporator operations. B, BX, and BY tanks also received uranium recovery wastes from U Plant. The critical shortage of tank space during this time led to extensive discharges of tank wastes to the soil column in and around the 200 East Area (Waite 1991). The 200 East Area tank waste discharges went to the BY cribs, BX trenches, and the BC cribs and trenches.

In 1956, the PUREX process came online in the A Plant. The PUREX process was far more complex than previous plutonium recovery operations. Prior to 1968, the neutralized PUREX high-fission product wastes were routed mainly to tanks in the A and AX tank farms for boiling wastes. However, waste transfer records indicate that some B, BX, and BY tanks received relatively small amounts of PUREX high-fission product wastes (likely associated with the Phase 1 strontium-90/technetium-99/cesium-137 isotope recovery activities in the B Plant). In the late 1960s, the tanks in WMA B-BX-BY were used to support the B Plant isotope recovery/ITS projects.

Although the major focus of Hanford Site operations has been the production of plutonium, historical records indicate that from the beginning, Hanford Site facilities were used for the production and/or recovery of radioactive isotopes other than plutonium. For example, in the early 1960s, quantities of strontium-90 were recovered from PUREX waste steams for potential use as heat sources. In the 1960s, there was a serious attempt to find viable markets for a number of isotopes, such technetium-99, palladium, and rhodium (Godfrey 1971) that could be recovered from tank wastes. However, the major isotope recovery programs at Hanford were driven by tank waste management requirements. By the late 1950s, it was clear that a number of single-shell tanks (SSTs) had likely leaked and the long-term storage of large volumes of liquid radioactive wastes was untenable. Hanford Site contractors were directed to convert liquid radioactive waste to saltcake as soon as practicable. The problems associated with converting liquid wastes to saltcake have long been appreciated. These included aluminum solubility issues (Barney 1976) and controlling heat production in stored saltcake (Smith and Tomlinson 1967).

The conversion of high-fission product radioactive waste supernatants into saltcake required both a 3 to 5-year cooling-off period to allow short-lived radionuclides to decay (thus, the need for boiling waste tanks in the S, SX, A, and AX tank farms) and removal of a significant amount of the longer-lived, heat-generating radionuclides such as strontium-90 and cesium-137. In 1967, B Plant was reactivated to support an isotope recovery program. Beginning in 1967, PUREX current acid wastes were processed through B Plant for cesium-137 and strontium-90 recovery, prior to the 3 to 5-year cooling-off period. Aged PUREX supernatants and sludges were recovered from the tanks and processed through the B Plant for strontium-90 and cesium-137 recovery. The aged reduction-oxidation (REDOX) supernatants were transferred to 200 East Area tanks and processed through B Plant for cesium-137 recovery. After cesium-137 removal, REDOX supernatants were transferred back to the 200 West Area for saltcake production in the T and S Evaporators. The REDOX sludges, which contained essentially all of the strontium-90, were left in SX tanks and air-cooled.

After the cesium-137 was removed (or at least greatly reduced) in the aged PUREX supernatants, the wastes were transferred to various B, BX, and BY tanks, leading to conversion of supernatants into saltcake using the BY farm in-tank solidification (ITS) process. In the ITS process, heater units were installed in three tanks in the BY tank farm. Waste supernatants were rotated through the ITS process tanks and out to the B, BX, and BY tanks so as to produce saltcake. The available tank space in the B, BX, and BY farms was filled with saltcake using the BY ITS process.

C.3.1.3 B, BX, and BY Tank Waste Transfers

The extensive waste reprocessing operations in the B Plant led to very large volumes of tank waste being transferred through certain tanks. Such tanks were generally referred to as receiver tanks. For example, tank BX-101 was the receiver tank for B Plant cesium-137 recovery wastes from 1968 through 1972. Tank B-101 was the receiver tank for Cell 23 wastes until the tank was removed from service in 1974. Tank BX-104 was the 200 East Area receiver tank for the aged REDOX supernatants coming from the 200 West Area. The aged REDOX supernatants were transferred to tank C-105 that acted as the feeder tank for supernatants going to B Plant. After being processed in the B Plant, the REDOX supernatants were transferred to tank BX-101 (after 1972, tank BX-104 was used) and then back to the 200 West Area for conversion to saltcake in S and T Evaporators. Available waste transfer records (Agnew et al. 1997) lack the detail required to develop an adequate understanding of real-time waste transfers through the tank system. For example, it is not uncommon to see the total volume of waste in the tank listed as much larger than the known tank volume. This occurs because waste transfers into and out of the tank were not listed chronologically but rather only reconciled on a quarterly basis in the waste transfer records (Agnew et al. 1997). Note that the waste transfer records in Agnew et al. (1997) were developed to support estimating the current tank waste compositions and inventories as of January 1, 1994 and not to provide real-time tank information over the complete operating lifetime of the tank. However, the records are adequate to track gross movement of waste types through the specific receiver tanks.

C.3.1.4 Reassessment of the Composition of Wastes in Tanks BX-101 and BX-102 During Leak Events Between 1968 and 1972

Preliminary estimates of tank wastes compositions in tanks BX-101 and BX-102 during the times of expected leak events have been published (Jones et al. 2001). The tank waste composition and leak volume for the waste loss event at tank BX-102 published in Jones et al. (2001) was based on published data on a 1951 tank overfill event that led to the loss of 91,600 gal of bismuth phosphate metal waste. The published waste composition and inventory estimates associated with the 1951 waste loss event accurately reflect the current state of knowledge. However, assumptions made in developing tank waste composition estimates for tank BX-102 (as published in Jones et al. 2001) failed to account for any waste losses from tank BX-102 in the 1968 to ~1972 time period. In fact, current geophysical physical logging data indicate the 1968 to ~1972 leak event likely originated from tank BX-101 rather than BX-102 (DOE-GJPO 1998, 2000c). However, both tanks contained essentially identical waste compositions from 1968 through mid-1970. Both of these tanks contained a B Plant waste stream associated with the cesium-137 recovery from aged PUREX supernatants.

In 1970, tank BX-102 was suspected of being a leaker. An extensive field investigation program was conducted that year. Tank BX-102 was declared a leaker and removed from active service in 1970 (Womack and Larkin 1971). In September 1971, because of continuing increasing gamma activity in drywells near tank B-102, the decision was made to add 50 tons of diatomaceous earth to tank B-102 to sorb residual tank liquor (Metz 1971). In 1972, continuing increasing gamma activity in drywells around BX-101 was noted. Additional field investigations identified a sluice pit on top of tank BX-101 as the source of tank waste leaking into the soil column (Jensen 1972). Tank BX-101 was taken out of service at the end of 1972. Tank B-101

was identified as an assumed leaker in 1974 (Hanlon 2002). It is interesting to note that all of the tank waste contamination near tanks BX-101 and BX-102 can be explained from the well-documented 1951 metal waste loss and a BX-101 leaking sluice pit over the time period of 1968 through 1972. Following is a discussion of the waste types being stored in tanks BX-101 and BX-102 over this time period.

In late 1967, a large-scale fission-product recovery program was begun in the B Plant (Buckingham 1967). The major focus of this effort was to remove sufficient amounts of cesium-137 and strontium-90 from various process streams and tank wastes so that the resulting supernatants could be converted to saltcakes without further processing (Larson 1967). A number of tanks in the BY farm were used in the ITS program. Many tanks in the B, BX, and C tank farms were used to support movement of wastes to B Plant for reprocessing and transfers of resulting waste streams to the BY ITS processing tanks. Beginning in early 1968, both tanks BX-101 and BX-102 received wastes from the B Plant cesium-137 recovery process. Waste transfer records indicate that tank BX-102 held this waste type until it was deactivated in mid-1970. Tank BX-101 continued to receive the cesium-137 recovery wastes until it was deactivated at the end of 1972. However, waste transfer records indicate that from mid-1970 until being deactivated, tank BX-101 was used as a waste blending tank for supernatants going to the BY farm ITS process. Thus, an understanding of the waste composition in tanks BX-101 and BX-102 during the times of suspected waste-loss events requires some knowledge about the compositions of waste streams going to the B Plant for cesium-137 recovery.

There were five major waste types transferred to the B Plant for cesium-137 recovery and, in addition, there were a number of minor recycle streams also being reprocessed. Three of the major waste streams were processed with only minor head-in treatment whereas the other two were processed extensively before cesium-137 recovery. The compositions of the five waste streams are shown in Table C.2. The three waste streams that were processed directly were the aged PUREX supernatant (PSN), the PUREX-sludge supernatant (PSS), and the aged REDOX supernatants (RSN). It appears the only pre-treatment these waste streams received before being passed through ion exchange column was the addition of complexants to bind polyvalent metal ions to prevent their interactions with the cation ion exchange resin used for cesium-137 recovery (Gasper 1989). Three waste streams (PSN, PSS, and RSN) accounted for essentially all of volume of waste processed through B Plant for cesium-137 recovery.

Table C.2. High-Level Waste Streams Feeding the B Plant Cesium-137 Recovery Process [(a) (b)]

Chemical/ Radionuclide	Waste Type				
	PSN	PSS	PAW	ZAW	RSN
Na (M)	4.0 – 6.0	1.8 – 5.4	0.2 – 0.7	0.2 – 0.35	4.9 – 5.5
Al (M)	NR	0.005 – 0.04	0.03 – 0.08	0.8	0.3 – 0.8
Fe (M)	NR	NR	0.1 – 0.3	0.1	NR
Cr (M)	NR	0.002 – 0.004	0.018 – 0.032	0.014 – 0.016	NR
H (M)	—	—	0.5 – 0.9	0.2 – 1	—
Hydroxide (M)	—	0.08 – 0.5	—	--	0.9 – 1.6
Nitrate (M)	0.6	0.9 – 4.2	1.2 – 2.1	0.9	2.6 – 3.5
Nitrite (M)	0.6 –3.2	0.2 – 0.5	NR	NR	0.4
Sulfate (M)	0.1 – 0.16	0.25 – 0.4	0.24 – 0.58	0.12 – 0.18	0.9 – 1.6
Phosphate (M)	0.02	0.031	<0.012	0.01	NR
Chloride (M)	0.09	0.002	NR	NR	NR
Carbonate (M)	0.8 – 0.9	0.24 – 0.7	—	—	NR
Fluoride	NR	NR	0.0044	0.30	NR
Cs-137 (Ci/gal)	13 – 15	1.8 – 2.3	38 – 400	50 – 800	0.3 – 2
Sr-90 (Ci/gal)	1.8 – 2.3	0.16	16 – 37	45 – 79	NR
Ru-106 (Ci/gal)	0.01 – 0.5	NR	NR	150	0.01 – 0.08
Tc-99	100 mg/gal, 0.00044 M	1.1 E-05 M	7.0 E-04 M	1.2 E-03 M	3 – 17 mg/gal
pH	10 - 11	10 - 13	—	—	—

[(a)] From Gasper 1989, "By-Product Recovery from High-Level Wastes", WHC-EP-0244 and Larson 1967, "B Plant Phase III Flowsheets", ISO-986.
[(b)] Data in this table are reproduced from the primary references and include a number of mixed, non-standard units
PSN = aged PUREX high-level waste supernatant
PSS = PUREX sludge supernatant
PAW = PUREX Current Acid Waste generated from aluminum-clad fuel
ZAW = PUREX Current Acid Waste generated from zirconium-clad fuel
RSN = aged REDOX high-level waste supernatant
NR = not reported

The remaining waste streams (PAW and ZAW), generally referred to as current acid wastes (CAW), were the acidic high-level waste streams coming directly from PUREX after the sugar-denitrification process. The goal was to remove cesium-137 and strontium-90 from these wastes before they were neutralized and transferred to boiling waste tanks. The obvious advantage was in recovering cesium-137 and strontium-90 from a low sodium waste stream. The first step in recovering cesium-137 from the CAW waste types was to clarify the supernatant by centrifugation and then precipitation of cesium-137 with phosphotungstate. The aqueous phase then was transferred to the strontium-90 recovery process. The flowsheets developed for processing the CAW waste streams indicate that high fission-product aqueous waste streams

generated during cesium-137 and strontium-90 recovery were diverted to the waste tanks designated for B Plant boiling wastes (Larson 1967, 1968). Thus, it is assumed that the processing of CAW in the B Plant during the 1967 through 1972 period would have contributed little to the fission-product load in waste streams transferred to tanks BX-101 and BX-102. The development of composition estimates for wastes in tanks BX-101 and BX-102 in the time period of interest focuses on the three high-volume cesium-137 recovery waste streams coming from the B Plant: PSN, PSS, and RSN.

Data for the three B Plant cesium-137 recovery waste types of interest (i.e., PSN, PSS, and RSN) are reproduced in standard units of moles/L and Ci/L in Table C.3. Activities are reported for three radionuclides, cesium-137, strontium-90, and technetium-99. The conversion factors are: 3.8 L per gallon for volumes and for technetium-99, a mass to activity ratio of 58.2 g/Ci. When Table C.3 provides a range of concentration values, the larger value was generally chosen because more dilute waste streams were processed through the Cell 23 Evaporator for volume reduction. It is assumed the target value for sodium would have been around 5 M, based on waste volume reduction goals and the requirement to be able to pump the wastes.

The variability in the data listed in Table C.3 clearly points out the challenges in reprocessing Hanford wastes. Gasper (1989) outlines some of the problems encountered in the cesium-137 recovery process. The first ion exchange material (i.e., Linde AW-500) proved to be chemically unstable in long-term processing of alkaline waste solutions. Other ion exchange materials were used but proved to be problematic. It appears in many cases, the goal of 95% removal of cesium-137 was not met. The co-mixing of waste types in tank BX-101 prior to being transferred to the ITS process during 1971 and 1972 may have been required to further dilute the cesium-137 concentrations in the waste batches to meet the saltcake heat-load specifications.

The tank waste composition estimate published in Jones et al. (2001) for tank BX-101 is a reasonable waste composition estimate of materials that may have been lost from tanks BX-101 and BX-102 in the 1968 through 1972 time period. This waste composition estimate is reproduced from Jones et al. (2001) in Table C.4.

Table C.3. Estimates of B Plant Cesium-137 Recovery Process High-Level Waste Streams Compositions

Chemicals (M)	Waste Type					
	PSN	PSS	RSN	1XW PSN [a]	"CSR" from HDW Model [b]	RPP-7389 BX-101 1972 Composition [c]
Na	5.0	5.4	5.2	5.15	5.0	3.9
Al	NR	0.04	0.8	NR	0.45	0.32
Fe	NR	NR	NR	NR	0.0055	0.003
Cr	NR	0.004	NR	NR	0.056	0.016
PH	11	13	—	10 – 11	NR	NR
Hydroxide	—	0.5	1.6	—	NR	NR
Nitrate	0.6	4.2	3.5	0.52	1.43	1.0
Nitrite	0.6 – 3.2	0.5	0.4	2.78	1.09	0.36
Sulfate	0.16	0.4	1.6	0.14	0.13	0.070
Phosphate	0.02	0.031	NR	0.013	0.014	0.011
Chloride	0.09	0.002	NR	0.078	0.005	0.069
Carbonate	0.8 – 0.9	0.7	NR	0.73	0.23	0.259
Complexant (e.g., HEDTA)	—	—	—	—	0.001	NR
Radionuclides						
Cs-137 (Ci/L)	[d]	[d]	[d]	<0.18	0.04	0.012
Sr-90 (Ci/L)	0.47 – 0.61	0.042	NR	NR	0.07	0.045
Tc-99 (Ci/L)	4.5 E-04 to 7.5 E-04	1.9 E-05	1.4 E-05 to 7.7 E-05	NR	2.2 E-04	7.28 E-05
Specific Gravity				1.25	1.20	

[a] From Table 28 of Larson 1967 (ISO-986)
[b] From Agnew 1997
[c] From Jones et al. 2001
[d] Flowsheets from Larson 1967 assumed a 95% recovery; however, Gasper (1989) notes that between 1967 and June 1969, 25% of the Cs-137 product (10 MCi) were lost back to process waste streams.
PSN = aged PUREX high-level waste supernatant
PSS = PUREX sludge supernatant
RSN = aged REDOX high-level waste supernatant
NR = not reported
References:
Agnew 1997, "Hanford Tank Chemical and Radionuclide Inventories: HDW Model Rev. 4", LA-UR-96-3860.
Gasper 1989, "By-Product Recovery from High-Level Wastes", WHC-EP-0244.
Jones et al. 2001, "Preliminary Inventory Estimates for Single-Shell Leaks in B, BX, and BY Tank Farms", RPP-7389, Rev. 0.
Larson 1967, "B Plant Phase III Flowsheets", ISO-986.

Table C.4. Composition Estimate for Wastes in Tanks BX-101 and BX-102 During Leak Events

Assumed Leak Event Dates – 1968 through 1972			
Analyte	**moles/L**	**Analyte**	**Ci/L**
Na	3.90 E+00	Nb-93m	4.98 E-06
Al	3.19 E-01	Tc-99	7.28 E-05
Fe	3.03E-03	Ru-106	4.95 E-09
Cr	1.63 E-02	Cd-113m	3.01 E-05
Bi	3.55 E-05	Sb-125	6.22 E-05
La	4.25 E-10	Sn-126	2.16 E-06
Hg	3.68 E-07	I-129	1.41 E-07
Zr	4.65 E-06	Cs-134	8.73 E-08
Pb	4.92 E-05	Cs-137	1.16 E-02
Ni	1.82 E-03	Ba-137m	1.10 E-02
Sr	0.00 E+00	Sm-151	4.99 E-03
Mn	1.13 E-03	Eu-152	1.46 E-06
Ca	9.10 E-03	Eu-154	2.29 E-04
K	1.67 E-02	Eu-155	8.55 E-05
NO3	1.02 E+00	Ra-226	6.26 E-11
NO2	3.57 E-01	Ra-228	3.16E-10
CO3	2.59 E-01	Ac-227	3.64 E-10
PO4	1.12 E-02	Pa-231	1.31 E-09
SO4	6.96 E-02	Th-229	1.43 E-11
Si	3.44 E-02	Th-232	1.31 E-10
F	1.56 E-03	U-232	1.91 E-08
Cl	6.90 E-02	U-233	7.38 E-08
DBP	6.79 E-03	U-234	1.06 E-07
Butanol	5.23 E-03	U-235	4.35 E-09
TBP	0.00 E+00	U-236	3.56 E-09
NPH	0.00 E+00	U-238	9.81 E-08
U-Total	1.23 E-03	Np-237	2.45 E-07
Analyte	**Ci/L**	**Analyte**	**Ci/L**
H-3	6.17 E-05	Pu-238	6.49 E-07
C-14	1.04 E-05	Pu-239	1.56 E-05
Ni-59	6.38 E-07	Pu-240	2.99 E-06
Ni-63	6.32 E-05	Pu-241	4.54 E-05
Co-60	1.32 E-05	Pu-242	2.76 E-10
Se-79	1.40 E-06	Am-241	3.03 E-05
Sr-90	4.46 E-02	Am-243	1.90 E-09
Y-90	4.48 E-02	Cm-242	6.92 E-08
Zr-93	6.58 E-06	Cm-243	7.07 E-09
		Cm-244	1.01 E-07

B Plant Process records indicate the cesium recovery wastes were pH = 10.
Complexant concentration likely to have been 115% of sum of iron, aluminum, and manganese.

The waste composition listed in Table C.4 and published in Jones et al. (2001) is a composite of B Plant waste stream estimates generated from three major waste types: aged PSN, PSS, and diluted aged RSN. PSN carried the highest fission-product load and RSN had the highest hydroxide and aluminum concentrations. The pH of the PSN and PSS was between 10 and 13 while the RSN contained molar concentrations of hydroxide.

The technetium-99 concentrations were highest in PSN (~6 E-04 Ci/L) and much lower in PSS and RSN (1 to 8 E-05 Ci/L). The leak inventory estimate developed in Jones et al. (2001) used a technetium-99 concentration of 7.28×10^{-5} Ci/L. The most concentrated PSN waste stream had a technetium-99 concentration of 7.5×10^{-4} Ci/L, or an order of magnitude higher than the value used for estimates in Jones et al. (2001).

The PSN was processed through B Plant from 1968 through mid-1970. The RSN was processed through B Plant after mid-1970. Leak events between 1968 through mid-1970 would have involved primarily a PSN waste type. Jones et al. (2001) composition estimates underestimate the technetium-99 concentrations for any PSN waste leaks (possibly by a factor of 5). Likewise, the Jones et al. (2001) values overestimate the technetium-99 loss estimates for RSN waste types (processed through tank BX-101 after mid-1970).

C.3.1.5 Tank B-110 Fill History

Tank B-110 is the first 530,000-gallon tank in the 3-tank cascade (i.e., B-110, B-111, and B-112). It began receiving second cycle bismuth phosphate waste in early 1945 and was filled by the fourth quarter of 1945 (Agnew et al. 1997). This tank continued to receive second cycle waste until 1953. Waste transfer records indicate that approximately 6.3 million gallons was added to this 3-tank cascade. The records indicate that the cribbing of second cycle waste began in 1948 from tank B-112. Thus, it is likely tank B-110 would have maintained any sludge coming in with the incoming wastes. During the 1953 to 1954 period, tank B-110 was a receiver tank for supernatants coming from other B farm tanks to be cribbed. In 1954, tank B-110 began receiving evaporator bottoms from the B Evaporator facility. From 1955 through 1962, this tank received small additions of 5-6 cell waste from B Plant. The tank was projected to be about half-filled with sludge. In 1963, approximately 175,000 gal of tank space was freed up by pumping supernatant to tank B-112. From 1963 through 1967, tank B-110 received approximately 675,000 gal of PUREX high-level wastes, identified as fission product waste-type. The PUREX wastes were added in reasonably small batches (i.e., ~100,000 gal) with frequent transfers to boiling waste tanks in the A tank farm. A review of the isotope recovery process and waste transfer records suggests these PUREX waste streams transferred to tank B-110 likely came from the Phase I/II Isotope Recovery Program conducted in PUREX, Hot-Semiworks, and the B Plant. The Phase I/II Program involved, at different times, recovery of strontium-90, cesium-137, technetium-99, and other isotopes. During this time period, it appears the waste volume in tank B-110 was maintained above its nominal 530,000-gallon tank capacity.

In 1968, the waste storage mission of tank B-110 shifted to supporting the Phase III B Plant isotope recovery operations. In 1968 and 1969, tank B-110 received 645,000 gal of B Plant wastes. Waste transfer records suggest the waste levels were maintained well above the nominal tank capacity of 530,000-gallons. At the end of 1969, there was only a 10,000-gallon deficiency

between the measured waste volume and calculated volume based on waste transfer records. By the third quarter of 1971, the deficiency had grown to 31,000-gallons. At that point, 223,000-gallons of supernatant were transferred out of the tank. Essentially all of the waste remaining in this tank was listed as solids. The tank was saltwell pumped a number of times. In 1972, the waste deficiency increased to 44,000-gallons. In 1973, tank B-110 was listed as a suspected leaker and a number of drywells were installed. Intermittent saltwell pumping continued and by the end of 1975, the cumulative unknown had changed to a positive 25,000-gallons. Note that the waste volume measurements become highly uncertain when considering solid tank wastes.

In developing leak inventory estimates for tank B-110, a 25,000-gallon leak volume was assumed and the leak was assumed to have taken place in 1971 and 1972 (Jones et al. 2001). It was assumed the leaked supernatant would have carried substantial amounts of tank waste components, thus, leak inventory estimates were quite large. For example, the tank B-110 leak inventory estimate included 8,220 kg of sodium, 7,810 kg of nitrate, 134 kg of chromium, 13.8 Ci of technetium-99, and 16,000 Ci of cesium-137. The B-110 leak inventory estimates are considerably larger than the leak inventory estimates developed for tank SX-108. It was appreciated that the cesium-137 inventory estimates from the assumed B-110 leak event seemed to be inconsistent with recently measured spectral gamma logging data (DOE-GJPO 1999). However, the spectral gamma logging data did suggest the possibility of a strontium-90 plume between tanks B-107, B-108, B-110, and B-111. The drilling and sampling program conducted in fiscal year 2001 near tank B-110 was designed to address uncertainties raised by the inconsistencies in existing information about the B-110 leak event. Clearly, the soil analysis data from the B-110 borehole (Section 3.0) are inconsistent with the leak inventory estimate published in Jones et al. (2001).

As noted by Agnew et al. (1997) tank B-110 was half-filled with solids by 1954. By 1965, there was thought to be 330,000 gal of solids in this tank. Fluid transfers through this tank are thought to have involved minimal mixing of supernatants with pre-existing solids. Thus, leak events taking place in the late 1960s or early 1970s would likely have involved the batches of supernatants being stored in the tank at that time.

C.3.1.6 Composition Estimate of Tank Wastes Leading to B-110 Strontium-90 Plume

Historical records uncovered to date fail to provide definitive evidence of the time of waste losses from the B-110 tank system, nor the likely waste composition estimates. Because of the variable composition of waste types that passed through this tank, no direct estimate of the composition of wastes lost can be made. However, a likely waste type can be identified associated with the contamination plume by matching soil analysis data from the B-110 borehole with the major constituents with specific waste streams that were discharged to the tanks. This approach was used to identify a plausible B Plant waste stream that could have led to the strontium-90/fluoride/carbonate plume found near tank B-110. The combination of strontium-90 and fluoride in a waste stream prior to 1974 limits the waste-type to a zirconium-clad fuel processing origin.

Tank B-110 received high-activity waste from B Plant beginning in 1963. These wastes were received in 35 to 150,000-gallon batches and then forwarded to other tanks. No process records have been found that indicate these wastes would have contained fluoride. However, these

wastes would have contained mobile gamma-emitting radionuclides such as cobalt-60, europium-154, and antimony-125, none of which were found around tank B-110. Thus, it appears unlikely there were significant wastes lost during that time period.

In 1968, B Plant began to process PUREX CAW. The B Plant processing of the CAW stream generated from zirconium-clad fuels (ZAW) could have led to a waste composition that included (and was generally limited to) mobile strontium-90, fluoride, and carbonate. According to the flowsheet data (Larson 1967), ZAW contained 0.3 M fluoride. The fluoride originated from the zirconium decladding operation. The dissolution of the zirconium cladding required the use of ammonium hydrogen fluoride. Fluoride was a likely impurity in the dissolved uranium fuel processed in PUREX. After denitrification, the high fission product waste stream was transferred to B Plant for cesium-137 and strontium-90 recovery. First, the cesium-137 was removed using the phosphotungstate precipitation process (Larson 1968) with the aqueous phase going to the strontium-90 recovery process. The second step was the precipitation of strontium-90 using a lead sulfate carrier process (Larson 1967). The liquid waste stream was then transferred to B Plant boiling waste tanks.

The strontium/lead sulfate cake was then converted to a carbonate salt using a metathesis process. The carbonate cake was dissolved in nitric acid. After a pH adjustment and the addition of complexants, the strontium-90 was extracted into an organic phase in a solvent extraction column system (Larson 1967). The aqueous phase was then neutralized and sent to the tanks. The flowsheet information suggests this waste stream contained, among other things, 0.43 Ci/gal strontium-90, 0.52 M HEDTA, and 0.1 M fluoride, and had a pH of 3.9. The waste stream would have been neutralized to a pH >8 (pH 10 was optimal), probably with sodium carbonate or a combination of 50% sodium hydroxide and sodium carbonate. It is likely the strontium-90 concentrations would have been higher, perhaps much higher, than the value suggested in the flowsheet because of problems in adjusting the pH and complexant concentration correctly. Waste streams such as these were known to have contained mobile (i.e., complexed) strontium-90 and plutonium.

It can be hypothesized that the leak of strontium-90 containing waste from tank B-110 likely involved the piping/waste transfer system rather than structural failure of the tank because, for the last two or three years of active service, this tank contained cesium-137 recovery waste similar to the waste-type lost from tanks BX-101 and BX-102. There is no cesium-137 recovery waste-type fingerprint in the spectral gamma logging data from drywells around tank B-110. However, no documentation of losses during waste transfers involving tank B-110 have been found. Nor are realistic leak volume estimates currently available for losses around tank B-110. As discussed in Section 2.1.1.2, the spectral gamma logging data provide evidence for a substantial strontium-90 plume in the area between tanks B-110, B-111, B-107, and B-108. At this point in time, the strontium-90 gamma logging data cannot be quantified (McCain 2002). A partial list of constituents expected to be in a strontium-90 recovery waste stream coming from zirconium-clad fuel is provided in Table C.5. Based on process records, it is clear this waste could have been mixed with other B Plant waste streams and/or could have been concentrated in the Cell 23 Evaporator. However, some of the ratios (e.g., strontium-90 to fluoride) may be of interest.

Table C.5. Strontium-90 Recovery Waste Streams from Zirconium Clad Fuel [a]

Chemical/ Radionuclide (M)	Concentration	Chemical/ Radionuclide	Concentration
Na	3.3	Phosphate (M)	<0.003
Al	0.0305	Total Carbonate (M)	0.8[c]
Fe	<0.1	Fluoride	0.10
Cr	0.00545	HEDTA	0.52
H	(b)	Hydroxyacetic acid	0.25
Hydroxide	(b)	Cs-137 (Ci/gal)	Assumed ~2
Nitrate	3.1 – 4.0	Sr-90 (Ci/gal)	0.43
Nitrite	NR	Tc-99	0.00042 M
Sulfate	<1.8	pH [b]	~10 (assumed)

[a] Data in this includes the 1AW data from Table 11 of Larson 1967
[b] Assumed waste stream neutralized to pH ~10 with sodium carbonate.
[c] Assumed sodium carbonate used to neutralize HEDTA, AcOH, and initial acid.
Reference: Larson 1967, "B Plant Phase III Flowsheets", ISO-986.

C.3.2 TECHNETIUM-99 INVENTORY DISCUSSION

Technetium-99 was identified as the major radioisotope of concern in long-term risk evaluations in recent Hanford Site environmental investigations (Knepp 2002; Mann et al. 2001). Thus, the development of a better understanding of the nature and extent of technetium-99 contamination from tank leaks and intentional discharges of tank waste becomes a major focus of vadose zone characterization efforts. Technetium-99 is produced in about equal molar amounts with cesium-137 during the fission of uranium. Technetium-99 is of concern because of its relatively long half-life (i.e., ~200,000 years) and its tendency to form mobile species under vadose zone conditions. Technetium-99 decays by weak beta emissions that are not detectable with field instrumentation. Thus, any improvements in an understanding of the fate of technetium-99 in the vadose zone or in-tank inventories must come from an integration of data from a limited number of recent analyses and laboratory experiments with information from previous studies and historical process knowledge. This section provides an assessment of the state of knowledge of technetium-99 in WMA B-BX-BY.

The production of technetium-99 at the Hanford Site and its likely pathway through the Hanford plutonium processing and isotope recovery facilities has been completed. In addition, results from fundamental investigations of the radiolytic reduction of technetium(VII) in the presence of organic complexants have been published (Shuh et al. 2000). Focused laboratory tests were conducted to address specific technetium-99 chemistry issues associated with WMA B-BX-BY. Finally, a literature review of technetium-99 studies pertinent to the vadose studies was completed (Krupka and Serne 2002). Information from these sources are integrated with soil analyses data from test wells to develop a rationale for selection of technetium-99 values used in long-term risk modeling.

C.3.2.1 Technetium-99 Production and Processing at Hanford

Technetium-99 is a fission product resulting from the irradiation of uranium fuel rods in the Hanford plutonium reactors. Its production rate was controlled by the composition of the uranium fuel rods, reactor power level, and time the fuel was in the reactor. These parameters are well documented. The plutonium recovery process history for the irradiated fuel rods is also available. Thus, the expected inventory of technetium-99 produced at Hanford as a function of time and the plutonium recovery facility that processed it are well understood (Jones 2002) and are shown graphically in Figure C.12. Approximately 33,000 Ci of technetium-99 were processed through the plutonium recovery plants at Hanford. Approximately 77.7% of the technetium-99 was processed through PUREX, 19% through REDOX, and only 3.3% through the bismuth phosphate process in B and T Plants. Approximately 2,200 Ci of technetium-99 were produced at PUREX in the 1980s and wastes containing this technetium-99 went to double-shell tanks. Thus, the total amount of technetium-99 that could have reached the SSTs is approximately 31,000 Ci. However, it has long been known that some of the technetium-99 was co-extracted with uranium and was subsequently shipped off the Hanford Site.

It is generally accepted that approximately 20% of the technetium-99 processed through PUREX was co-extracted with the uranium (Roberts et al. 1962; Roberts 1971; Godfrey 1971). A similar percentage of technetium-99 was likely co-extracted during the uranium recovery process from metal waste. Process flow sheet information (Buckingham 1967) suggests that very little technetium-99 was co-extracted with the uranium in the REDOX process. Thus, approximately 19,000 Ci of technetium-99 from PUREX, 6,300 Ci from REDOX, and 870 Ci from the bismuth phosphate process were routed through the SSTs. The fate of technetium-99 that exited the process facilities into the waste tank system is far more uncertain.

As discussed in detail in Section C.3.2.3, essentially all of the technetium-99 exited the bismuth phosphate plants in the metal waste stream, which also included almost all of the uranium. Metal wastes were segregated in specific tanks and later retrieved for uranium recovery. It is assumed the technetium not co-extracted with the uranium remained with the aqueous waste stream discharged from the U Plant (designated as uranium recovery waste) as the mobile anion, pertechnetate. Some 40 million gallons of uranium recovery waste were discharged to the BY cribs, a BX- and a TX-specific retention trench, and the BC cribs and specific retention trenches (Waite 1991). Essentially all of this uranium recovery waste passed through tanks within WMA B-BX-BY. The detection of cyanide in soil or water samples is a definite marker for uranium recovery waste because of the apparently environmentally stable ferrocyanide component of that waste stream. Although the waste transfer records do not identify uranium recovery waste as having been received by tanks B-110, BX-101, or BX-102, cyanide was found in the waste currently in tank B-110 and one of the soil samples from the BX-102 borehole contained trace amounts of cyanide.

Figure C.12. Technetium-99 Production Inventories by Major Reprocessing Campaign and Fuel Type

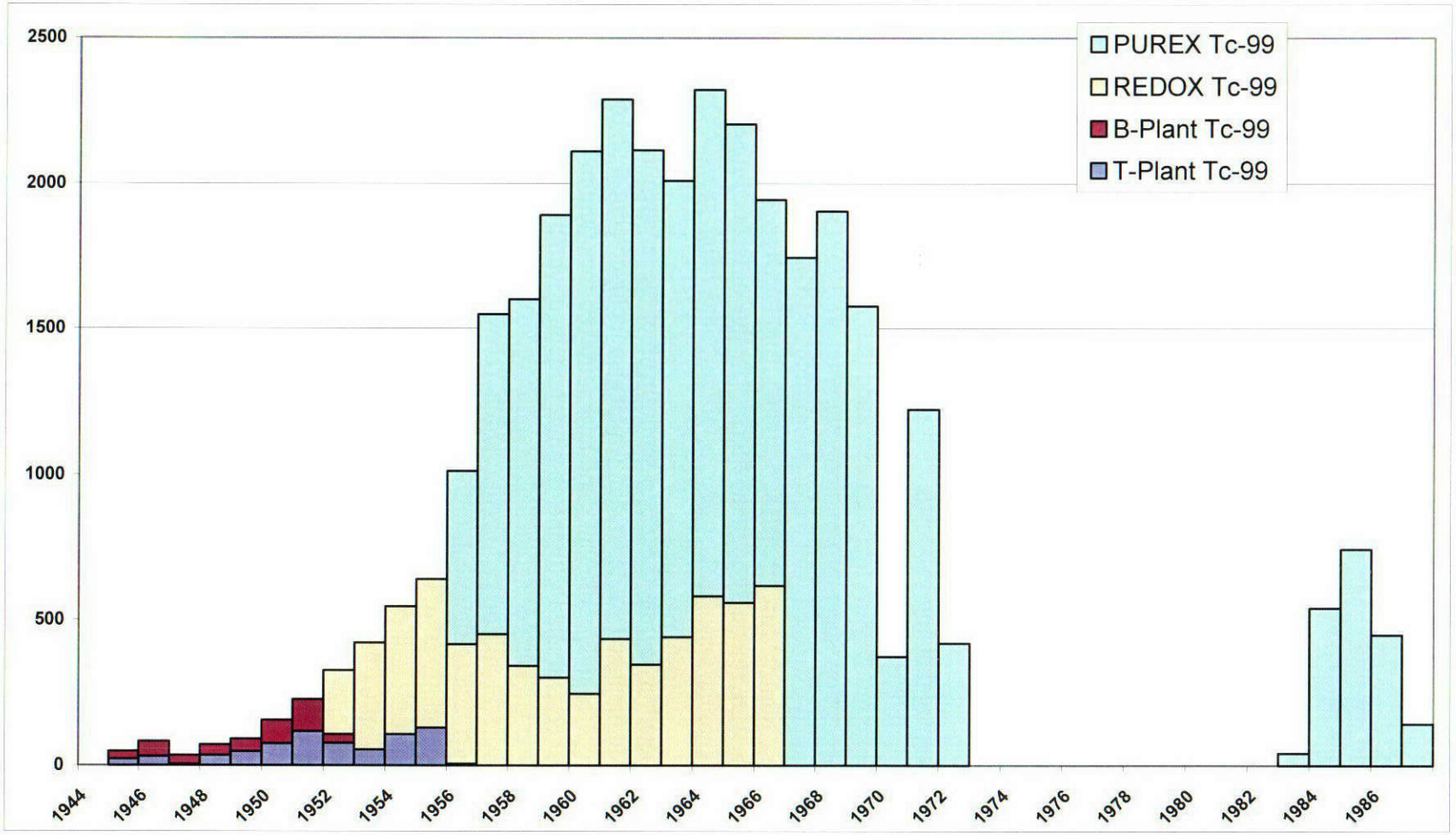

In both the REDOX and PUREX processes, technetium-99 followed other soluble fission products in the high-level waste stream that went to boiling waste tanks. In the late 1960s through the early 1970s, there was a serious attempt to find commercial markets for a number of fission products, including technetium-99. Inventories of the fission products in about 20 of the high-level waste tanks were determined and technetium recovery process methods were developed and partially implemented. It was known that the technetium-99 followed cesium-137 in the high-level waste streams. Technetium-99 recovery, based on an ion exchange process, was to have followed the cesium-137 recovery in ion exchange columns. Process records indicate that, at most, a few hundred Ci of technetium-99 were recovered during the isotope recovery program, an insignificant amount within the overall technetium inventory. However, it is important to note that the vast majority of the Hanford Site technetium-99 inventory passed through the B Plant in the late 1960s and early 1970s as part of the cesium-137 recovery program.

C.3.2.2 Technetium-99 Losses to the Vadose Zone

Historical process plant records and tank waste analysis data show that cesium recovery waste transferred from B Plant to WMA B-BX-BY tanks carried high levels of technetium-99. The current understanding of tank waste loss events around tanks BX-101 and BX-102 indicate that cesium recovery waste was a major component of the wastes passing through these tanks and presumably associated with late 1960s through early 1970s waste loss events. Thus, based on the current understanding, substantial amounts of technetium-99 were expected to be found in the vadose zone area east of tanks BX-101 and BX-102. However, as discussed in Section 3.0, the soils analysis data show far less technetium-99 than anticipated. There are a number of possible explanations as the discrepancies between estimates are based on process knowledge and the field observations.

B Plant process records and tank information for tanks BX-101 and BX-102 can be combined to suggest that tens of Ci of technetium-99 could have been lost to the environment. However, soil analysis data fail to support that hypothesis. One obvious explanation would be that technetium-99, as a mobile species, could have moved through the vadose zone to groundwater. However, the soil analysis data from trench B-38 strongly suggest that the mobile constituents (e.g., nitrate) discharged to this crib are currently located from about 50 to 150 ft below ground surface (bgs). Assuming that the geology and natural recharge are similar between these two facilities, it is difficult to accept the assumption that large quantities of technetium-99 could have been lost to the vadose zone and essentially all of it moved to the groundwater. However, as described in Section 5.0, it appears that "run-off" water may have been channeled into the contaminated soil column near tanks BX-101 and BX-102 over the last 20 years. In the early 1980s, a waste transfer line was placed on the surface between the B and BX tank farms (Williams 1999). Soil was mounded on top of the line for shielding creating a dam that subsequently ponded run-on water. It is likely that this ponded water drained into the contaminated soil east of tanks BX-101 and BX-102. Thus, it is possible that contaminated vadose zone soils east of tanks BX-101 and BX-102 were periodically flushed with sufficient water to have moved mobile contaminants to groundwater.

Since both the B Plant operations documentation and waste transfer records appear to be reliable, another possibility is that the technetium-99 may not have remained in the aqueous phase after

exiting the B Plant. Recently published results (Shuh et al. 2000) demonstrate that technetium(VII) can be reduced in a gamma field in the presence of certain organic compounds. Working with reasonably simple aqueous solutions, it was shown that gamma ray interactions with water molecules lead to the production of free radicals, some strongly oxidizing, and an equivalent amount strongly reducing. Shuh et al. (2000) reported that if organic reductants were present, the reductants would scavenge some of the strong oxidant free radicals leading to a situation where technetium(VII) would be reduced to technetium(IV). The technetium(IV) may or may not stay in solution depending on whether or not complexants were present. The cesium-137 recovery waste exiting B Plant was far more complex than the systems examined by Shuh et al. (2000) but the wastes did contain gamma emitting radionuclides and organic compounds that were similar or identical with the compounds studied by Shuh et al. (2000). To address this possibility, tank waste sludge samples from tank BX-101 were retrieved from archive and are being analyzed.

C.3.2.3 Tracking Technetium-99 Through the Bismuth Phosphate Process

The first plutonium recovery process implemented at Hanford was based on the co-precipitation of plutonium (IV) with bismuth phosphate. The plutonium product was decontaminated by a series of oxidation state changes and precipitation steps (Anderson 1990; Agnew 1997). Three major waste streams were produced that contained essentially all of the fission products. These are referred to as metal waste, first cycle waste, and second cycle waste. Frequently, an assumption is made that 90% of the fission products went with the metal waste, 9% with the first cycle waste, and 1% with the second cycle waste (Anderson 1990; Agnew 1997; Kupfer et al. 1999; Simpson et al. 2001; DOE-RL 2000). This assumption has been widely applied to Hanford waste management projects including the best-basis inventory data and Hanford defined model used to estimate current contents in Hanford waste tanks, and to the inventories of radionuclides discharged to cribs and trenches (Simpson et al. 2001). The fact that the soil analysis data from the B-38 crib show virtually no technetium-99 in the soil column but significant levels of nitrate suggests that the first cycle wastes discharged to this trench contained almost no technetium-99. This task was undertaken to resolve the question of how much technetium-99 should be expected in the first cycle waste stream.

The first step was to review the bismuth phosphate process technical manual (GE 1944). This manual states that approximately 90% of the total beta activity went with the metal waste, not 90% of the fission products. It further states the total beta activity remaining with the bismuth phosphate/plutonium precipitate (and thus going on to produce the first cycle waste stream) was primarily zirconium/niobium-95. Thus, a review of the technical manual clearly indicates the long held assumption about the split of fission products among the bismuth phosphate process waste streams is incorrect.

To provide conclusive evidence about the fate of technetium-99 in the initial plutonium separation step in the bismuth phosphate process, a laboratory experiment was designed to recreate the process flowsheet chemistry and follow technetium as well as other isotopes through the redox and precipitation steps. The results of these experiments will be reported separately, however, the laboratory results did demonstrate that 99+% of the technetium followed the metal waste stream. Thus, the first cycle waste discharged to the B-38 crib contained very little technetium-99, as indicated by the soil analysis data. Since 7 of the 8 specific retention trenches

in the BX trenches received first cycles wastes, it is appropriate to reduce the technetium-99 inventory estimates for discharges of first cycle wastes. Based on results of the laboratory work, the overall technetium-99 inventory estimate is reduced from 14.7 Ci to 1.5 Ci for the first cycle wastes discharged to the BX trenches.

C.3.3 GEOSTATISTICAL ANALYSIS OF SPECTRAL GAMMA LOGGING DATA FROM B, BX, AND BY TANK FARMS (KRIGING ANALYSIS)

The objective of the geostatistical analyses of existing spectral gamma logging data from drywells in the B, BX, and BY tank farms is to create estimates of the volumes of contaminated soils and their associated levels of gamma-emitting radionuclides. This geostatistical technique is referred to as kriging analysis. The kriging analysis results of spectral gamma logging data are potentially useful in establishing tank leak inventory estimates (Knepp 2002). This task involved two major efforts: one was to establish the zones where there was sufficient data density to support the mathematical analysis and the second component was the application of the geostatistical technique to the data sets of interest. The spectral gamma logging data provide the most current assessment of vadose zone contamination in the three SST farms of interest (DOE-GJPO 1997, 1998, 2000a through d) and are discussed in Section 2.0.

The kriging analysis was performed in four tasks, as shown in Table C.6: preliminary evaluation, spatial trend analysis, interpolation, and inventory estimation. During the preliminary evaluation, the raw data was analyzed to determine continuity and data density. This task identifies the regions where there is sufficient data density to support the geostatistical analysis. Gamma-emitting radionuclides included in the preliminary evaluation included cobalt-60, cesium-137, europium-152, europium-154, antimony-125, uranium-238, and uranium-235. No radionuclides passed the initial screening in the region of interest around tank B-110. However, in the region east of tanks BX-101 and BX-102, the radionuclides passing the initial screening process included cobalt-60, antimony-125, and the uranium isotopes 238 and 235. Because neither cobalt-60 nor antimony-125 could be adequately quantified in the waste streams passing through these two tanks, the gamma data from the processed uranium plume (e.g., uranium-238) found in the region east of tanks BX-101 and BX-102 was selected for additional analyses. Processed uranium was identified by daughter products which have grown in since the uranium exited the chemical processing facility.

The second step in the kriging task was to perform a spatial trend analysis. In this task, the spatial statistical trends or structure of the sampled data were described. The parameters that describe the spatial trends are used during the interpolation task. During the interpolation task, ordinary and trend kriging were used to interpolate process uranium point and confidence estimates for regions below and around the waste storage tanks.

Table C.6. Task Summary

Task	Preliminary Analysis	Spatial Trend Analysis	Interpolation	Inventory Estimation
Activity	Analysis of: • Data continuity • Data normality • Data density • Other physical processes	Correlation determination: • Vertical • Horizontal Anisotropy search	Use method of kriging to make process uranium activity estimates	Integration of the estimated process uranium activity field
Result	Site conceptual model Data transform Data compression or filter	Variogram parameters: • Variogram model • Range (X, Y, Z) • Sill • Nugget	Process uranium and variance of error estimates for all locations around and below tanks	Estimation of: • Gross process uranium activity levels • Contaminated soil volume

The final task was to use process uranium estimates to generate inventory and activity level estimates for the processed uranium plume east of tanks BX-101 and BX-102. After the contaminant distribution was estimated using the sample data and geostatistics, the volumes and activity levels were calculated. The bulk activities and associated volumes are summarized in Table C.7 by activity level. The projected three-dimensional images of the contaminated soil are shown in Figures C.13 through C.18.

Table C.7. Uranium Activities and Volumes by Activity Level

Cutoff Threshold	1 pCi/g	5 pCi/g	10 pCi/g	25 pCi/g	50 pCi/g	100 pCi/g	500 pCi/g
Volume (m^3)	8390.8	5764.0	4459.4	2703.1	1326.3	479.1	3.4
Activities (pCi)	4.15E+11	4.03E+11	3.86E+11	3.34E+11	2.45E+11	1.40E+11	3.54E+09

The method of ordinary kriging is used to make estimates of contaminant concentration values at locations where there are no samples within the conceptual model domain. It should be noted that the actual sample values are used and respected during the interpolation process. To estimate the volume and concentration of contaminated soil, a geostatistical approach is used. The approach incorporates a conceptual model using the geophysical data and the statistical or trend information (derived from the geophysical data). The conceptual model is comprised of a three-dimensional grid that represents the tanks and volume of soil around the tanks.

Figure C.13. Processed Uranium Greater than 1 pCi/g

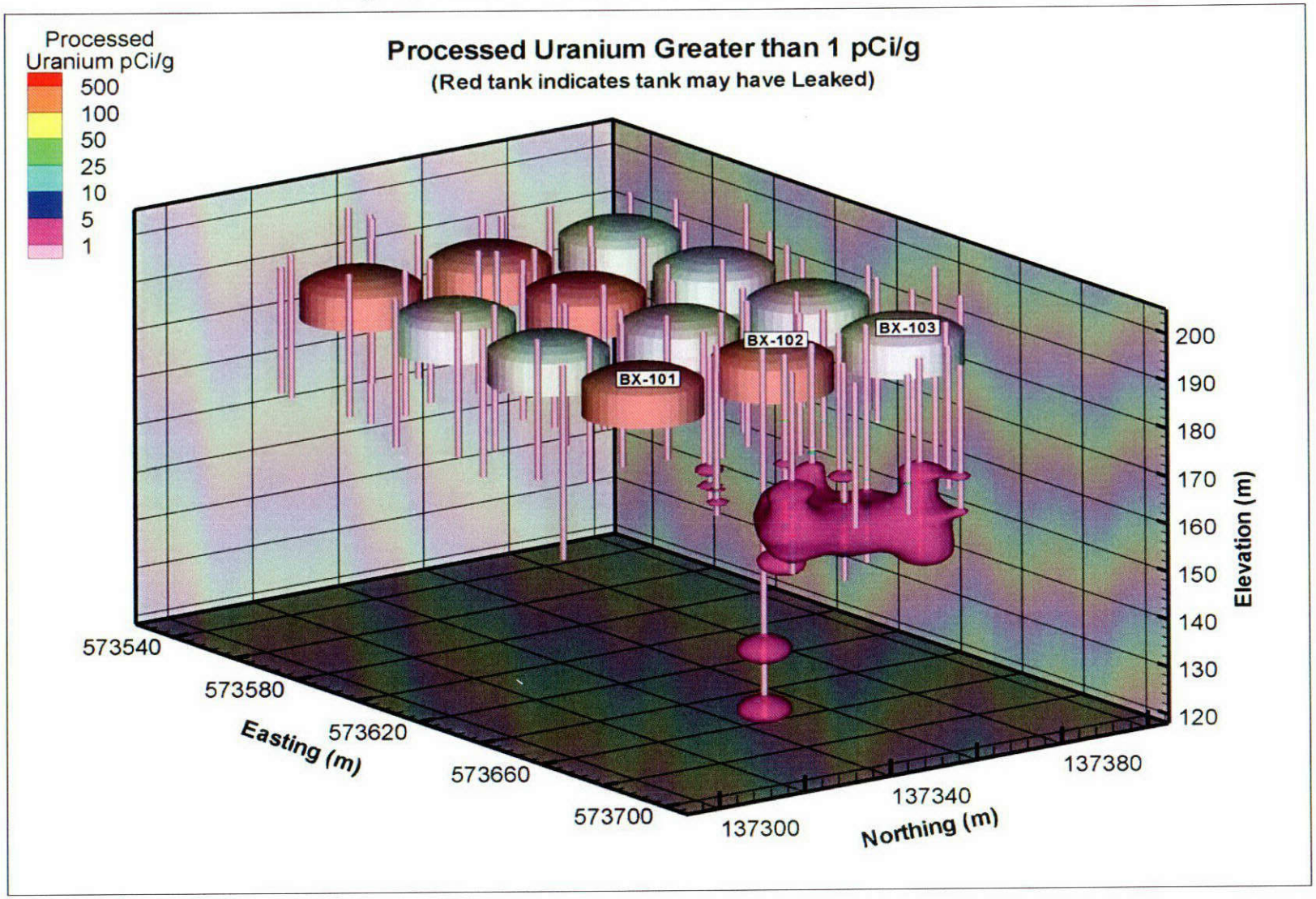

Krigged uranium-238 plumes indicating contamination below 120 feet in drywell 21-02-04 are based on somewhat less reliable uranium-238 spectral gamma logging data. These data are less reliable because of interferences from the high levels of cesium-137 in the soil.

Figure C.14. Processed Uranium Greater than 5 pCi/g

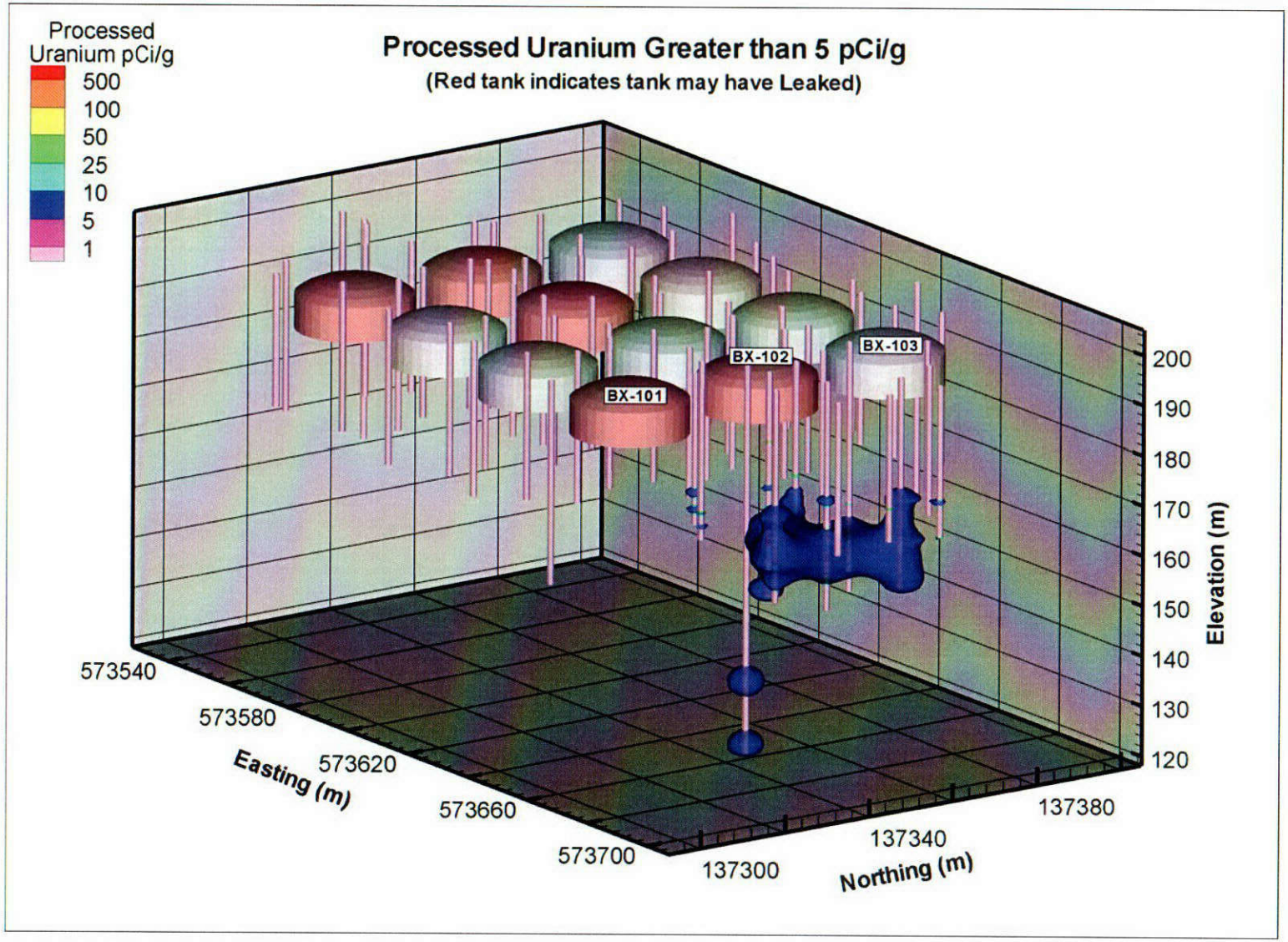

Krigged uranium-238 plumes indicating contamination below 120 feet in drywell 21-02-04 are based on somewhat less reliable uranium-238 spectral gamma logging data. These data are less reliable because of interferences from the high levels of cesium-137 in the soil.

Figure C.15. Processed Uranium Greater than 10 pCi/g

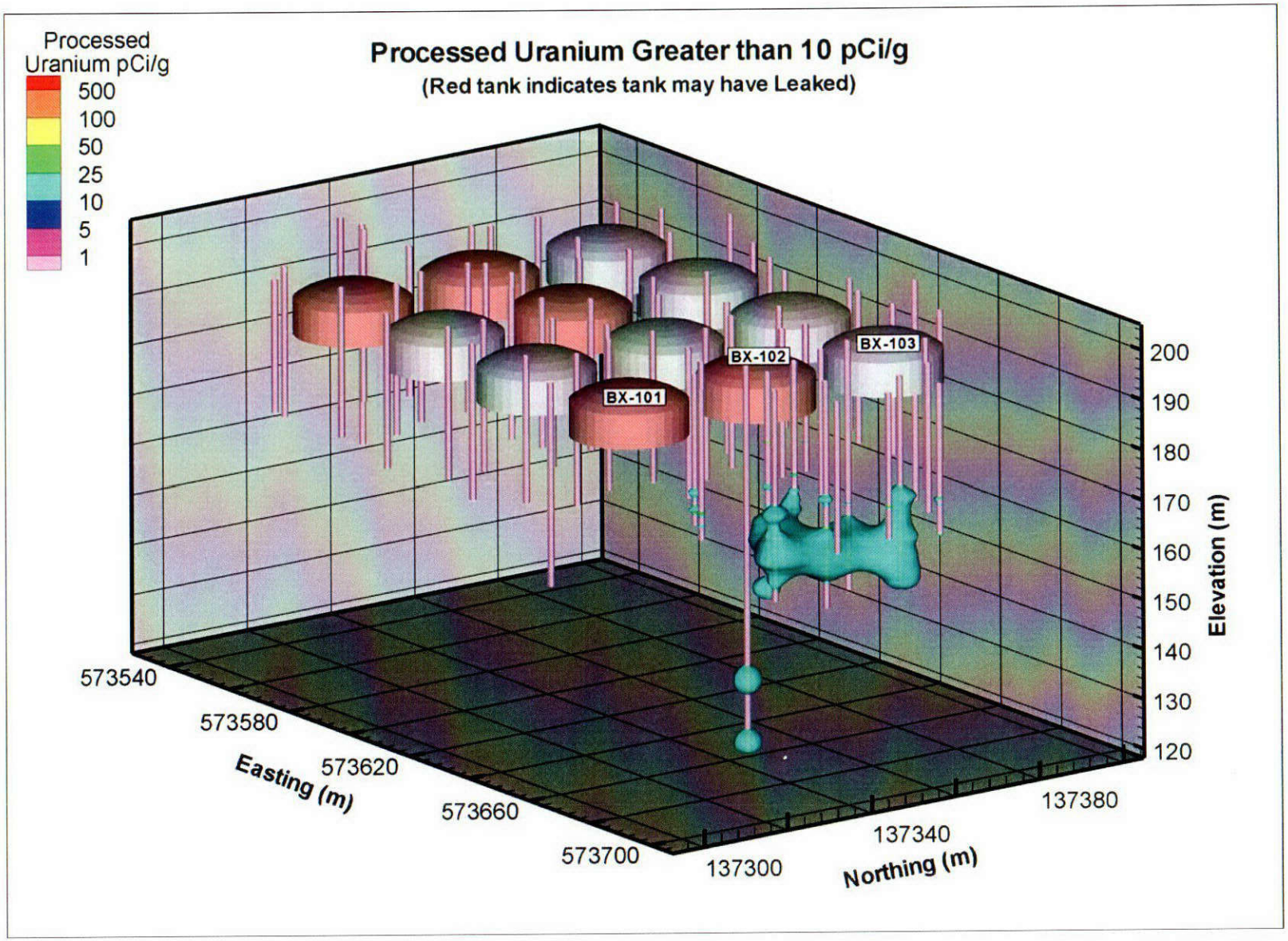

Krigged uranium-238 plumes indicating contamination below 120 feet in drywell 21-02-04 are based on somewhat less reliable uranium-238 spectral gamma logging data. These data are less reliable because of interferences from the high levels of cesium-137 in the soil.

Figure C.16. Processed Uranium Greater than 25 pCi/g

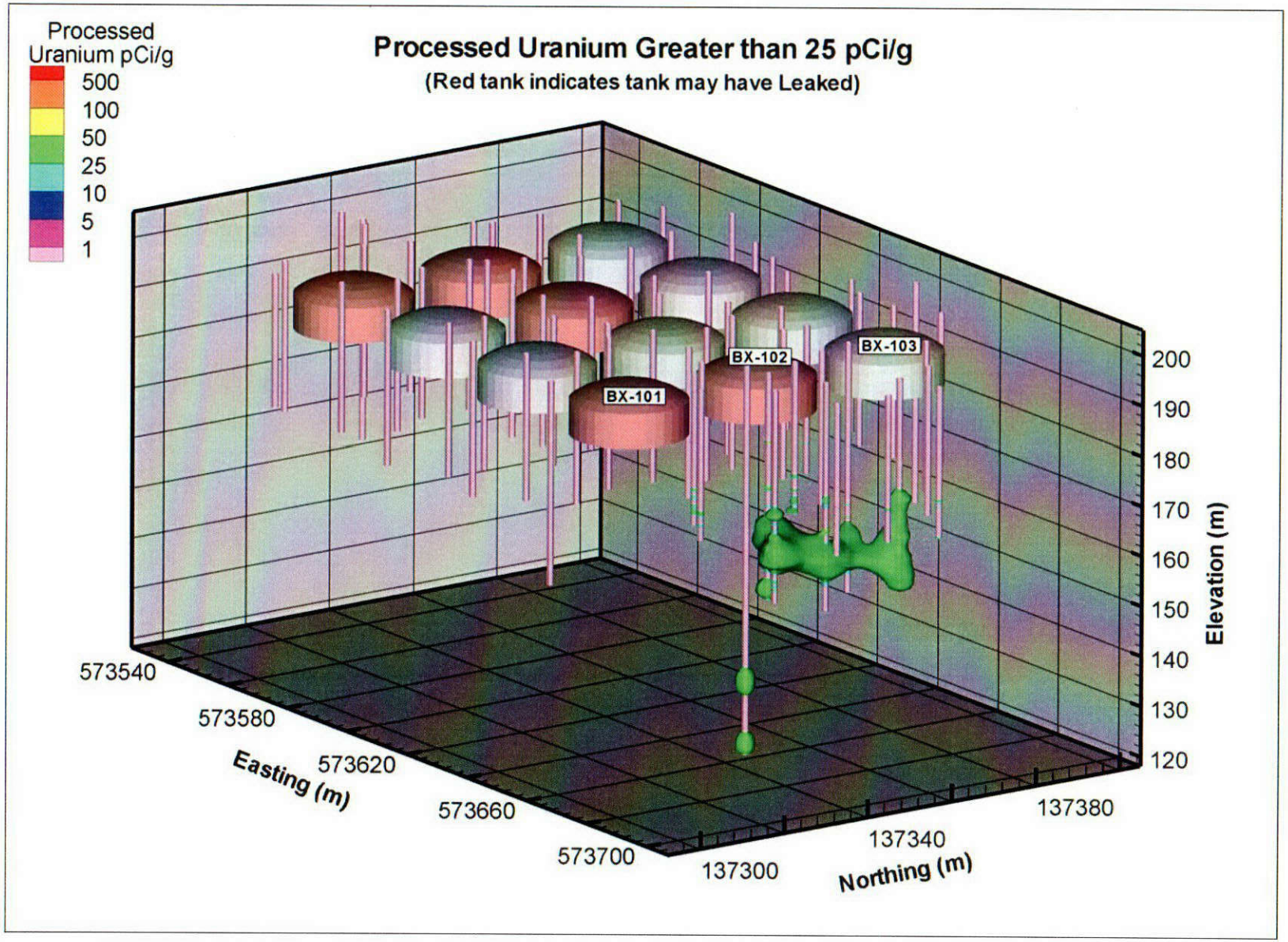

Krigged uranium-238 plumes indicating contamination below 120 feet in drywell 21-02-04 are based on somewhat less reliable uranium-238 spectral gamma logging data. These data are less reliable because of interferences from the high levels of cesium-137 in the soil.

Figure C.17. Processed Uranium Greater than 50 pCi/g

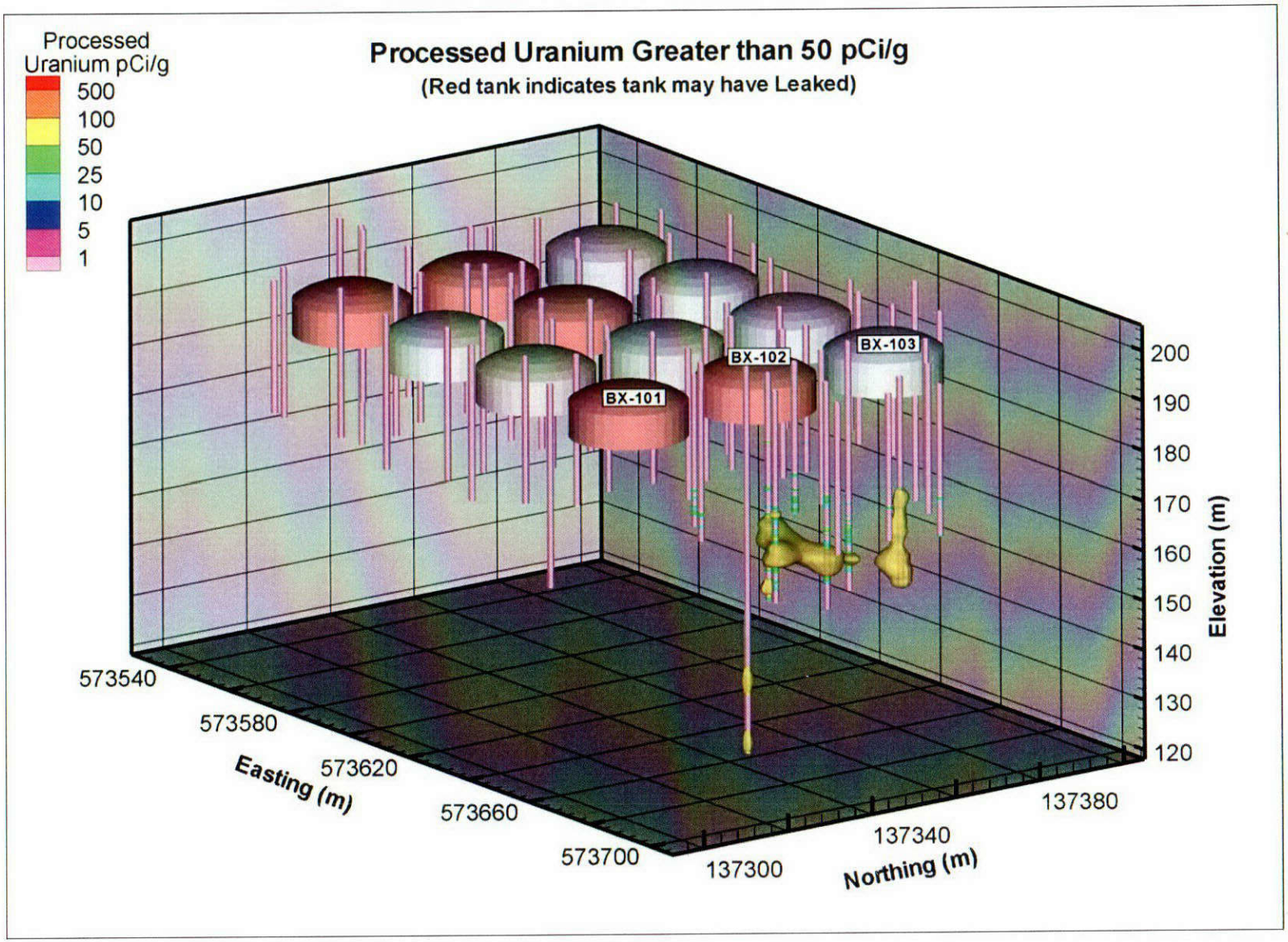

Krigged uranium-238 plumes indicating contamination below 120 feet in drywell 21-02-04 are based on somewhat less reliable uranium-238 spectral gamma logging data. These data are less reliable because of interferences from the high levels of cesium-137 in the soil.

Figure C.18. Processed Uranium Greater than 100 pCi/g

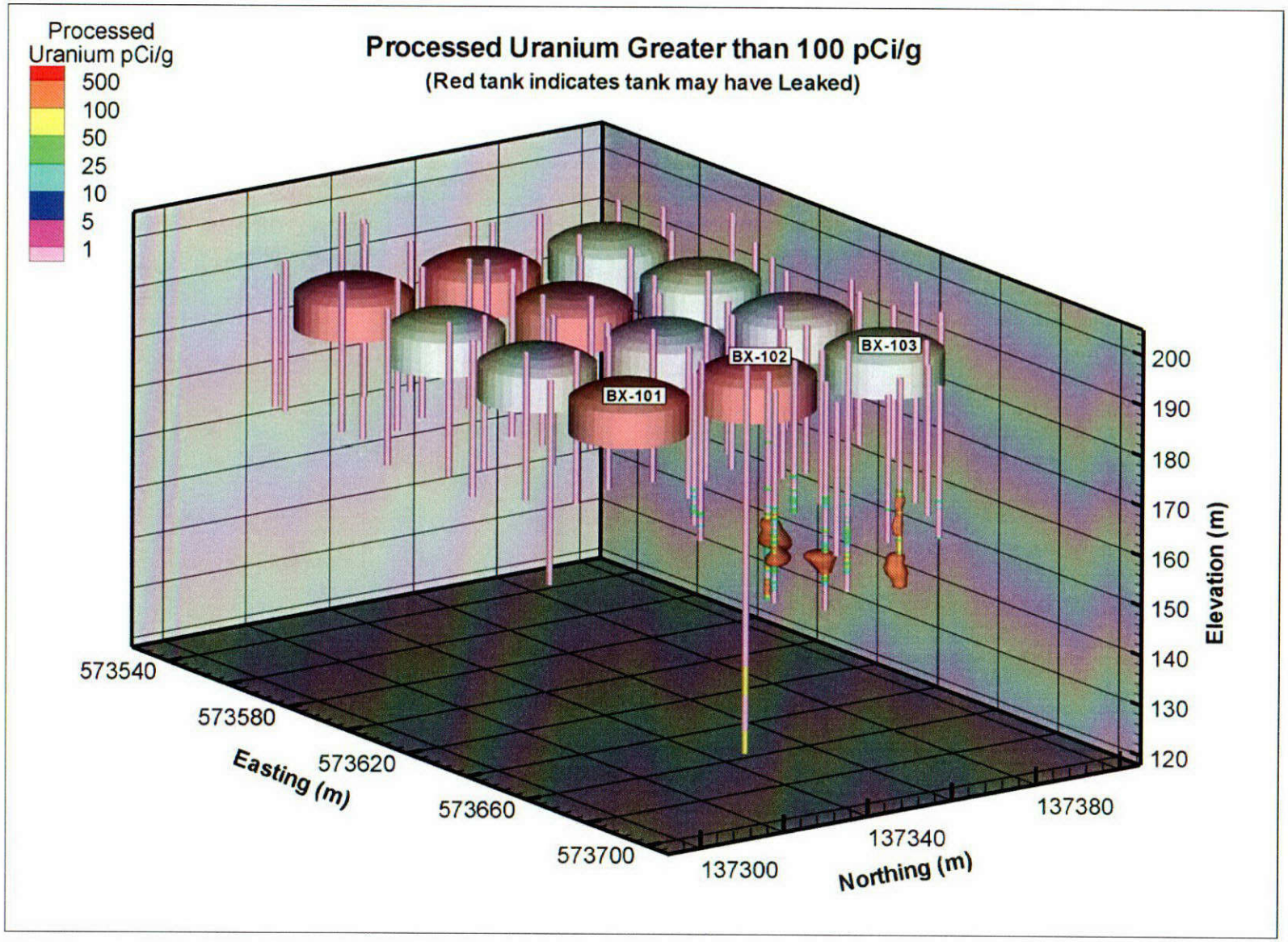

Krigged uranium-238 plumes indicating contamination below 120 feet in drywell 21-02-04 are based on somewhat less reliable uranium-238 spectral gamma logging data. These data are less reliable because of interferences from the high levels of cesium-137 in the soil

C.4.0 GEOLOGY

Wells 299-E33-337 and 299-E33-339 were drilled using a combination of cable-tool percussion and air-rotary methods. Cable-tool methods were used for well 299-E33-338. Samples were collected via splitspoon in a near continuous manner through the vadose zone. The wells were extended to or into the top of basalt to better define the surface of that geologic horizon.

The geology (Section 3.1.1) present in these wells is generally consistent with that described for the characterization boreholes 299-E33-45 (Section B.4.1) and 299-E33-46 (Section B.5.1).

that the lower depths contain coarse materials, so sample handling (e.g., drying) may be responsible for the apparent drier matric potentials.

For the B-110 borehole (299-E33-46), results are similar to those from the BX-102 borehole (299-E33-45). There are few erratic spikes and the matric potential generally stays much wetter than the gravity potential. As with the B-102 borehole, there is an apparent drying near the water table. As with the B-102 borehole, the soils at the greatest depths are coarse sands and gravels, and as a result may have been impacted by sample handling. Both the B-110 borehole and BX-102 borehole matric potential profiles strongly suggest that drainage is occurring.

For borehole 299-E33-338, located on the southeast corner of the B tank farm, the samples are considerably drier than for the two other boreholes (299-E33-45 and 299-E33-46), particularly near the surface. These data are consistent with the hypothesis that non-vegetated areas, with coarse-textured surfaces, drain more than areas with similar soil, but with vegetation present. It appears that the wetting from meteoric sources has not reached the water table at this site.

that the lower depths contain coarse materials, so sample handling (e.g., drying) may be responsible for the apparent drier matric potentials.

For the B-110 borehole (299-E33-46), results are similar to those from the BX-102 borehole (299-E33-45). There are few erratic spikes and the matric potential generally stays much wetter than the gravity potential. As with the B-102 borehole, there is an apparent drying near the water table. As with the B-102 borehole, the soils at the greatest depths are coarse sands and gravels, and as a result may have been impacted by sample handling. Both the B-110 borehole and BX-102 borehole matric potential profiles strongly suggest that drainage is occurring.

For borehole 299-E33-338, located on the southeast corner of the B tank farm, the samples are considerably drier than for the two other boreholes (299-E33-45 and 299-E33-46), particularly near the surface. These data are consistent with the hypothesis that non-vegetated areas, with coarse-textured surfaces, drain more than areas with similar soil, but with vegetation present. It appears that the wetting from meteoric sources has not reached the water table at this site.

Figure C.19. Matric Water Potential Measured by Filter Paper Technique on Core Samples from Borehole 299-E33-45 Located Near Tank BX-102 in the BX Tank Farm

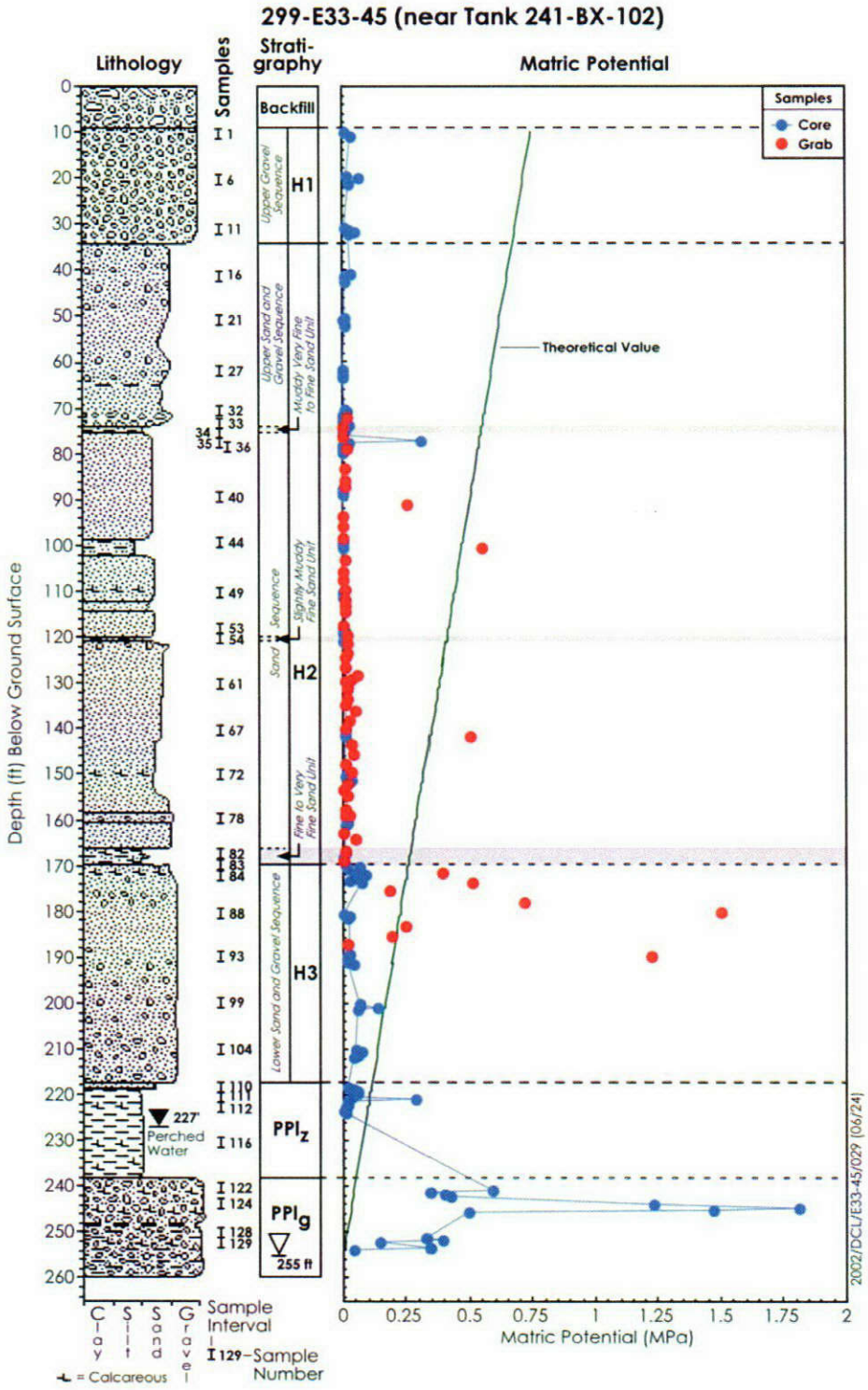

Figure C.20. Matric Water Potential Measured by Filter Paper Technique on Core Samples from Borehole 299-E33-46 Located Near Tank B-110 in the B Tank Farm

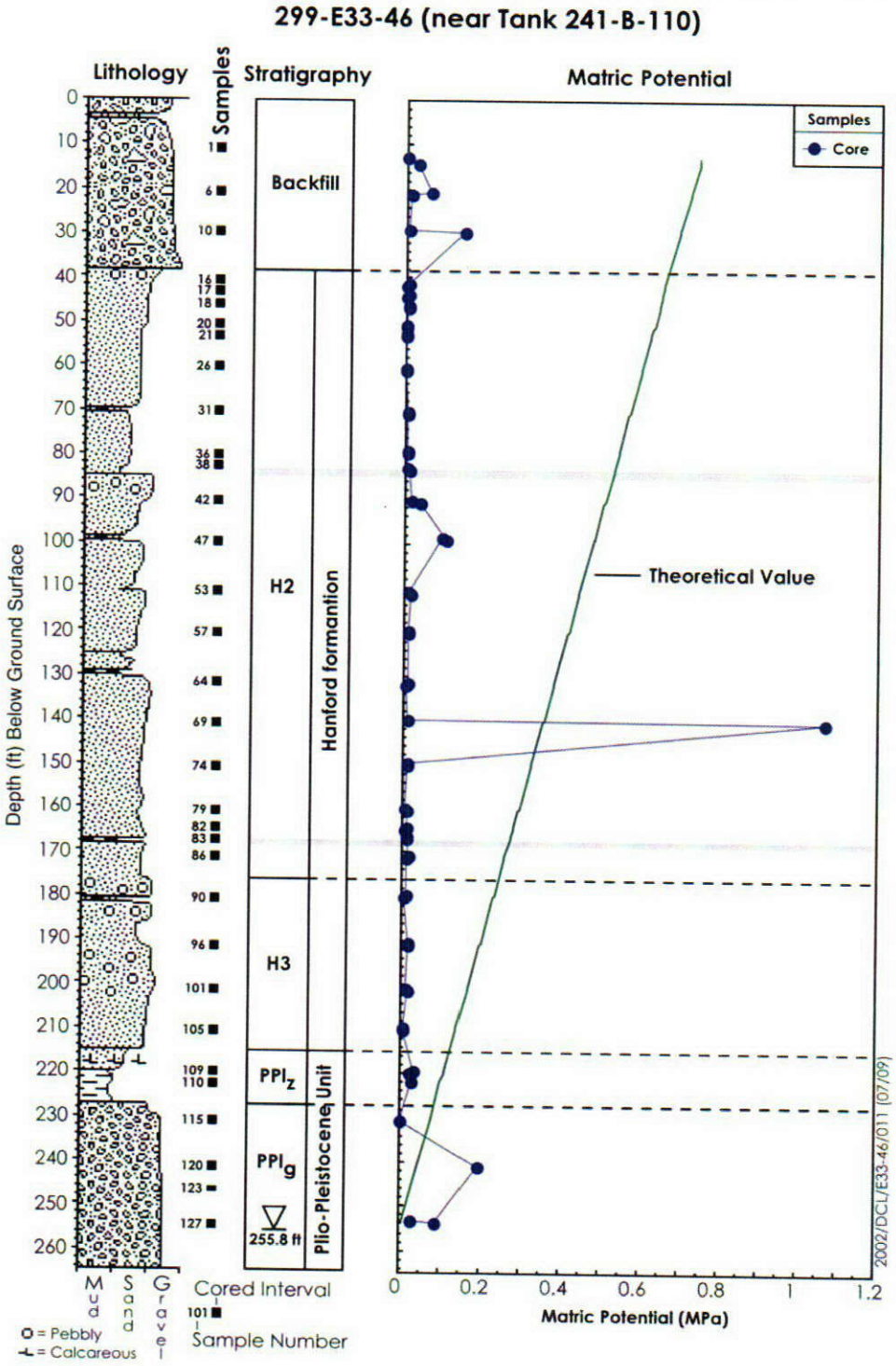

Figure C.21. Matric Water Potential Measured by Filter Paper Technique on Core Samples from Borehole 299-E33-338 Located to the Southeast near the Perimeter of the B Tank Farm

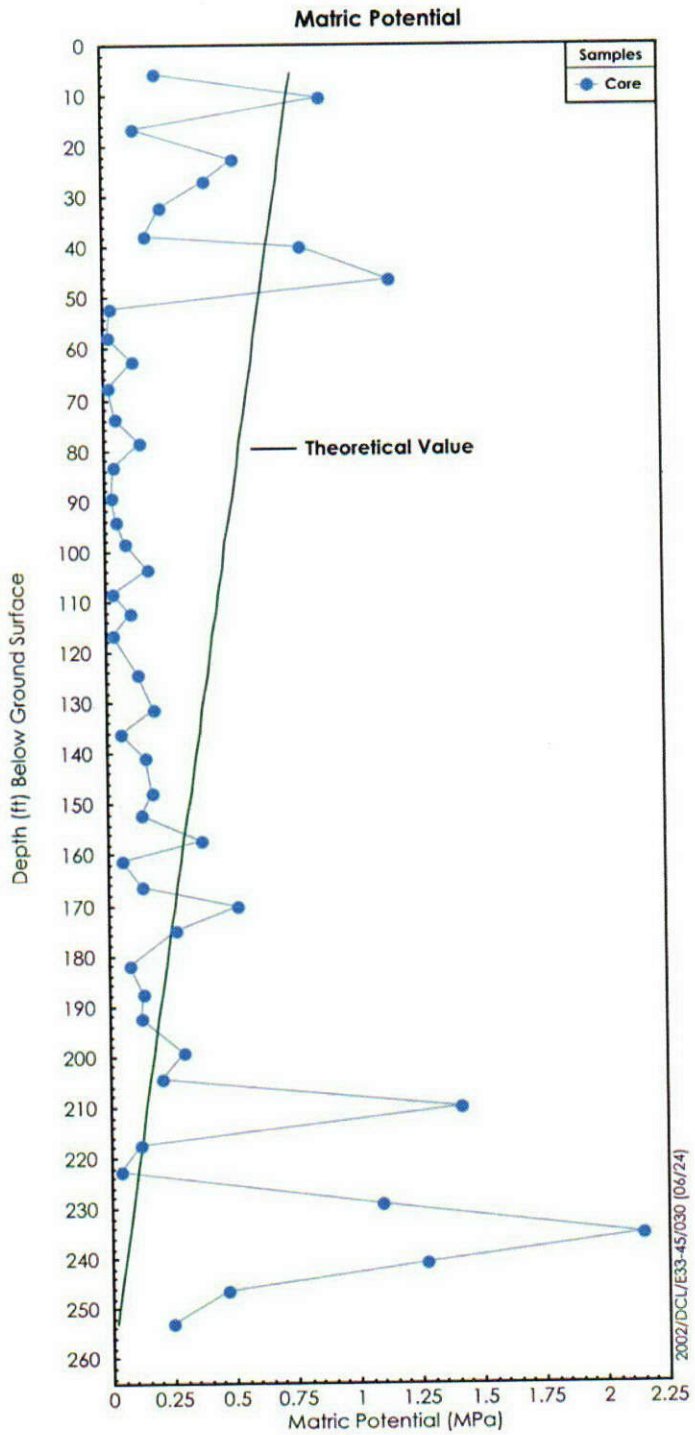

C.5.3 VADOSE ZONE INSTRUMENTATION

A series of instruments was placed in the B tank farm in July and August 2001 and installed near tank B-110. The Vadose Zone Monitoring System consists of eight sets of sensors placed at depths ranging from 0.9 m (3 ft) to 68.9 m (226 ft) bgs. Duratek Federal Services drilled the borehole, under the direction of CH2M HILL Hanford Group, Inc. (CH2M HILL), for chemical and hydrologic characterization as part of the SST Phase 1 RFI/CMS[1] characterization effort (Rogers and Knepp 2000). The sensors are used for continuous monitoring of vadose zone hydraulic properties at and beneath the surface of the tank farm. The VZMS sensor arrays consisted of advanced tensiometers, water content sensors, heat dissipation units, solution samplers, temperature sensors, and a water flux meter. Figure C.22 shows the configuration of the sensor nest before insertion into the B tank farm. Gee et al. (2001) provides details of the installation and description of each instrument.

Figure C.22. Vadose-Zone Monitoring System Before Deployment in B Tank Farm

(Without Water Flux Meter and Temperature Sensor)

Sensors from left to right are the Modified CSI Water Content Sensor, Advanced Tensiometer, Solution Sampler, and Heat Dissipation Unit.

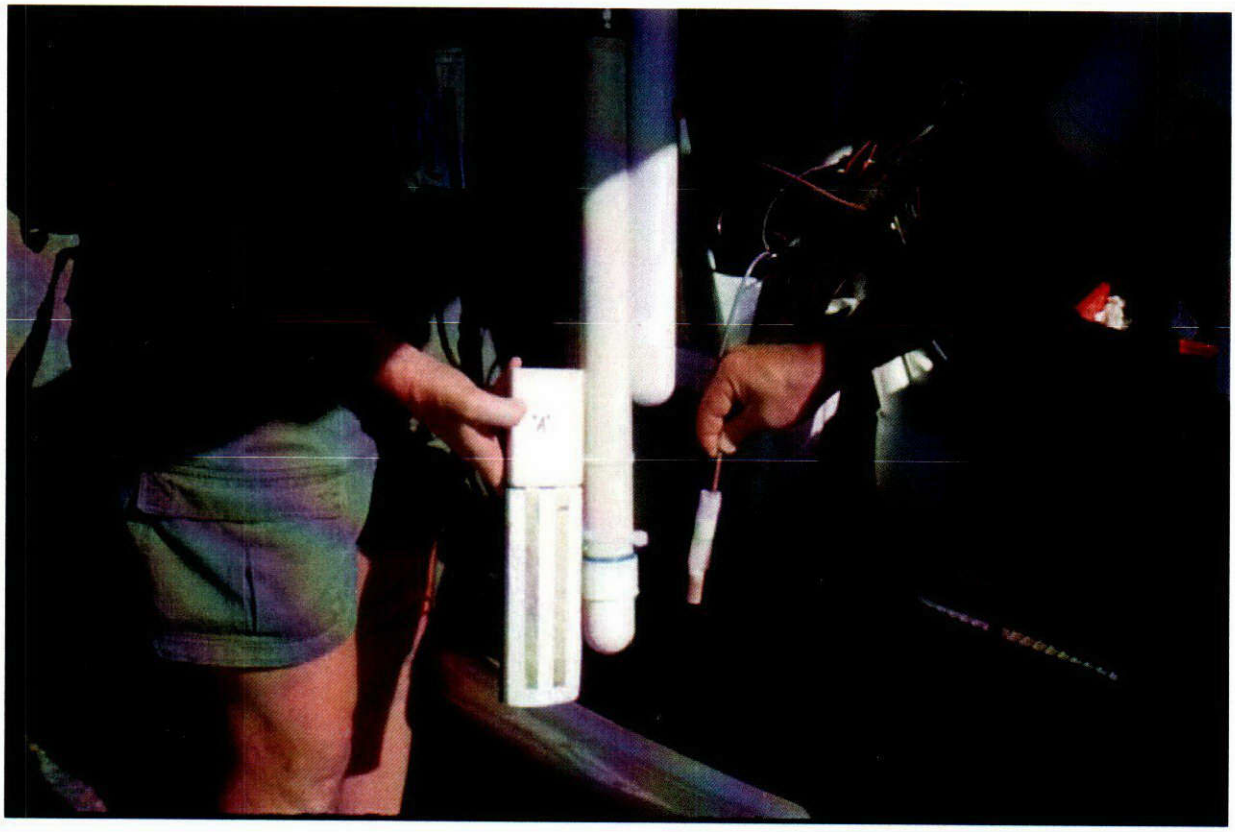

[1] RFI = remedial feasibility investigation; CMS = corrective measures study

C.5.4 ADVANCED TENSIOMETERS

Tensiometers (water filled porous cups attached to a pressure transducer) are used to directly measure matric water potential in the subsurface in the operational range from 0 to -0.07 MPa (0 to -700 mbar). Tensiometers can also be used to measure positive pressures in soils that are saturated and thus act as piezometers for monitoring perched water bodies or water table elevations. Advanced tensiometers (ATs) (Sisson and Hubbell 1999) incorporate the pressure transducer directly into the porous cup to minimize the length of the water column that hydraulically connects the pressure transducer to the cup. By minimizing the water column length, the tensiometer performance is enhanced by eliminating or minimizing several problems encountered in conventional tensiometers, i.e., excessive thermal noise, sluggish response, and limited depth placement (Hubbell and Sisson 1996, 1998; Sisson and Hubbell 1999). Placement of the pressure transducer, porous cup, and the water column at depths where diurnal temperature fluctuations are dampened minimizes the problem of thermally affected fluid movement into and out of the tensiometer. In addition to reducing the noise level from temperature fluctuations, the length of time between refilling the tensiometer was extended from once per week to once per year or longer, depending on the depth of placement and the in situ capillary pressures. The short length of the sealed portion of the AT makes it possible to place it at almost any depth (Figure C.23).

Technical issues with respect to durability of sensors, data acquisition systems, and reliability of data have largely been resolved. Typically, sensors have been easily installed under conditions where monitoring points have been relatively easy to access. The major technical issue for the Hanford Site relates to deployment into contaminated sites and in deep vadose zone materials (i.e., deeper than 15 m [50 ft]). Where open boreholes are available, these units can be installed in a semi-permanent installation.

Figure C.23. Schematic of Advanced Tensiometers Showing the Porous Cup and Pressure Transducer System for a Typical Deployment

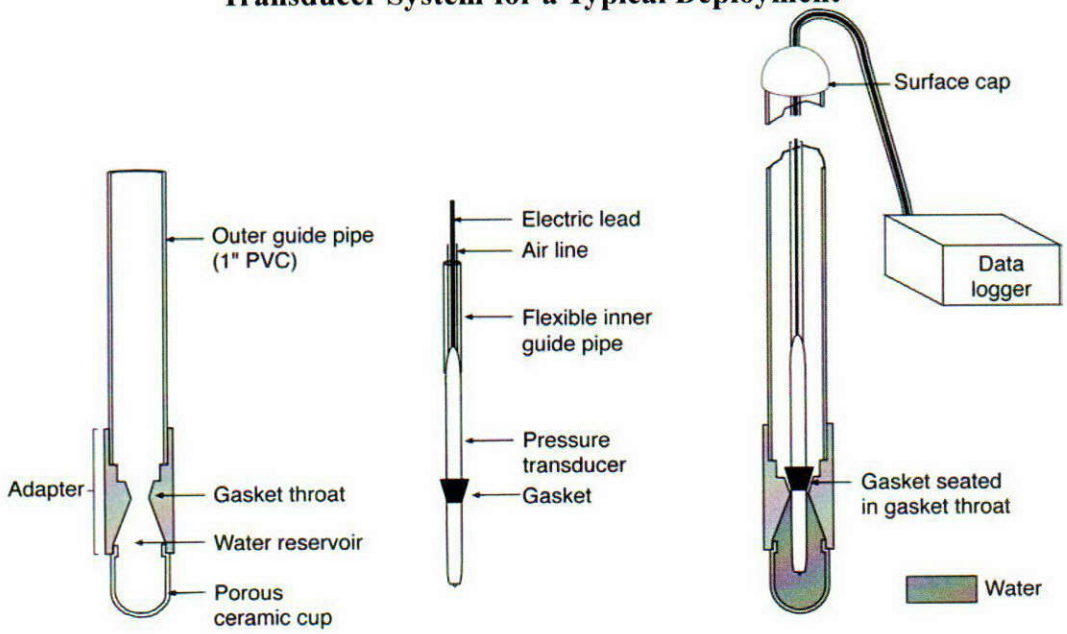

The design for the Hanford Site tank farms was modified from a series of observations suggesting that for the most part, matric potentials in Hanford sediments are within the range of 0 to -0.01 MPa (0 to -100 mbar). Based on these anticipated pressures, the water losses from the cups should be very low. Therefore, the life of the units can be extended almost indefinitely in the wet-draining sandy sediments by optimizing the volume of water in the tensiometer. Such sediments are present in abundance in the subsurface at most Hanford waste sites. The high anticipated water potential and limited access to the site for refilling the instrument combined to make this design more applicable than the standard configuration for this particular site. Based on these observations, the tensiometer was constructed so that it could be filled and sealed in place. The basic AT design was slightly modified to remove the outer and inner guide pipe that normally extends to the land surface and enlarges the water reservoir. The pressure transducers used in the tensiometer are a type that can over-range beyond the typical pressure limit of 15 psi. The pressure sensor is placed adjacent to the measurement location so that no further manipulation of pressure data is required. The pressure range of the sensor will allow the detection of perched water if the sediments become saturated. Sensor placement depths are shown in Table C.8.

Table C.8. Vadose Zone Monitoring System Sensor Placement in Borehole 299-E33-46 near Tank B-110 in B Tank Farm

Depth (bgs)	Water Flux Meter	Advanced Tensiometer	Heat Dissipation Unit	Water Content Sensor	Temperature	Solution Sampler
226		X	X	X	X	X
218		X		X	X	X
82		X	X	X	X	X
53		X		X	X	X
15		X	X	X	X	X
9		X		X	X	X
6	X	X	X	X	X	X
3		X		X	X	X

Tests are ongoing with the instrumented site. Preliminary data indicate that the soil water has not equilibrated chemically with the porewaters in the formation. Data were collected from the water flux meter beginning in early March 2002 so annual flux rates are not yet available. However, the data suggest that net infiltration (drainage) is occurring at the B-110 borehole.

Pressures have not yet equilibrated, but the tensiometers appear to be reasonably stable in time, with all water potentials wetter than -100 mbar, indicating nearly steady state drainage conditions. These data support the observations from the water flux meter and the soil cores, i.e., that unit gradient conditions exist at the B tank farm and thus, drainage is occurring. As more data are collected, they will be analyzed in terms of the observed water potentials and the measured water flux based on water flux meter.

C.6.0 GROUNDWATER CONTAMINATION

C.6.1 INTRODUCTION

This section summarizes historical as well as recent groundwater data related to the nature and extent of contamination in the uppermost aquifer in the vicinity of WMA B-BX-BY. The primary focus is on relating ambient groundwater contamination to releases from waste storage and disposal facilities within or associated with the WMA. Accordingly, historical water levels, wastewater discharges, inferred flow directions, and contaminant history in key wells near the WMA were reviewed as background for understanding current groundwater contaminant distribution patterns and their relationship to possible waste management area sources.

C.6.2 WASTEWATER DISCHARGE HISTORY

Discharge of large volumes of cooling water to the B-Pond system and Gable Mountain Pond account for most of the liquid waste volume discharged to the ground in the 200 East Area. Numerous crib discharges over the operating history were secondary sources that influenced water table elevations locally at the discharge sites. However, the major control on water levels and flow direction and rate was the balance between cooling water discharged to either B Pond or Gable Mountain Pond. The locations of these two major discharge facilities with respect to WMA B-BX-BY and the relative discharge volumes to each facility created groundwater mounds that competed with each other in controlling the movement of groundwater in the vicinity of the WMA.

C.6.2.1 Discharge Volumes

The annual discharge volumes to B Pond and Gable Mountain Pond from 1945 through 1995 are compared in Figure C.24. The top panel provides a bar graph of the annual volumes to each facility separately and as a total (maximum height of each bar). The center panel provides a percentage of the total that was discharged to Gable Mountain Pond and the bottom panel shows the ratio of discharge volumes to the two facilities.

As illustrated in Figure C. 24, from 1945 to about 1956, cooling water was discharged to only B Pond. Beginning in 1957, discharge to Gable Mountain Pond increased rapidly and overshadowed input to B Pond. The relative volume of water discharged to these two facilities is dramatically illustrated in the bottom panel of Figure C. 24. This plot demonstrates the dominating influence of Gable Mountain Pond from 1958 to 1972. Annual discharge volumes to Gable Mountain Pond relative to B Pond were less dramatic after 1972 until closure of Gable Mountain Pond in 1985. The impact of the changes in discharge volumes to the two facilities on water level and flow direction near WMA B-BX-BY are discussed in the following sections.

Figure C.24. Discharge History for Gable Mountain Pond and the B Pond System from 1945 to 1995

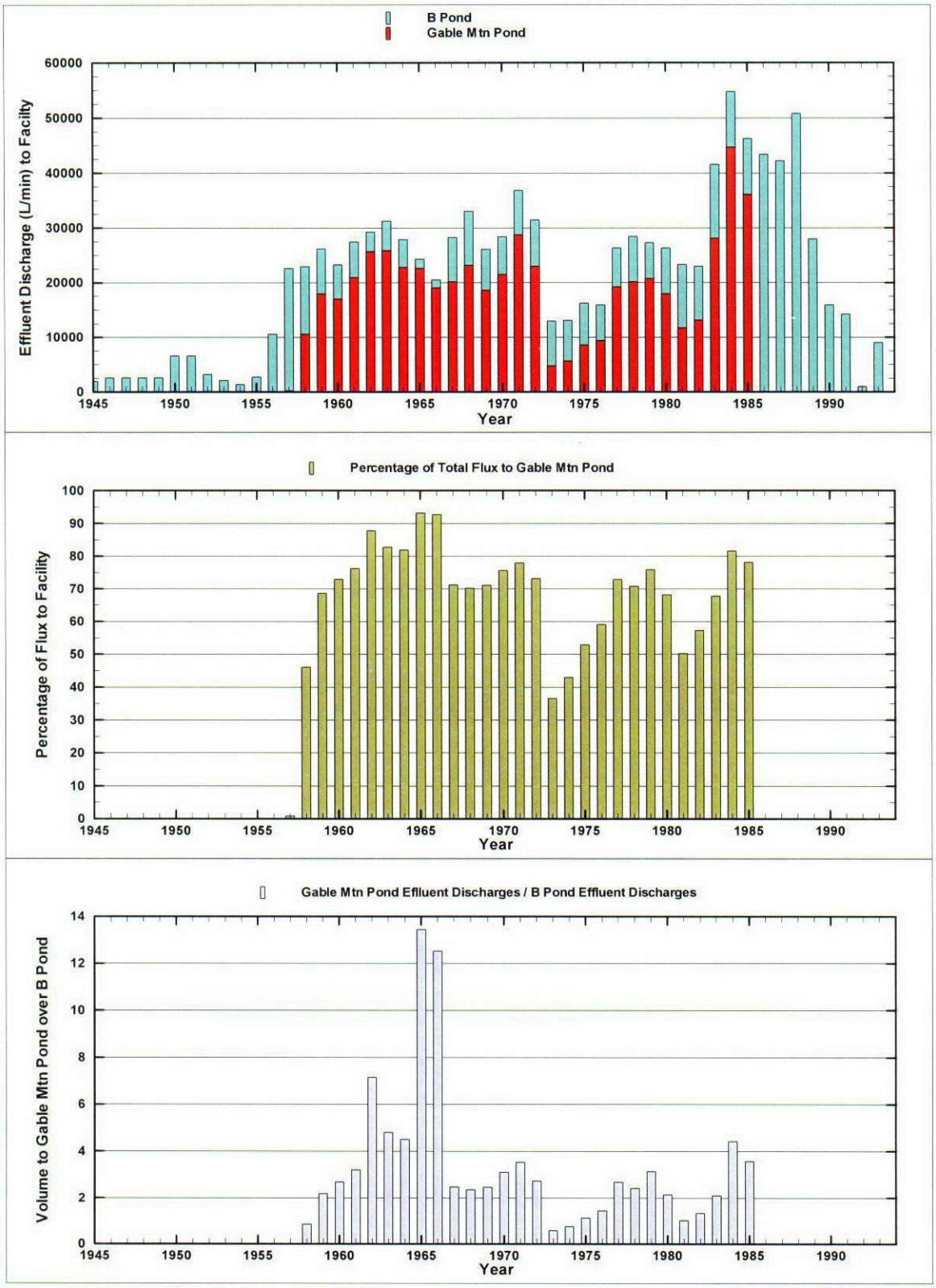

C.6.2.2 Water Table Elevations in the 200 East Area

The response of the water table to discharges at B Pond and Gable Mountain Pond is illustrated in Figure C.25. The data are normalized to the maximum discharge and maximum increase in water level over the time period shown. This allows direct comparison of changes in discharge and change in water level on the same scale (i.e., as per cent where the maximum in each case is 100% or full scale). The wells selected for this comparison are among the few in the vicinity of WMA B-BX-BY that have relatively complete measurement records over the period of interest. The spacing among the three wells is also optimal for analysis of relative changes in flow direction discussed in the following section.

As illustrated in Figure C.25, the rapid increase in water table elevation beginning in 1958 is primarily a result of the discharge to Gable Mountain Pond. The maxima in the hydrographs for these wells correspond to the two periods of maximum discharge. Gable Mountain Pond dominates the earlier maximum whereas the more recent maximum is primarily due to B Pond. Interestingly, the minimum in water levels between about 1975 and 1985 do not decline as sharply as the discharges to the ponds. This may be due to aquifer storage (i.e., drainage following decreased discharge creates a lag in the decline in water table elevation). Also, the 1990 maximum water level is less than the 1970 maximum even though greater annual discharge volumes occurred during the 1990 buildup. During the latter period, only B Pond was receiving cooling water. One explanation for this apparent discrepancy is that B Pond is underlain by an extensive perching layer (Ringold mud unit) just above the water table. This may act as a buffer that attenuates the response of the aquifer to discharges in that area (Figure C.26).

C.6.2.3 Hanford Site Water Table

The Hanford Site water table map and inferred flow directions for two time periods are shown in Figure C.26. The 1997 water table map shows the residual groundwater mound at B Pond and flow directions with a westerly component in the central 200 East Area. By March 1999, the mound diminished and there is an inferred flow reversal to the southeast in the same central 200 East Area. Northward flow is implied in the Gable Gap area. There is very little gradient in the region around WMA B-BX-BY making flow direction inferences based on water table elevations difficult at best.

The area shown in yellow (Figure C.26) illustrates the location of the Ringold mud unit in relation to B Pond and the surrounding area. It is important to note that no impediment (i.e., Ringold mud unit) to downward flow lies beneath the Gable Mountain Pond area. It should also be noted that during the maximum discharge period to the ponds, the gray shaded area (basalt outcrop) immediately northeast of the 200 East Area was below the water table. During the more recent period, the saturated portion of the aquifer is restricted in areal extent by the basalt. Whether or not the basalt in this area is capable of storing water or is impermeable is still uncertain. If it is semi-permeable and was capable of storing high salt waste from past discharges, this could be a source of slow drainage back into the periphery of the adjacent aquifer.

Figure C.25. Percent Change in Water Table Elevations at Three Key Locations versus Percent Change in Discharge Volumes to Gable Mountain Pond and B Pond

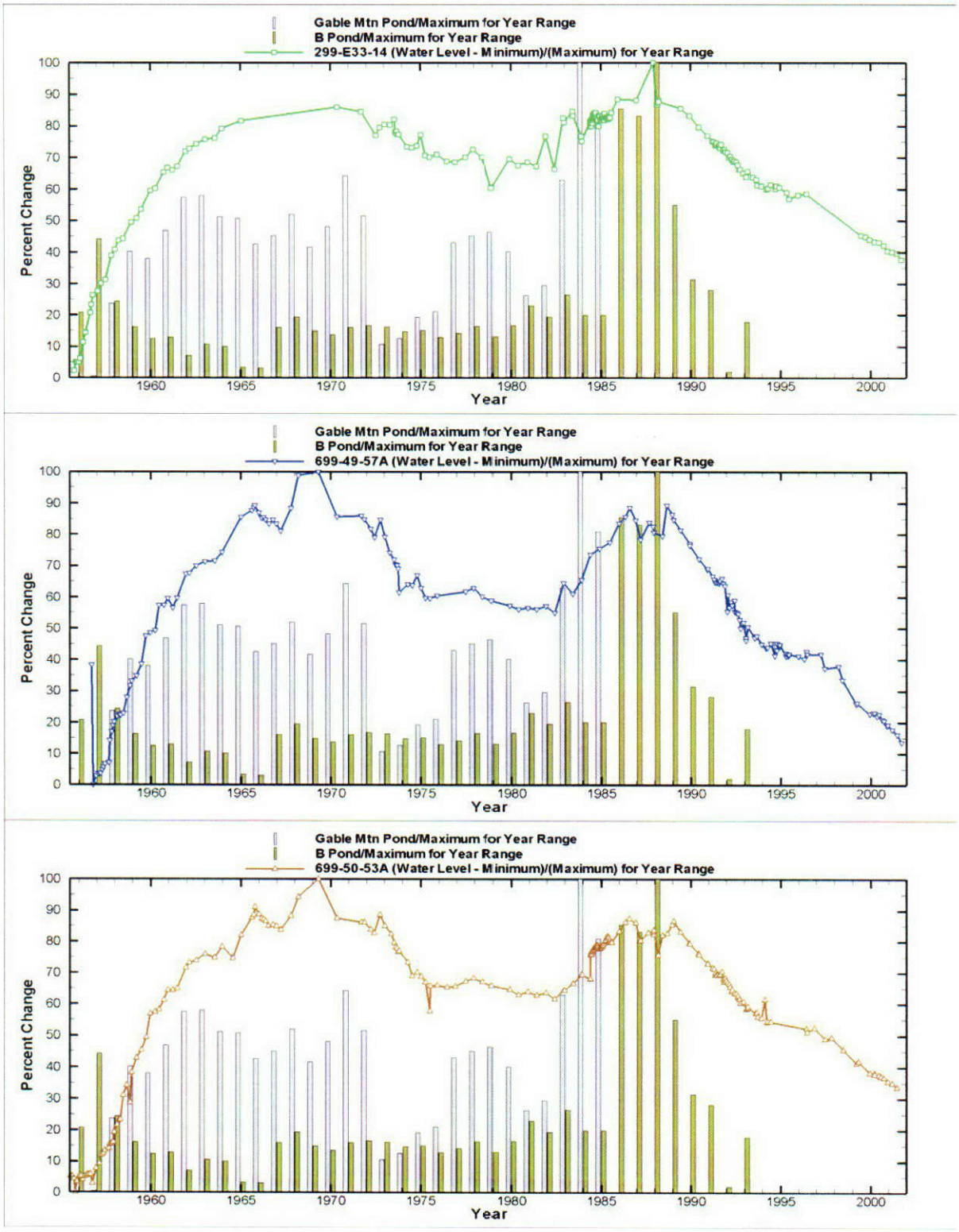

Figure C.26. Water Table Map for the Hanford Site Showing Recent Changes in the 200 East Area, 1997 (left) versus 1999 (right)

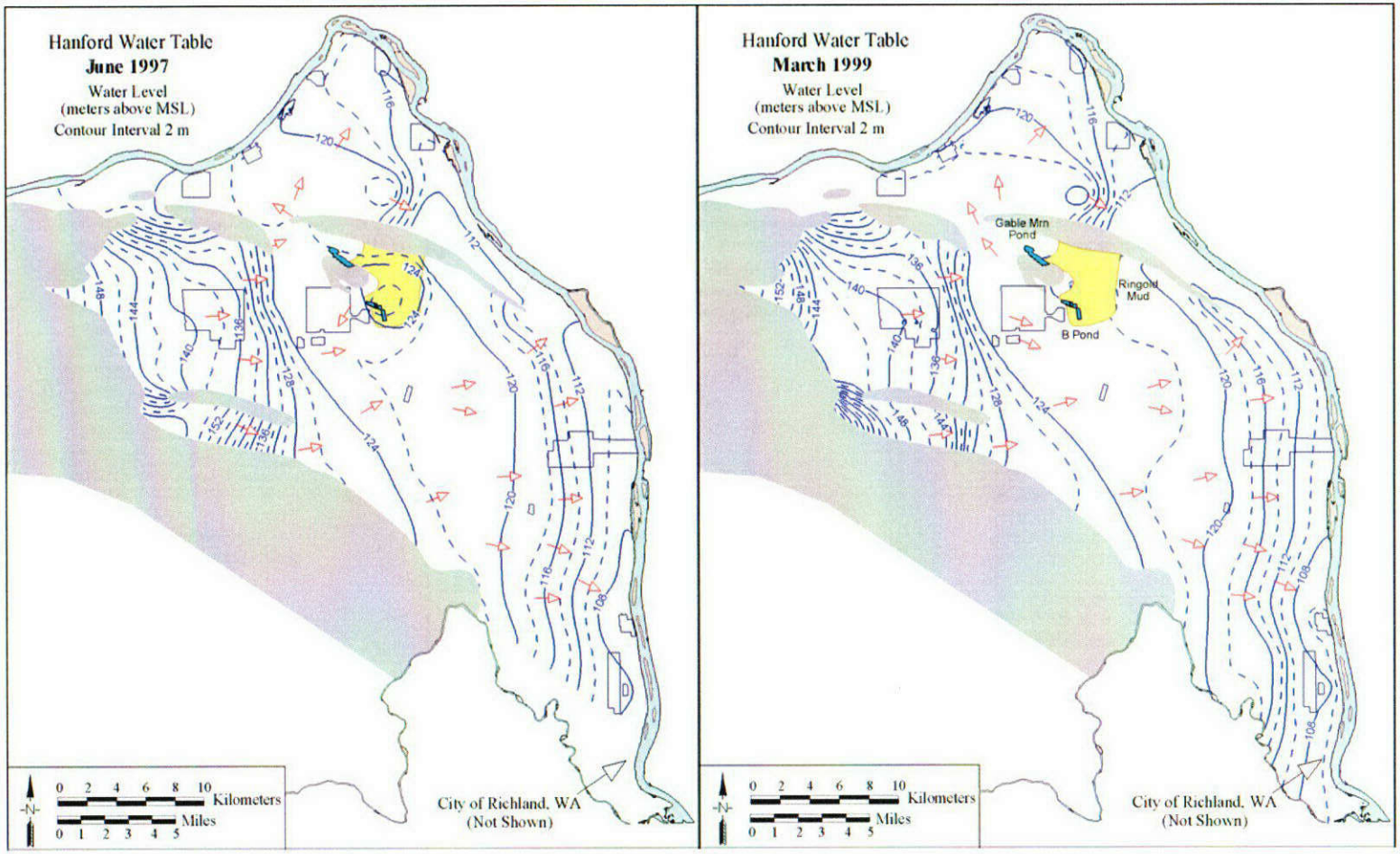

C.6.3 CHANGES IN FLOW DIRECTION

An attempt was made to analyze historical changes in flow direction using the three-point problem trend surface analysis (Spane 1999). Review of water level data for all wells within a 1000-m radius of the WMA resulted in finding only a limited number of wells with continuous water level data from the 1950s to the present. Fortunately, three monitoring wells with suitable records were found in s strategic location near the WMA:

- Well 699-49-57A located northwest of the WMA
- Well 699-50-53A located to the northeast
- Well 299-E33-14 near the east side of the BY cribs area.

Locations of these wells in relation to the WMA and other facilities in the northern 200 East Area are shown in Figure C.27. Data for these three wells were retrieved and grouped according to time of measurement. Ideally, water levels should be measured on at least the same day for each of the three wells in the group (Spane 1999). However, only about half of the data set met this requirement. Some data set groupings included measurements that were up to 30 days apart. Rather than reject such groupings, they were included in the analysis. The maximum spread in days between measurements for each time grouping is recorded in the data table included as column 3 of Table C.9. Also, obvious outlying data points were eliminated from the analysis.

It should also be noted that aside from possible barometric pressure effects (Spane 1999), well straightness might influence the results of this type of analysis. While these effects are acknowledged as important corrections, especially where there is very little gradient between wells, these effects are assumed to be secondary for purposes of identifying major periods where flow reversal may have occurred. However, follow up evaluations (e.g., slug testing to check for skin effects, well straightness, and barometric pressure response in each well) could improve the analysis.

Another basic assumption is that wells 699-50-53A and 699-49-57A are in communication with the unconfined aquifer. Some problems have been noted suggesting stagnation effects in 699-49-57A and the decline in the water table below the top of basalt in 699-50-53A in more recent years. However, based on the general response exhibited by the hydrographs for each of these wells (Figure C.25), it was assumed the wells reflect long-term changes in water table elevation at their respective locations. If either well was not in communication with the aquifer at all, the hydrographs would not track the recognized downward trends exhibited in all monitoring wells in this area.

Given the above limitations in the data set, the trend surface method described in Spane (1999) was used to estimate apparent flow direction and gradient for each three-well data grouping for points in time from 1956 to the present. Numerical results are included in Table C.9, which contains historical water level data for three selected wells near the north end of WMA B-BX-BY. No adjustments were made in any of the data to account for well straightness or other factors that could influence the inferred flow directions (azimuth in degrees with north as zero). The flow directions are based on trend surface analysis of water level data from the three wells as indicated in Table C.9.

Inspection of the numerical values shown in Table C.9 suggests four distinct time periods with either northerly or southerly flow directions. Flow direction for each grouping in each of the four time periods identified is shown in Figure C.28. The average gradient for each of the four time periods is shown in the legend box for each period. The length of the arrows shown indicates relative magnitude of the gradient (proportional to flow rate through the Darcy equation).

The trend analysis suggests flow direction was to the north during the late 1950s. The directions are fairly consistent in one direction during this period. The gradient was also the largest during this time period, which very likely damped out the uncertainties discussed above. The second time period extends from December 1958 through April 1974 during which the general flow direction was southerly. However, closer inspection of the data shows that during the first half of this period, the flow direction was more southeast to south and then began shifting to the west in 1971. The average gradient for this time period was about 5 fold lower than for the first time period.

The third major period appears to be from July 1974 to June 1996 when flow was consistently to the north and the average gradient was also about 5 times less than the late 1950s time period. After this time, the flow direction appears to have reversed again from a northerly to a southerly direction (i.e., sometime after 1996). The gradient in the latter case is more than a factor of 10 lower than during the early 1950s. It should also be noted that discharge volumes to Gable Mountain Pond were greater than volumes discharge to B Pond by about a factor of 3 from 1973 to 1985. Intuitively, this imbalance would seemingly favor a southerly flow direction rather than the northerly direction as indicated by the trend surface results for this period. Apparently, discharges to B Pond during this period exerted a greater influence on the gradient in the vicinity of WMA B-BX-BY than expected based solely on discharge volumes alone. More recently, as the water table continues to decline, the gradient is returning to pre-Hanford conditions with a southeast to easterly flow direction.

Because of the uncertainty in flow direction based on trend surface analysis of historical data, it was deemed important to compare results with alternative methods. Direct measurements of flow direction were made in the B-BX-BY area in 1999 and 2000 as reported by Narbutovskih in Hartman et al. (2001). While the flow meter results were variable, the general flow direction suggested by these measurements was to the south and southwest. This is consistent with the trend surface result from 1999 to the present for the three wells chosen in this study (Figure C.28).

Some additional checks on the reliability of the trend surface flow direction analysis (as applied here) can be made by inspection of contaminant history in wells that have been monitored over the period of interest, as discussed in the following section.

Figure C.27. Location of Key Monitoring Wells Used for Assessing Long-Term Changes in Flow Direction Near Waste Management Area B-BX-BY

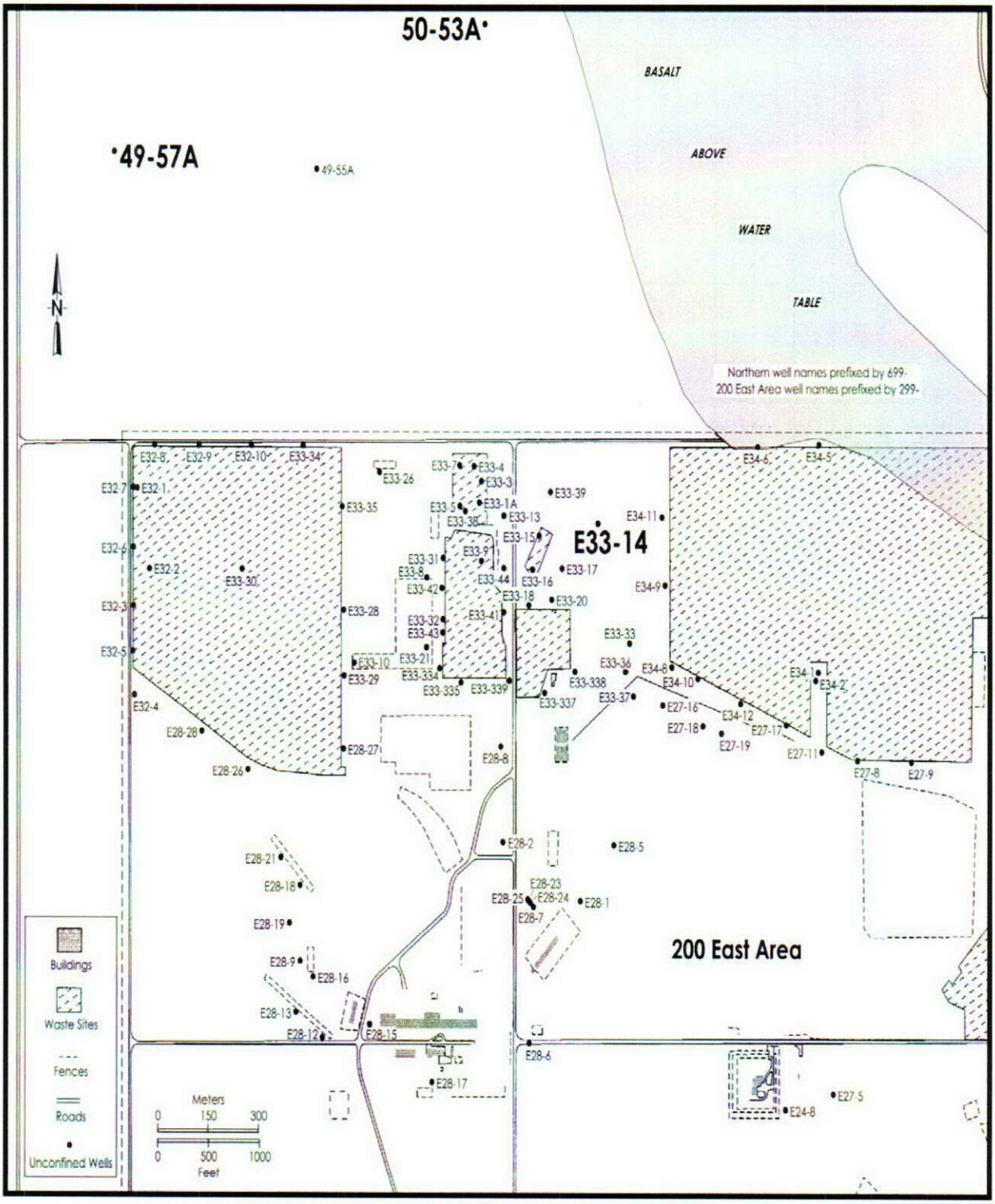

Table C.9. Historical Water Levels and Inferred Flow Directions(Azimuth) (5 pages)

Start Date	End Date	Number of Days in Group	299-E33-14	699-49-57A	699-50-53A	DiffMinMax Water	Gradient (m/m)	Azimuth (North = 0)	Grad in X Direction	Grad in Y Direction
14 Sep 1956	09-Oct-1956	25	121.902	123.185	121.446	1.739	1.594E-03	58.71	1.362E-03	8.282E-04
25 Jan 1957	21-Feb-1957	27	122.085	122.16	121.687	0.473	5.523E-04	34.39	3.119E-04	4.557E-04
13 Mar 1957	29-Mar-1957	16	122.186	122.163	121.785	0.401	4.919E-04	28.08	2.315E-04	4.340E-04
14 Jun 1957	27-Jun-1957	13	122.231	122.255	121.84	0.415	5.092E-04	31.32	2.647E-04	4.350E-04
25 Oct 1957	25-Oct-1957	0	122.554	122.554	121.925	0.629	7.942E-04	29.70	3.935E-04	6.899E-04
19 Dec 1957	31 Dec 1957	12	122.631	122.648	122.059	0.589	7.332E-04	30.50	3.721E-04	6.318E-04
24 Mar 1958	26 Mar 1958	2	122.752	122.718	122.199	0.553	6.769E-04	27.96	3.174E-04	5.979E-04
20 Jun 1958	23 Jun 1958	3	122.774	122.73	122.498	0.276	3.215E-04	24.97	1.357E-04	2.915E-04
10 Nov 1958	09 Dec 1958	29	122.993	122.989	122.41	0.583	7.336E-04	29.51	3.613E-04	6.385E-04
18 Mar 1959	23 Mar 1959	5	123.048	123.084	122.937	0.147	1.646E-04	37.27	9.966E-05	1.310E-04
24 Jun 1959	29 Jun 1959	5	123.167	123.194	123.028	0.166	1.934E-04	34.52	1.096E-04	1.594E-04
23 Dec 1959	28 Dec 1959	5	123.417	123.489	123.461	0.072	4.445E-05	132.20	3.293E-05	-2.986E-05
30 Mar 1960	04 Apr 1960	5	123.444	123.508	123.485	0.064	4.009E-05	135.53	2.809E-05	-2.861E-05
23 Sep 1960	27 Sep 1960	4	123.655	123.748	123.623	0.125	1.144E-04	59.03	9.810E-05	5.888E-05
08 Dec 1960	14 Dec 1960	6	123.716	123.812	123.741	0.096	6.502E-05	92.54	6.496E-05	-2.880E-06
23 Mar 1961	24 Mar 1961	1	123.688	123.721	123.745	0.057	5.467E-05	188.36	-7.950E-06	-5.409E-05
23 Jun 1961	28 Jun 1961	5	123.731	123.815	123.763	0.084	5.231E-05	105.10	5.051E-05	-1.363E-05
11 Dec 1961	14 Dec 1961	3	123.935	124.038	124.013	0.103	7.020E-05	147.53	3.768E-05	-5.922E-05
26 Feb 1962	06 Mar 1962	8	123.969	124.047	124.074	0.105	9.523E-05	180.12	-1.955E-07	-9.523E-05
10 Jul 1962	19 Jul 1962	9	124.03	124.117	124.098	0.087	6.059E-05	149.77	3.051E-05	-5.235E-05

Table C.9. Historical Water Levels and Inferred Flow Directions(Azimuth) (5 pages)

Start Date	End Date	Number of Days in Group	299-E33-14	699-49-57A	699-50-53A	DiffMinMax Water	Gradient (m/m)	Azimuth (North = 0)	Grad in X Direction	Grad in Y Direction
09 Jan 1963	17 Jan 1963	8	124.091	124.154	124.174	0.083	7.494E-05	179.26	9.729E-07	-7.493E-05
25 Jul 1963	05 Aug 1963	11	124.106	124.163	124.132	0.057	3.453E-05	113.82	3.159E-05	-1.395E-05
17 Dec 1963	23 Dec 1963	6	124.231	124.242	124.26	0.029	3.033E-05	197.07	-8.906E-06	-2.900E-05
11 Jan 1965	19 Jan 1965	8	124.334	124.574	124.403	0.24	1.590E-04	95.17	1.583E-04	-1.433E-05
14 Sep 1971	14 Sep 1971	0	124.459	124.587	124.555	0.128	8.669E-05	146.84	4.741E-05	-7.258E-05
02 Jun 1972	11 Jul 1972	39	124.145	124.385	124.427	0.282	2.492E-04	174.22	2.509E-05	-2.480E-04
02 Oct 1972	05 Oct 1972	3	124.246	124.55	124.65	0.404	3.654E-04	179.61	2.510E-06	-3.654E-04
05 Jan 1973	08 Jan 1973	3	124.286	124.389	124.513	0.227	2.295E-04	194.00	-5.552E-05	-2.227E-04
10 Apr 1973	10 May 1973	30	124.28	124.239	124.415	0.176	1.982E-04	216.86	-1.189E-04	-1.586E-04
10 Jul 1973	20 Jul 1973	10	124.356	124.175	124.308	0.181	1.221E-04	272.99	-1.219E-04	6.378E-06
13 Aug 1973	15 Aug 1973	2	124.194	124.129	124.26	0.131	1.308E-04	227.12	-9.586E-05	-8.901E-05
10 Sep 1973	11 Sep 1973	1	124.2	124.12	124.244	0.124	1.170E-04	234.03	-9.469E-05	-6.871E-05
03 Oct 1973	08 Oct 1973	5	124.155	124.09	124.202	0.112	1.082E-04	230.93	-8.397E-05	-6.817E-05
16 Oct 1973	17 Oct 1973	1	124.155	123.867	124.214	0.347	3.112E-04	243.60	-2.787E-04	-1.383E-04
11 Apr 1974	18 Apr 1974	7	123.993	123.943	124.077	0.134	1.412E-04	222.02	-9.452E-05	-1.049E-04
12 Jul 1974	16 Jul 1974	4	123.978	123.934	123.915	0.063	5.791E-05	2.44	2.468E-06	5.785E-05
18 Oct 1974	18 Oct 1974	0	124.005	124.026	123.958	0.068	7.384E-05	39.57	4.703E-05	5.692E-05
08 Jan 1975	08 Jan 1975	0	124.148	123.907	123.912	0.241	2.047E-04	344.50	-5.471E-05	1.973E-04
14 Apr 1975	14 Apr 1975	0	123.877	123.815	123.842	0.062	3.765E-05	306.77	-3.016E-05	2.254E-05
07 Jul 1975	07 Jul 1975	0	123.856	123.809	123.495	0.361	4.268E-04	25.89	1.864E-04	3.840E-04

Table C.9. Historical Water Levels and Inferred Flow Directions(Azimuth) (5 pages)

Start Date	End Date	Number of Days in Group	299-E33-14	699-49-57A	699-50-53A	DiffMinMax Water	Gradient (m/m)	Azimuth (North = 0)	Grad in X Direction	Grad in Y Direction
03 Dec 1975	03 Dec 1975	0	123.892	123.834	123.802	0.09	8.424E-05	5.18	7.604E-06	8.389E-05
01 Jul 1977	01 Jul 1977	0	123.853	123.873	123.848	0.025	2.256E-05	61.99	1.992E-05	1.060E-05
07 Dec 1977	07 Dec 1977	0	123.956	123.907	123.888	0.068	6.208E-05	1.29	1.398E-06	6.206E-05
01 Jun 1978	01 Jun 1978	0	123.856	123.825	123.845	0.031	1.959E-05	282.20	-1.915E-05	4.141E-06
01 Dec 1978	01 Dec 1978	0	123.45	123.788	123.796	0.346	3.007E-04	167.06	6.734E-05	-2.931E-04
01 Dec 1979	01 Dec 1979	0	123.831	123.742	123.751	0.089	6.952E-05	339.21	-2.468E-05	6.500E-05
01 Jun 1980	01 Jun 1980	0	123.743	123.706	123.69	0.053	4.872E-05	2.46	2.090E-06	4.868E-05
01 Dec 1980	01 Dec 1980	0	123.789	123.721	123.729	0.068	5.223E-05	338.01	-1.956E-05	4.843E-05
01 Jun 1981	01 Jun 1981	0	123.734	123.706	123.681	0.053	5.188E-05	10.71	9.646E-06	5.098E-05
01 Dec 1981	01 Dec 1981	0	124.13	123.739	123.717	0.413	3.599E-04	348.80	-6.992E-05	3.531E-04
01 Jun 1982	01 Jun 1982	0	123.7	123.675	123.641	0.059	6.046E-05	15.27	1.592E-05	5.832E-05
01 Dec 1982	01 Dec 1982	0	124.374	123.953	123.741	0.633	5.882E-04	4.14	4.251E-05	5.867E-04
01 Jun 1983	01 Jun 1983	0	124.462	123.852	123.821	0.641	5.583E-04	348.52	-1.112E-04	5.472E-04
01 Dec 1983	01 Dec 1983	0	124.133	123.983	123.934	0.199	1.799E-04	359.54	-1.453E-06	1.799E-04
01 Jun 1984	01 Jun 1984	0	124.325	124.224	124.171	0.154	1.436E-04	4.61	1.154E-05	1.431E-04
01 Dec 1984	01 Dec 1984	0	124.405	124.279	124.257	0.148	1.308E-04	354.21	-1.321E-05	1.301E-04
14 Jun 1985	27 Jun 1985	13	124.398	124.337	124.345	0.061	4.621E-05	337.00	-1.806E-05	4.254E-05
17 Dec 1985	30 Dec 1985	13	124.618	124.514	124.449	0.169	1.598E-04	6.61	1.840E-05	1.588E-04
09 Dec 1986	29 Dec 1986	20	124.608	124.544	124.549	0.064	5.120E-05	340.81	-1.683E-05	4.835E-05
08 Dec 1987	10 Dec 1987	2	125.099	124.431	124.464	0.668	5.506E-04	342.71	-1.636E-04	5.257E-04

Table C.9. Historical Water Levels and Inferred Flow Directions(Azimuth) (5 pages)

Start Date	End Date	Number of Days in Group	299-E33-14	699-49-57A	699-50-53A	DiffMinMax Water	Gradient (m/m)	Azimuth (North = 0)	Grad in X Direction	Grad in Y Direction
08 Jun 1989	20 Jun 1989	12	124.499	124.45	124.443	0.056	4.928E-05	352.88	-6.109E-06	4.890E-05
06 Dec 1989	08 Dec 1989	2	124.401	124.325	124.309	0.092	8.172E-05	355.61	-6.257E-06	8.148E-05
12 Dec 1989	13 Dec 1989	1	124.404	124.309	124.299	0.105	9.197E-05	351.20	-1.408E-05	9.089E-05
18 Jun 1990	19 Jun 1990	1	124.246	124.178	124.171	0.075	6.567E-05	351.09	-1.018E-05	6.488E-05
10 Dec 1990	12 Dec 1990	2	124.136	124.09	124.065	0.071	6.637E-05	5.01	5.793E-06	6.612E-05
19 Mar 1991	19 Mar 1991	0	124.066	124.02	124.01	0.056	4.979E-05	355.87	-3.590E-06	4.967E-05
23 Apr 1991	24 Apr 1991	1	124.057	123.989	124.001	0.068	4.926E-05	333.39	-2.206E-05	4.404E-05
16 May 1991	20 May 1991	4	124.011	123.962	123.931	0.08	7.575E-05	6.75	8.905E-06	7.522E-05
21 May 1991	29 May 1991	8	124.02	123.965	123.958	0.062	5.445E-05	352.20	-7.393E-06	5.395E-05
18 Jun 1991	19 Jun 1991	1	124.038	123.965	123.949	0.089	7.916E-05	355.93	-5.615E-06	7.896E-05
29 Jul 1991	30 Jul 1991	1	123.996	123.956	123.925	0.071	6.851E-05	9.10	1.083E-05	6.765E-05
20 Aug 1991	21 Aug 1991	1	124.014	123.977	123.937	0.077	7.693E-05	12.85	1.710E-05	7.500E-05
25 Oct 1991	28 Oct 1991	3	123.947	123.95	123.883	0.067	8.275E-05	30.95	4.255E-05	7.097E-05
22 Nov 1991	22 Nov 1991	0	123.956	123.931	123.865	0.091	1.001E-04	21.04	3.594E-05	9.342E-05
20 Dec 1991	14 Jan 1992	25	123.929	123.687	123.859	0.242	1.601E-04	275.35	-1.594E-04	1.491E-05
22 Jan 1992	23 Jan 1992	1	123.913	123.846	123.84	0.073	6.383E-05	350.45	-1.059E-05	6.294E-05
20 Feb 1992	25 Feb 1992	5	123.849	123.727	123.816	0.122	8.194E-05	273.50	-8.179E-05	5.008E-06
19 Mar 1992	20 Mar 1992	1	123.865	123.778	123.786	0.087	6.861E-05	339.86	-2.362E-05	6.441E-05
14 Apr 1992	27 Apr 1992	13	123.822	123.748	123.731	0.091	8.107E-05	356.32	-5.204E-06	8.090E-05
17 Jun 1992	17 Jun 1992	0	123.804	123.794	123.709	0.095	1.137E-04	26.66	5.103E-05	1.016E-04

Table C.9. Historical Water Levels and Inferred Flow Directions(Azimuth) (5 pages)

Start Date	End Date	Number of Days in Group	299-E33-14	699-49-57A	699-50-53A	DiffMinMax Water	Gradient (m/m)	Azimuth (North = 0)	Grad in X Direction	Grad in Y Direction
21 Jul 1992	22 Jul 1992	1	123.785	123.678	123.703	0.107	7.350E-05	328.38	-3.854E-05	6.259E-05
19 Aug 192	20 Aug 1992	1	123.749	123.666	123.676	0.083	6.357E-05	337.80	-2.402E-05	5.885E-05
17 Sep 1992	18 Sep 1992	1	123.694	123.611	123.639	0.083	5.267E-05	317.95	-3.528E-05	3.911E-05
08 Oct 1992	11 Oct-1992	3	123.691	123.529	123.591	0.162	1.003E-04	312.91	-7.346E-05	6.827E-05
09 Dec 1992	10 Dec 1992	1	123.645	123.586	123.609	0.059	3.641E-05	312.09	-2.702E-05	2.440E-05
29 Jan 1993	08 Feb 1993	10	123.593	123.428	123.52	0.165	1.003E-04	292.20	-9.287E-05	3.789E-05
12 Mar 1993	12 Mar 1993	0	123.667	123.541	123.548	0.126	1.032E-04	342.32	-3.135E-05	9.832E-05
01 Sep 1993	01 Sep 1993	0	123.557	123.458	123.478	0.099	6.999E-05	331.22	-3.370E-05	6.134E-05
14 Dec 1993	14 Dec 1993	0	123.475	123.379	123.411	0.096	6.107E-05	318.38	-4.056E-05	4.566E-05
28 Mar 1994	28 Mar 1994	0	123.435	123.352	123.365	0.083	6.130E-05	335.01	-2.590E-05	5.556E-05
11 Apr 1994	28 Apr 1994	17	123.444	123.349	123.377	0.095	6.208E-05	322.43	-3.785E-05	4.920E-05
21 Jun 1994	21 Jun 1994	0	123.493	123.391	123.368	0.125	1.113E-04	356.16	-7.443E-06	1.110E-04
14 Jun 1996	25 Jun 1996	11	123.374	123.288	123.246	0.128	1.187E-04	3.80	7.866E-06	1.184E-04
13 Dec 1999	16 Dec 1999	3	122.764	122.727	122.768	0.041	3.631E-05	247.58	-3.357E-05	-1.385E-05
21 Mar 2000	21 Mar 2000	0	122.734	122.733	122.762	0.029	3.600E-05	210.66	-1.835E-05	-3.097E-05
21 Jun 2000	21 Jun 2000	0	122.726	122.72	122.74	0.02	2.181E-05	219.24	-1.380E-05	-1.689E-05
21 Sep 2000	21 Sep 2000	0	122.684	122.663	122.705	0.042	4.187E-05	227.29	-3.077E-05	-2.840E-05
14 Dec 2000	15 Dec 2000	1	122.61	122.622	122.661	0.051	5.720E-05	202.43	-2.183E-05	-5.287E-05
12 Mar 2001	12 Mar 2001	0	122.598	122.577	122.64	0.063	6.763E-05	220.48	-4.390E-05	-5.144E-05
21 Jun 2001	21 Jun 2001	0	122.583	122.53	122.591	0.061	5.430E-05	245.73	-4.950E-05	-2.232E-05

Figure C.28. Summary of Trend Surface Flow Direction Results

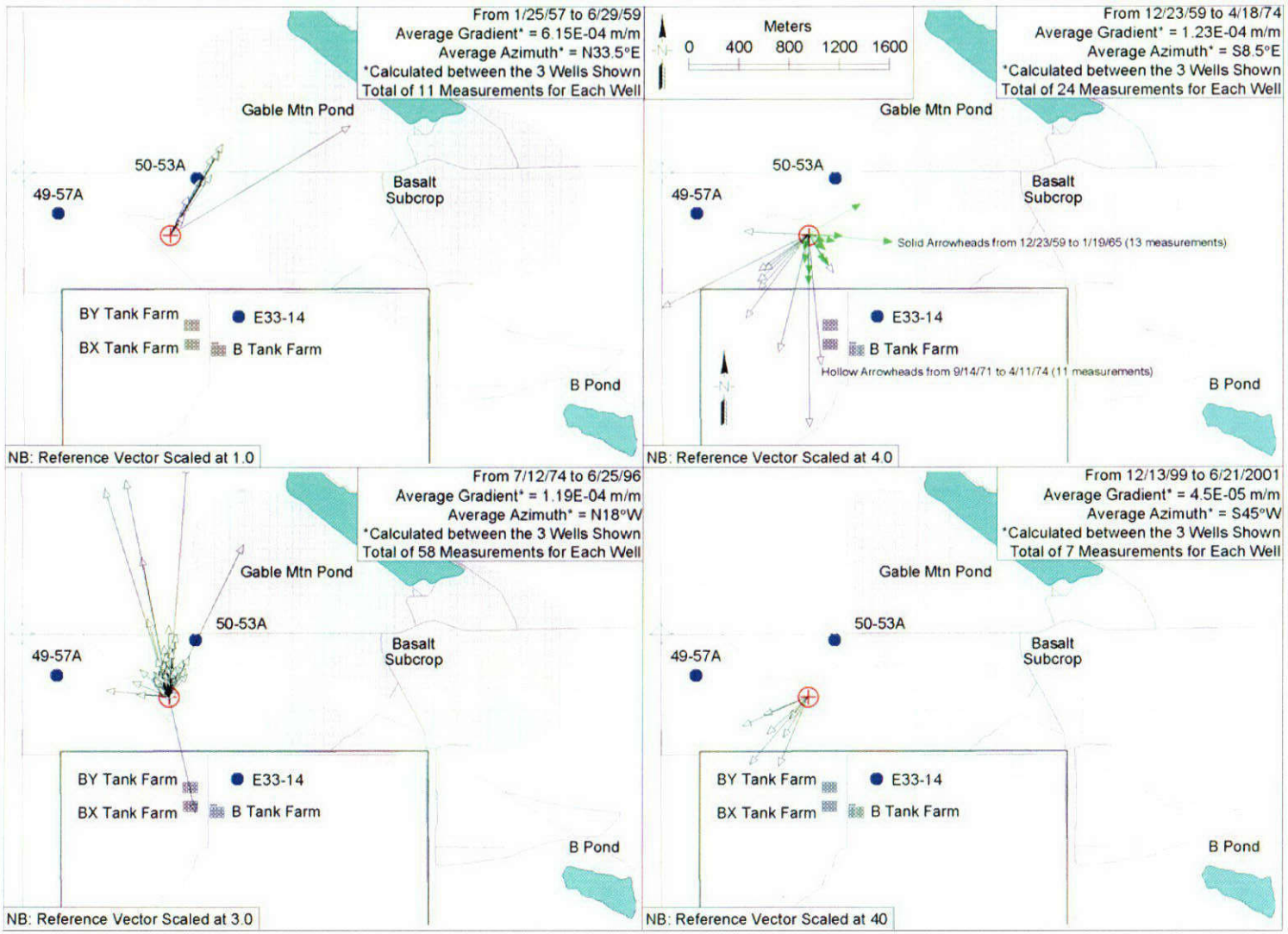

Velocity is proportional to the gradient which is indicated by the lengths of the arrows. A relative scale referenced to the first panel was used. Scaling factors are shown in the lower left hand corner. For example, a factor of 3 means that the arrow length or gradient in this panel is 1/3 the length shown in the first panel with a scaling factor of 1, and so on.

C.6.4 MONITORING WELL CONTAMINANT HISTORY

Nitrate, cobalt-60, and gross beta emitting contaminants were commonly analyzed in monitoring wells since the 1950s in a few selected wells. Such data are available for the same wells used for the trend surface analysis described above. The location of the two northerly wells (i.e., 699-49-57A and 699-50-53A) are separated sufficiently to potentially provide an indication of certain flow directions during critical time periods when major discharges of waste to the ground occurred. For example, the release to the BY cribs occurred over a relatively short time period (primarily in 1955). This event occurred at a time when the trend surface results suggest a northeasterly flow direction. If this inferred flow direction is correct, nitrate and cobalt-60 should have arrived at downgradient well 699-50-53A sometime after 1956 when the peak concentrations in groundwater occurred beneath the BY cribs. Likewise, if flow direction was as indicated in Figure C.28, contamination from this release event should not have arrived at well 699-49-57A since this well is located too far to the west to intersect the north-northeasterly flow direction suggested by the trend analysis for this time period.

To test the foregoing inference, nitrate and cobalt-60 concentrations were plotted versus time for the subject wells together with results for a well (299-E33-5) at the BY cribs (Figure C.29). The top panel shows the very high concentrations that occurred in groundwater at the crib source. The crib releases were over a short time period with high but variable concentrations. This pattern is completely absent in well 699-49-57A (center panel of Figure C.29) during this time period but is clearly evident in well 699-50-53A (bottom panel). Thus, these concentration history plots support the predicted trend surface flow directions for the late 1960s time period.

Figure C.29 also suggests a different contaminant plume arrived at well 699-49-57A in the early 1970s and persisted for over 10 years. This pattern does not occur in well 699-50-53A. A search of historical monitoring well data in the vicinity of WMA B-BX-BY revealed a match in well 299-E33-26. This well is located northwest of the BY cribs at crib 216-B-61. Waste Information Data System (WIDS) records state that the latter crib was never used so the contamination must have originated upgradient from the 216-B-61 crib. The source is not clear but may have been a secondary release from the BY cribs due to drainage or washdown of the residual waste beneath the BY cribs. Nevertheless, the time period for this release is appropriate to test a different time segment of the flow direction trend analysis.

Review of historical contaminant data for well 299-E33-26 and well 299-49-57A indicated only gross beta was common in both wells over the period of interest. Thus, only gross beta results for the two wells were plotted together as shown in Figure C.30. This plot indicates a similar pattern for both wells except that the sharp initial upward increase occurs in well 699-49-57A about 2.5 years after it first appeared in well 299-E33-26. This clearly implies a flow direction that was west to northwest during this period. As noted above, the trend surface results suggest a shift in flow direction (Figure C.28) from the southwest to the west and then northwest during the 1971 through 1974 time period. The straight line distance between the two wells is 1200 m. The trajectory may have been somewhat longer due to the shift from west to northwest during this period. Assuming a straight line distance between the two wells, an apparent flow rate of 1.3 m/day is implied (i.e., 1200 m/2.5 years = 480 m/yr or 1.3 m/day). The actual flow rate may have been somewhat greater than this if the flow due to path was non-linear due to curvature in the trajectory.

Figure C.29. Nitrate and Cobalt-60 Concentration History in Wells 299-E33-5, 699-50-53A, and 699-49-57A

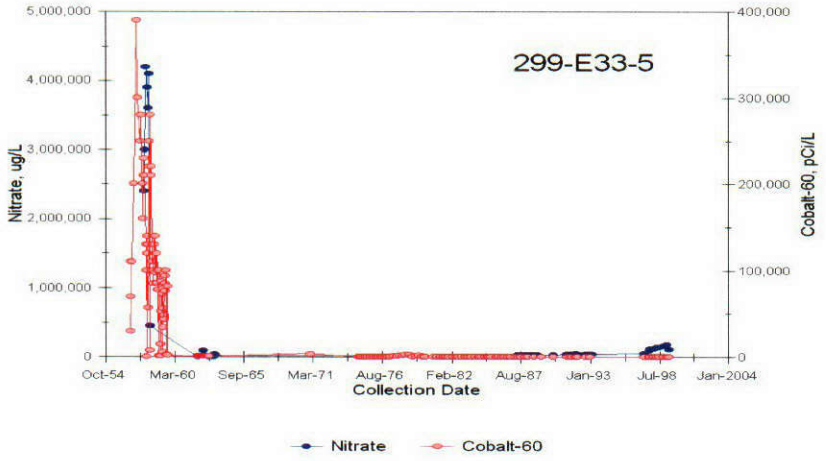

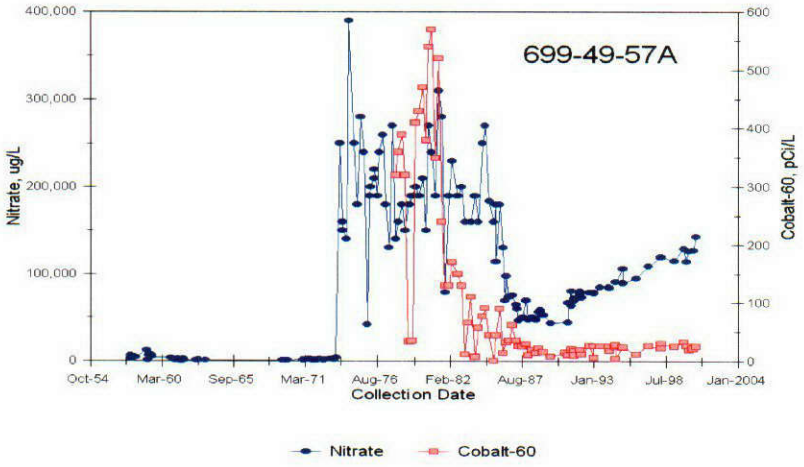

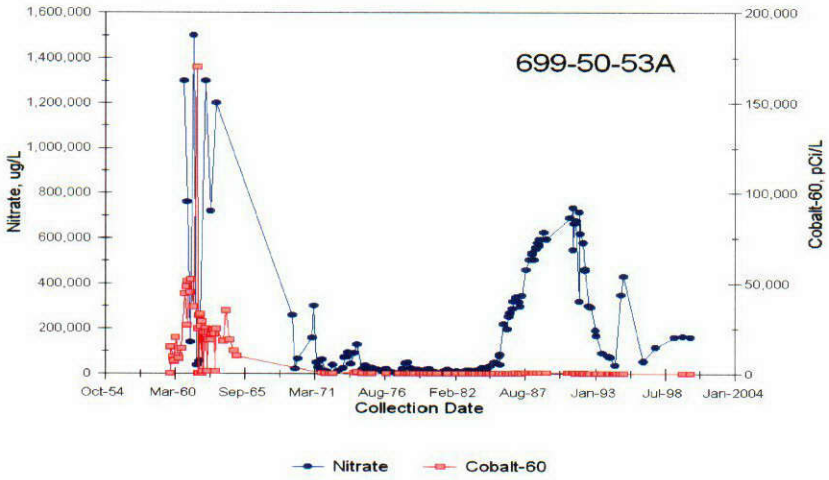

Figure C.30. Gross Beta Concentration History in Wells 299-E33-26 and 699-49-57A

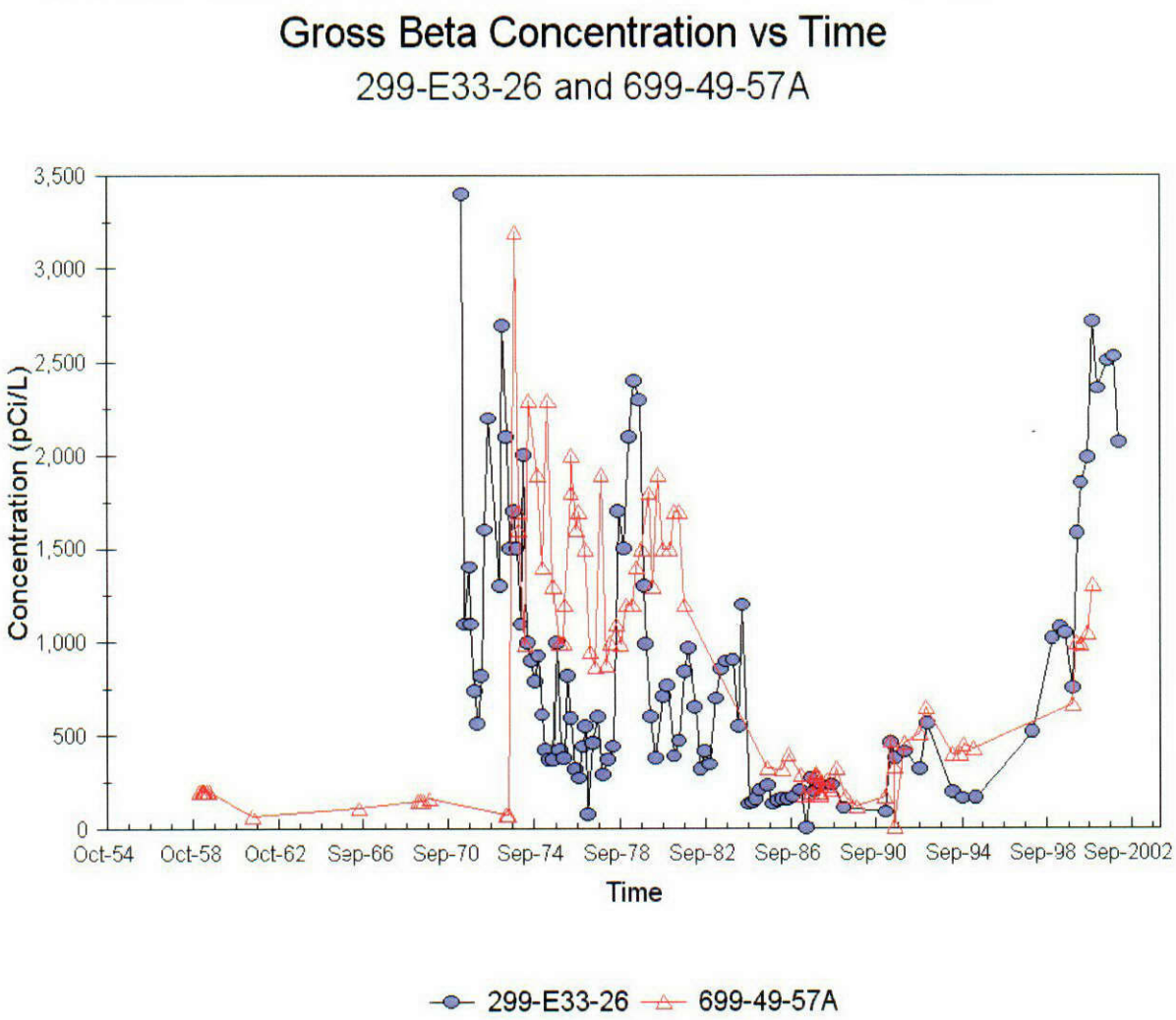

Assuming that: 1) the flow rate estimated above for the 1971 through 1974 time period is representative, 2) the aquifer properties are similar over the time period of interest, and 3) velocity is proportional to gradient (Darcy flow), flow rates based on the average gradient for all four time periods summarized in Figure C.28 can be estimated as follows. Divide the apparent flow rate for the 1971 through 1974 time period (1.3 m/day) by the average gradient ($1.68 \times 10\text{-}4$) for 1971 through 1974 (from Table C.9), and then multiply this ratio (0.744) times the average gradient in the other time periods of interest. Results of this exercise are shown in Table C.10.

The much lower contemporary or recent flow rate suggested in Table C.10 is also reasonable considering the continual decline in water levels and gradient as the B Pond mound dissipates. Also, as the water table declines, a less permeable portion of the aquifer may be encountered than in the past. For example, Spane et al. (2001) reported hydraulic conductivities of 22 to 56 m/day for three new wells at WMA B-BX-BY as compared to several hundred m/day reported in the past for this same area.

Table C.10. Estimated Average Flow Rates Near Waste Management Area B-BX-BY for Different Time Periods

Time Period	Average Gradient	Flow Rate, m/day
01/25/1957 to 06/29/1959	6.15E-04	4.8
12/23/1959 to 04/18/1974	1.23E-04	0.95
07/12/1974 to 06/25/1996	1.19E-04	0.95
12/13/1999 to 06/21/2001	4.5E-04	0.35

The higher estimated average flow rate for the 1957 through 1959 period (Table C.10) is reasonable since the gradient at this time was significantly greater than for subsequent periods. Also, by way of comparison, tritium travel times from PUREX to the Columbia River suggest an average flow rate of 3 to 4 m/day when discharges to the B-Pond/Gable Mountain Pond complex were high.

It should be emphasized that the estimated flow rates in Table C.10 are approximate and are intended only to provide some indication of relative magnitudes and average conditions for the time periods identified. At any one point in time, there is a high degree of uncertainty as evident from the coefficient of variation for the average value used for the reference period 1971 to 1974. For example, the coefficient of variation (%) for the 13 water table gradient values used between 1971 and 1974 (Table C.9) was 56%. Hopefully, averaging over long time periods helps to damp out the various contributors to the uncertainties in historical water level measurements.

C.6.5 CURRENT GROUNDWATER CONTAMINATION

The following summary of recent groundwater contamination in the vicinity of WMA B-BX-BY (Figure C.31 for well locations) was condensed from *Hanford Site Groundwater Monitoring for Fiscal Year 2001* (Hartman et al. 2002). Editorial modifications, including updated graphics and incorporation of new information acquired for this field investigation, were made as deemed appropriate.

The RCRA groundwater assessment studies at WMA B-BX-BY identified distinct groups of contaminants based on chemical associations, spatial relationships, historic plume movement, knowledge of process chemistry, and characteristic chemical ratios of contaminant concentrations (Hartman et al. 2001, 2002). The most relevant contaminants for tank waste source considerations include nitrate, technetium-99, cobalt-60, uranium, and tritium that are discussed below.

C.6.5.1 Contaminant Dynamics

Contaminant concentrations in groundwater beneath and in the vicinity of WMA B-BX-BY have exhibited rapid changes during the last 5 to 6 years. These changes are discussed first followed by a discussion of areal distribution patterns for the most recent results. Table C.11 indicates groundwater concentrations that have exceeded maximum contaminant levels or drinking water standards (40 CFR 141) for fiscal year 2001.

Figure C.31. Well Location Map for Waste Management Area B-BX-BY

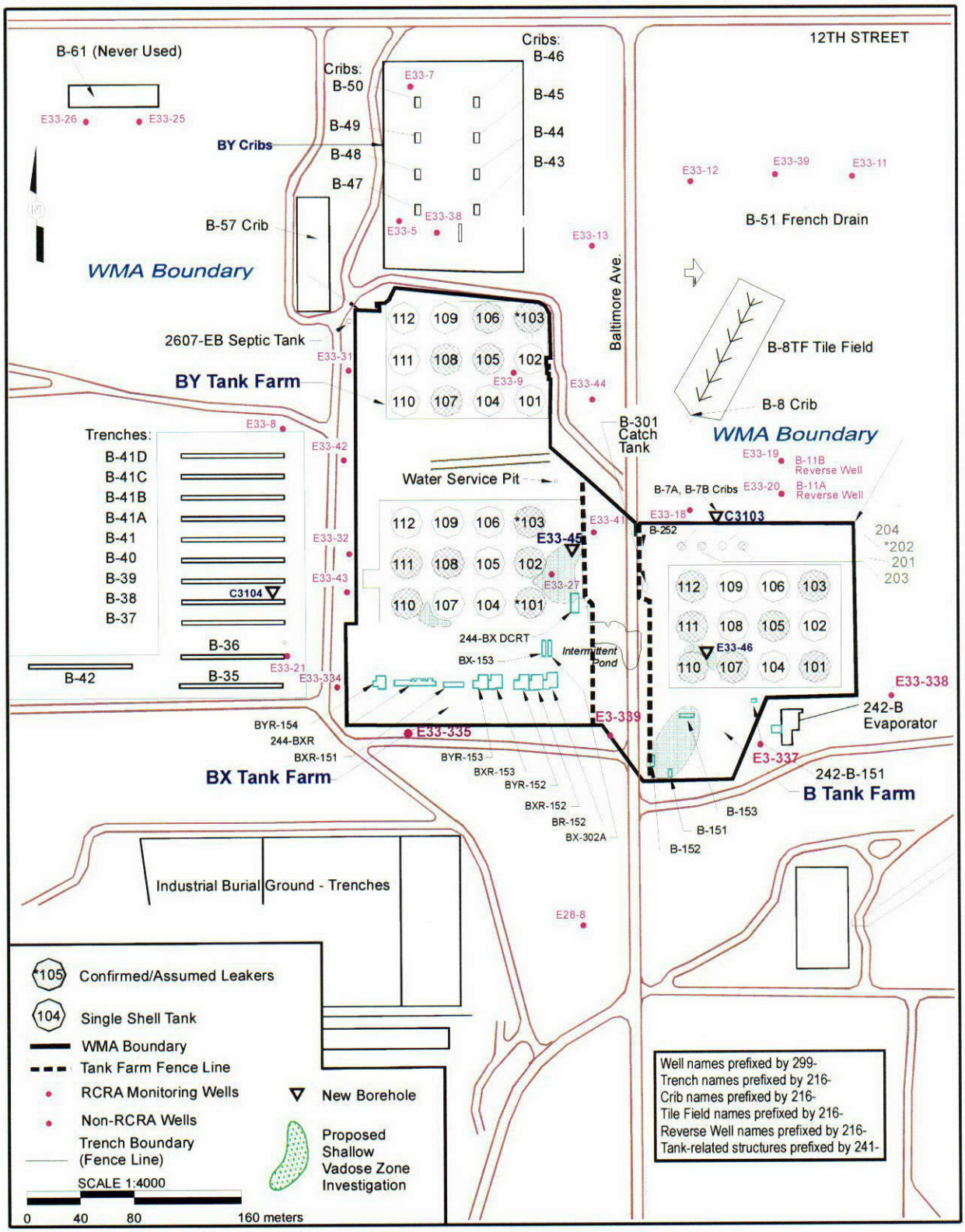

Note: All wells are preceded by 299-.
Note: The intermittent pond between the B and BX tank farms has been addressed by interim measures.

Table C.11. Groundwater Monitoring Results Exceeding Maximum Contaminant Levels or Drinking Water Standards at Waste Management Area B-BX-BY

Well Number	Antimony (µg/L)	Cyanide (µg/L)	Gross Alpha (pCi/L)	Gross Beta (pCi/L)	Nitrate (µg/L)	Iodine-129 (pCi/L)	Technetium-99 (pCi/L)	Tritium (pCi/L)	Uranium (µg/L)
299-E32-9	NA	NA	NA	58 (1)	NA	3 (1)	NA	NA	NA
299-E32-10	17 (1)	NA	NA	1,200 (2)	178,000 (4)	NA	3,490 (4)	NA	NA
299-E33-7	NA	423 (3)	NA	4,210 (3)	748,000 (4)	NA	11,600 (4)	NA	NA
299-E33-9	NA	NA	357 (2)	3,090 (3)	212,000 (4)	NA	7,660 (4)	NA	678 (4)
299-E33-13	NA	NA	16 (1)	975 (2)	425,000 (2)	NA	3,290 (2)	NA	NA
299-E33-15	NA	NA	NA	80 (1)	441,000 (2)	NA	NA	NA	NA
299-E33-16	NA	NA	NA	1,400 (3)	695,000 (4)	NA	5,780 (4)	NA	NA
299-E33-17	NA	NA	NA	NA	267,000 (1)	NA	NA	NA	NA
299-E33-18	NA	NA	108 (2)	1,200 (3)	205,000 (4)	NA	3,810 (4)	NA	193 (4)
299-E33-20	NA	NA	NA	103 (1)	460,000 (3)	NA	NA	NA	NA
299-E33-26	NA	NA	53 (2)	2,720 (3)	441,000 (4)	NA	7,510 (4)	NA	137 (4)
299-E33-28	NA	NA	NA	55 (1)	NA	NA	NA	NA	NA
299-E33-31	NA	NA	33 (1)	1,310 (3)	259,000 (3)	NA	3,800 (4)	NA	79 (4)
299-E33-32	NA	NA	NA	739 (4)	98,700 (4)	NA	2,090 (5)	NA	NA
299-E33-34	NA	333 (3)	21 (1)	3,060 (4)	456,000 (4)	NA	8,170 (4)	NA	46 (2)
299-E33-35	NA	NA	NA	658 (3)	120,000 (4)	4 (1)	2,420 (4)	NA	NA
299-E33-38	NA	383 (3)	84 (2)	4,600 (3)	531,000 (4)	NA	13,000 (4)	NA	165 (4)
299-E33-41	NA	NA	70 (2)	1,140 (2)	52,700 (1)	NA	3,290 (4)	NA	118 (2)
299-E33-42	NA	NA	NA	1,190 (3)	136,000 (4)	NA	3,380 (4)	NA	31 (1)
299-E33-43	NA	NA	NA	229 (3)	77,500 (1)	NA	915 (1)	NA	NA
299-E33-44	NA	NA	245 (2)	3,320 (3)	224,000 (4)	NA	8,230 (4)	NA	567 (4)
299-E33-339	NA	NA	NA	NA	NA	NA	NA	21,400 (1)	NA
DWS or MCL	6	200	15	50	45,000	1	900	20,000	30

Number indicates the maximum result for that well during the monitoring period from October 1, 2000 to September 30, 2001. Parenthesis indicates the number of exceedances in the particular well.
DWS = drinking water standard (40 CFR 141)
MCL = maximum contaminant level
NA = well did not exceed MCLs for the constituent

C.6.5.1.1 Technetium-99 and Nitrate. Concentrations of technetium-99 generally decreased during fiscal year 2001 following a period of steadily increasing concentrations since about 1997 (Figure C.32). Concentrations are higher at well 299-E33-38, located at the BY cribs, than in wells along the west side of WMA B-BX-BY. Concentrations range from 3,570 pCi/L at well 299-E33-31 west of the BY tank farm to 195 pCi/L in well 299-E33-43 to the south. The two new wells completed in early fiscal year 2000 show no upward trend in technetium-99, remaining below 70 pCi/L for the last 2 years. Although technetium-99 continued to increase early in fiscal year 2001 in the central part of the waste management area, concentrations declined in wells 299-E33-9, 299-E33-44, and 299-E33-41, mirroring the decrease in technetium-99 seen further north at the BY cribs in well 299-E33-38 (Figure C.33). Whether the decline is caused by local differences in the BY cribs plume or reflects mixing with another source is unknown.

Figure C.32. Technetium-99 Concentrations in Well 299-E33-38 at the BY Cribs and Wells Along the Western Side of Waste Management Area B-BX-BY

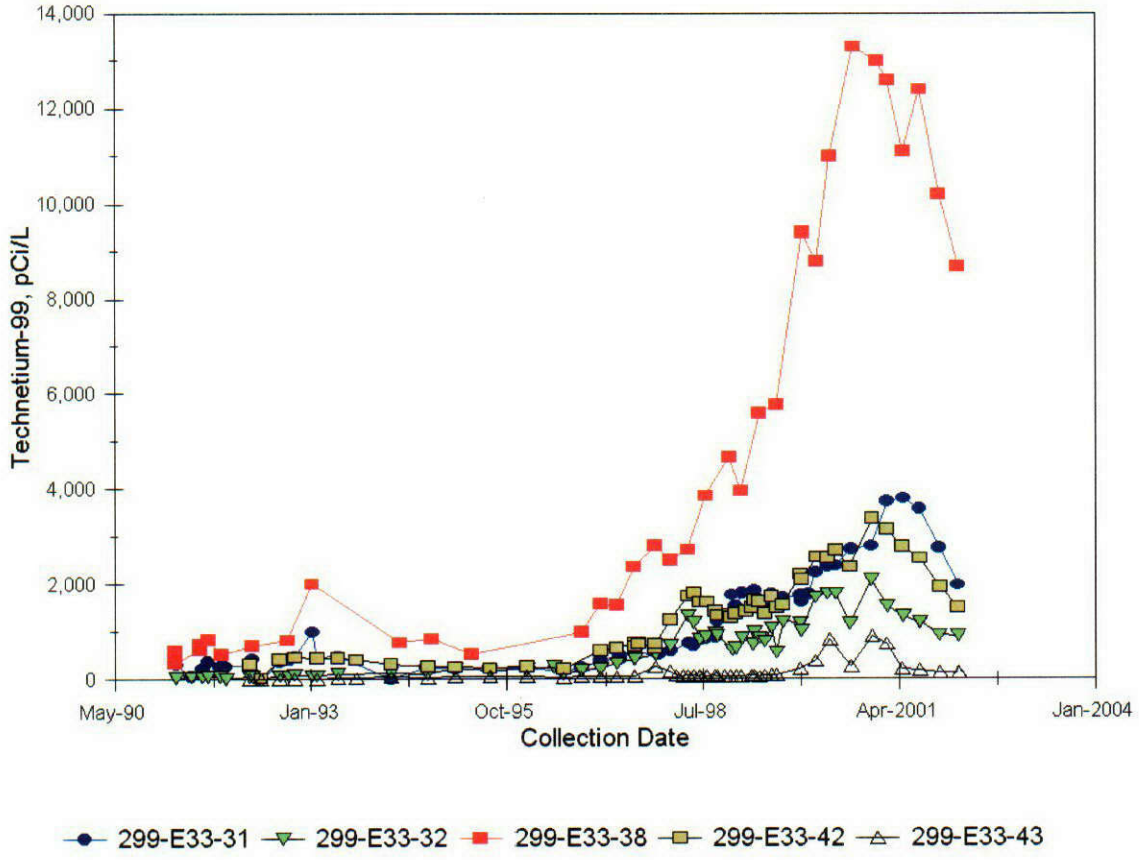

Figure C.33. Technetium-99 Concentrations in Wells in the Central Part of Waste Management Area B-BX-BY

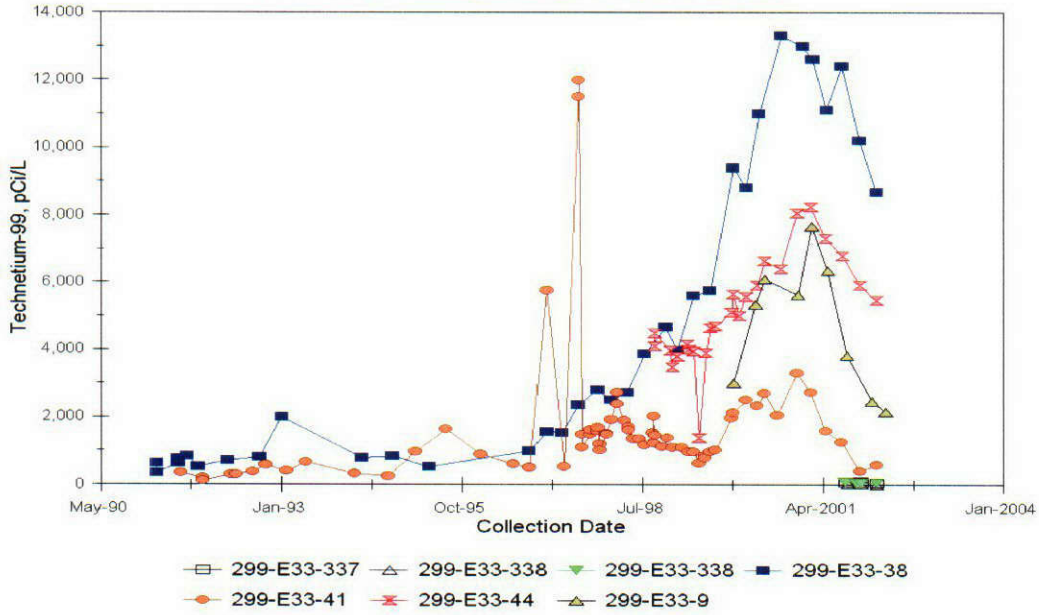

Nitrate concentrations exhibit similar trends as seen for technetium-99 as illustrated in Figures C.34 and C.35. While the general concentration trends for technetium-99 and nitrate are similar, there are differences in their ratios that provide clues to source areas and movement patterns.

Figure C.34. Nitrate Concentrations in Well 299-E33-38 at the BY Cribs and Along the Western Side of Waste Management Area B-BX-BY

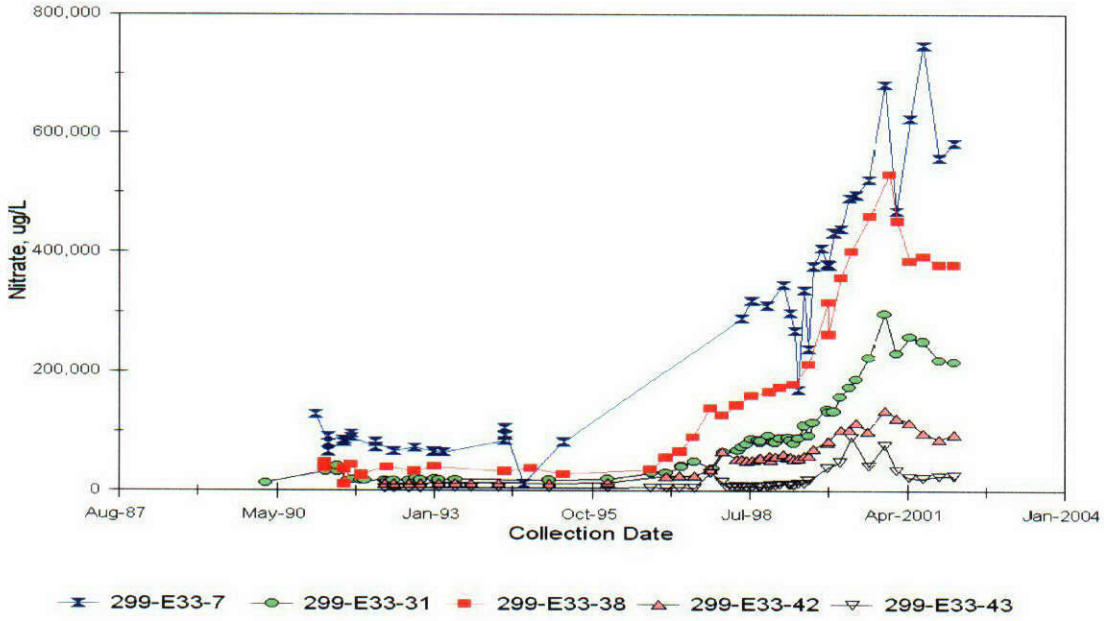

Figure C.35. Nitrate Concentrations at the BY Cribs and the Central Part of Waste Management Area B-BX-BY

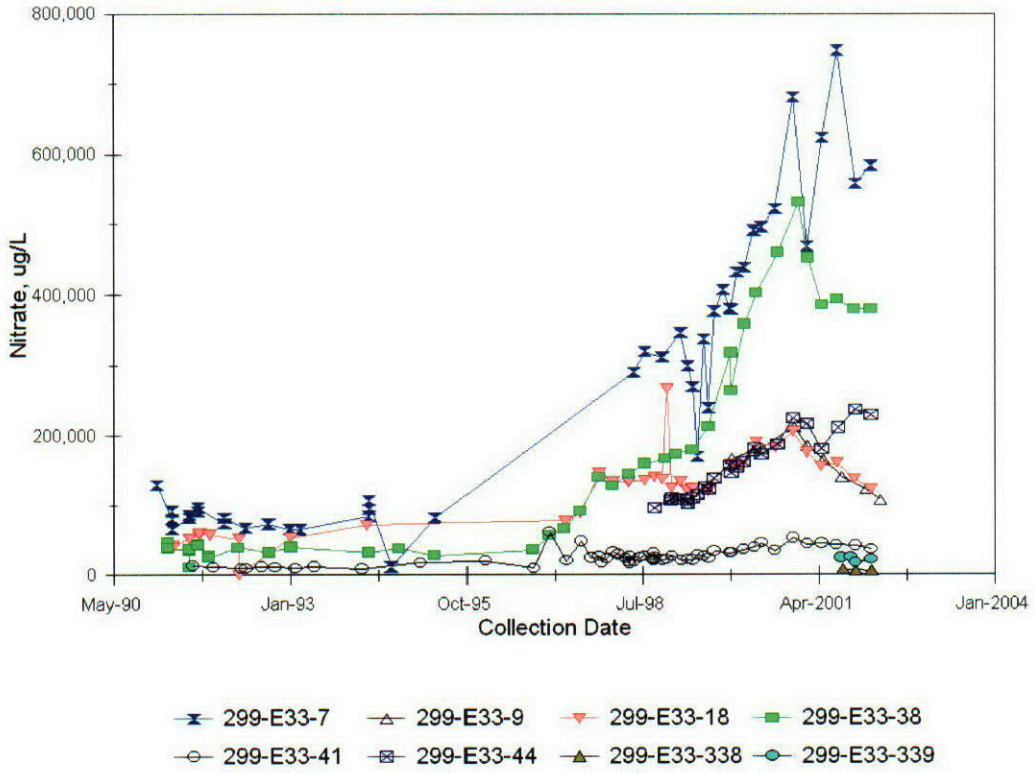

C.6.5.1.2 Cyanide. Cyanide occurs as a co-contaminant in the BY crib plume as identified in the early 1990s north of the BY cribs (Lindsey et al. 1992; Narbutovskih 2000). August 2001 concentrations in the vicinity of the BY cribs are currently at 341 µg/L for well 299-E33-7 and 192 µg/L for well 299-E33-38 (Figure C.36). In August 1999, this constituent was first detected south of the cribs in well 299-E33-44 (14 µg/L in August 2001) and later in February 2000, on the western side of the BY tank farm in well 299-E33-31 (28 µg/L in August 2001). During fiscal year 2001, cyanide was detected at low concentrations farther south on the western side in wells 299-E33-42 and 299-E33-32. Of the three newly installed wells along the southern border of the waste management area, cyanide was detected only in well 299-E33-337 at ~9 µg/L. Thus, cyanide from the BY cribs source appears to be spreading southward along with nitrate and technetium-99.

Figure C.36. Cyanide Concentrations in Wells at the BY Cribs and the Northern Portion of Waste Management Area B-BX-BY

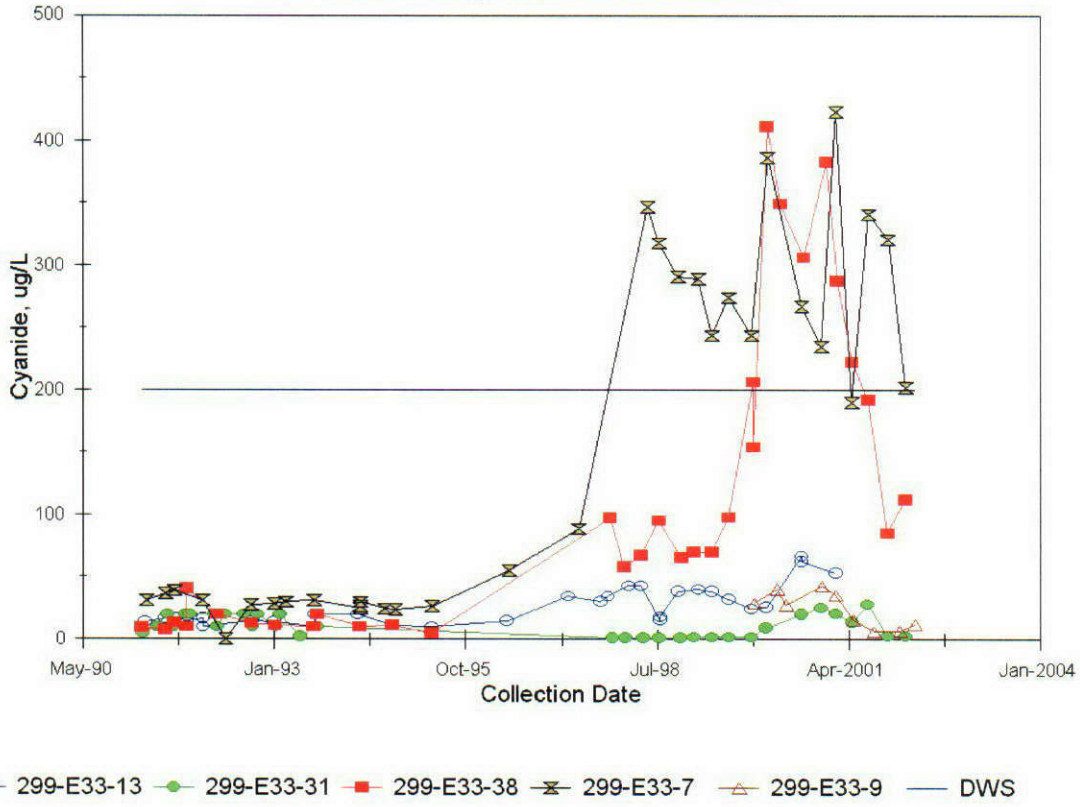

C.6.5.1.3 Uranium. Although uranium concentrations have been relatively static in the past and have not reflected the sharp increases seen in cyanide, nitrate, and technetium-99, uranium concentrations rose sharply in the central part of the waste management area (wells 299-E33-9 and 299-E33-44) after April 2000 to a maximum of 678 µg/L at the BY tank farm and now appear to be declining (Figure C.37). Uranium concentrations of this magnitude have not been observed either upgradient or downgradient from this central location. Upgradient, at the BY cribs, uranium was found at 165 µg/L during August 2001 in well 299-E33-38 while downgradient, in wells 299-E33-41 and 299-E33-18, values range from 133 µg/L to 24 µg/L. Although concentrations are somewhat variable over time, there is no obvious increase in uranium at either of these downgradient wells.

Figure C.37. Uranium Concentrations in Wells in the Central Part of Waste Management Area B-BX-BY

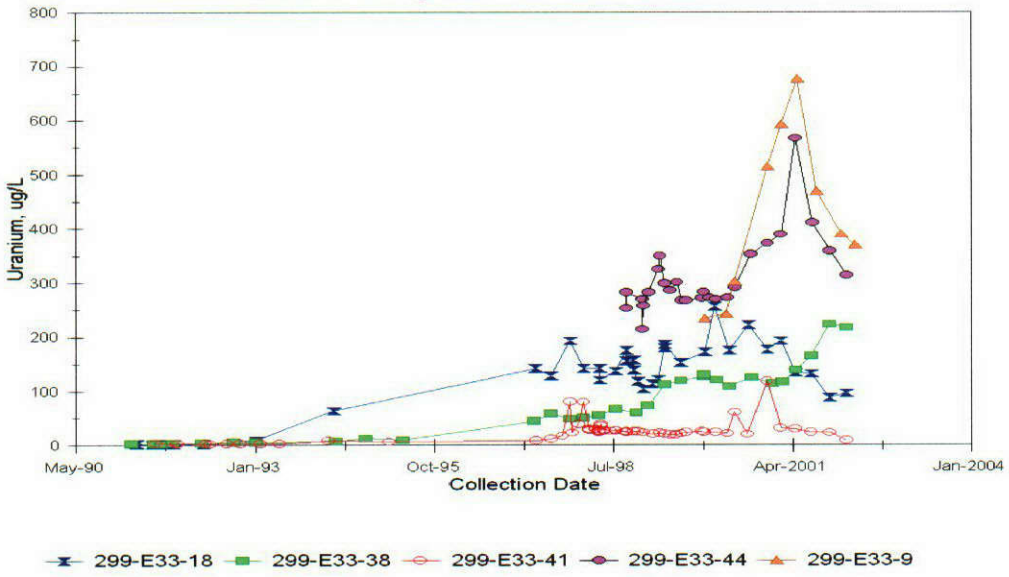

West of the waste management area, uranium increased steadily reaching a maximum in 2001 and now appears to be declining (Figure C.38). Values range from 66 µg/L in well 299-E33-31 to 29 µg/L in well 299-E33-42. Because uranium levels, both upgradient and downgradient of the BY tank farm, are either significantly lower or at background levels, the source of the uranium is, most likely, local.

Increasing uranium west of WMA B-BX-BY (e.g., wells 299-E33-26, 299-E33-31, and 299-E33-42) suggests that uranium may be migrating toward the west or southwest from the waste management area. Alternatively, the increasing uranium seen in wells 299-E33-31 and 299-E33-42 may be related to movement from the BY cribs region. A south or southwesterly direction is consistent with the inferred change in flow direction in the late 1990s (Figure C.28).

Figure C.38. Uranium Concentrations in Wells Northwest of Waste Management Area B-BX BY

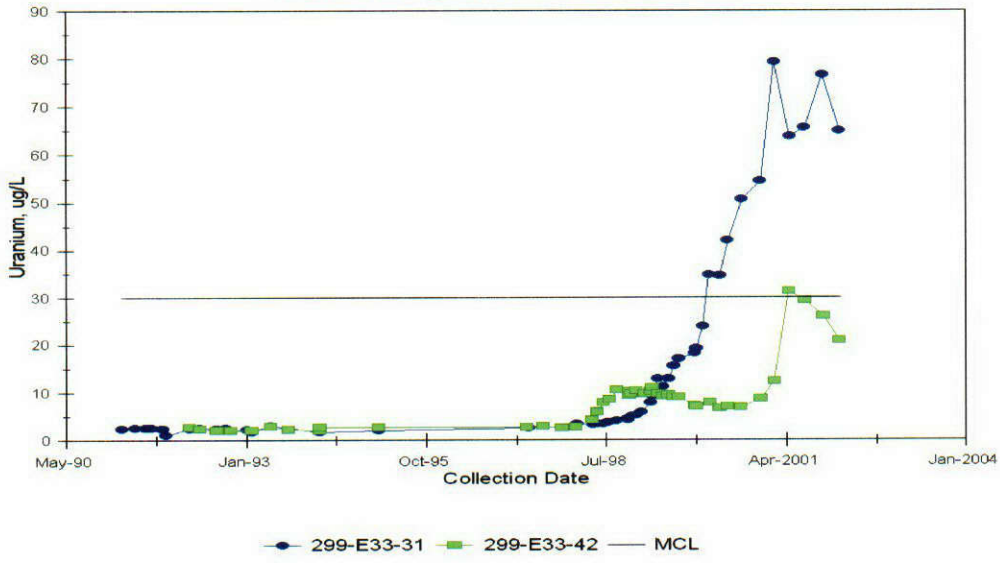

Cobalt-60. This neutron activation product was also associated with the large volume releases of waste to the BY cribs in the 1950s and appears to be correlated with cyanide. The high concentrations of cobalt-60 detected in the groundwater in the late 1950s provide direct evidence that mobile constituents from the BY crib discharges reached groundwater.

C.6.5.1.4 Tritium. Recently, tritium has become a contaminant of concern for WMA B-BX-BY (reported by Narbutovskih in Hartman et al. 2002). As shown in Figure C.39, tritium began rising abruptly in wells 299-E33-43 and 299-E33-32 on the western side of the BX tank farm from local background concentrations of ~2,000 pCi/L in early 1999. This trend is matched in wells 299-E33-334 and 299-E33-335 located in the southwestern corner of the site. The highest value of 21,400 pCi/L is found at the southeastern corner of the BX tank farm in the recently installed well 299-E33-339. This is above the drinking water standard of 20,000 pCi/L. Further to the east, a value of 14,500 pCi/L was detected in well 299-E33-337. To the north, tritium is still at background levels of 2,130 and 2,450 pCi/L in wells 299-E33-41 and 299-E33-42, respectively, indicating that tritium is not migrating into the local area from the north. Tritium values are also low in the southeastern corner of the waste management area in new well 299-E33-338.

Figure C.39. Comparison of Tritium Concentrations in the Southern Portion of Waste Management Area B-BX-BY to Upgradient Concentrations

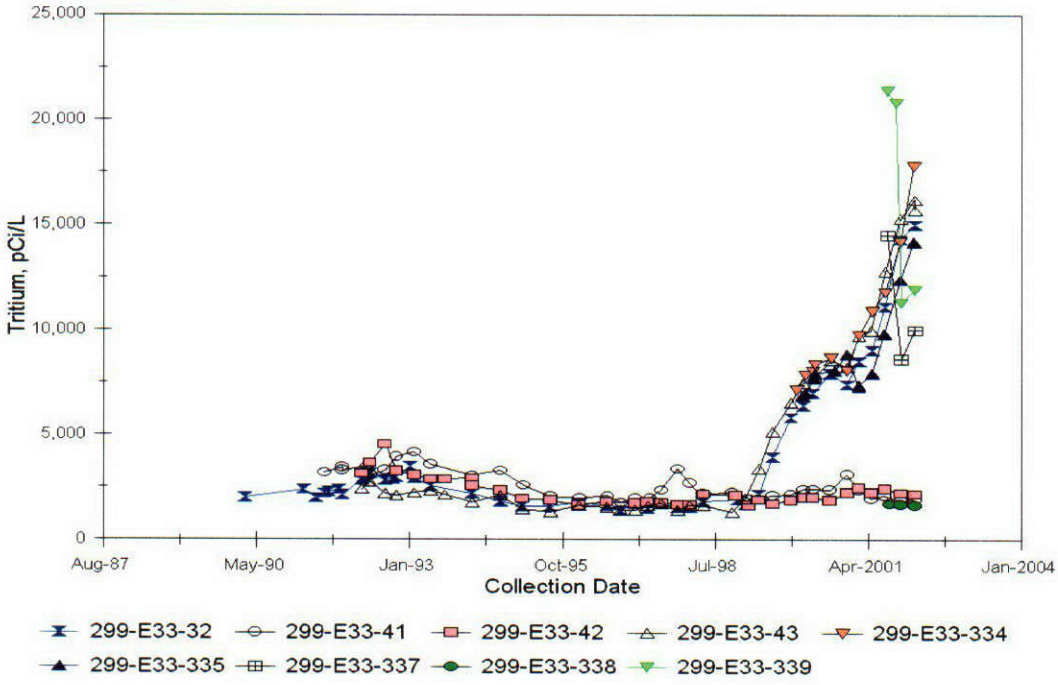

Also of interest was the discovery of elevated tritium in perched water during drilling of borehole 299-E33-45. The perched water zone was found on a local silt layer ~4.6 m above the water table. Perched water samples showed tritium concentrations of greater than 75,000 pCi/L. The tritium concentration in a groundwater sample collected from this well in January 2001 was only 2,410 pCi/L. The source of the much higher tritium concentrations in the perched water may be due to washdown of tritium from past leaks in evaporator (or tank condensate) transfer lines located nearby while the lower tritium concentration in the groundwater from the same well may be from a different source. Alternatively, the higher tritium source represented by the perched water results may be seeping through to the top of the underlying aquifer but dilution with deeper non-contaminated water may occur during sampling with a submersible pump (i.e., a borehole mixing or dilution effect). Depth discrete sampling is needed to evaluate the latter.

C.6.5.2 Areal Distribution Patterns

Spatial variation in contaminant concentrations may provide some clues about source areas. However, since concentrations change over time, a time-period must be chosen to examine spatial distribution patterns. For this purpose, the most recent data (average of last four sampling events) was chosen. Data were first grouped by geographic location and tabulated as shown in Table C.12. Data were then plotted and inspected for approximate distribution patterns or groupings. Contours of contaminant concentrations and selected contaminant ratios (e.g., nitrate/technetium-99) were then drawn to identify spatial patterns that might be indicative of source areas. Spatial distribution patterns are shown in Figures C.40 and C.41 and are discussed as follows.

Table C.12. Average Concentrations of Mobile Contaminants in Groundwater in the Vicinity of Waste Management Area B-BX-BY for Fiscal Year 2001

Wells [a]	NO_3 [b] (μg/L)	^{99}Tc [b] (pCi/L)	SO_4 [b] (μg/L)	Cyanide [b] (μg/L)	Tritium [b] (pCi/L)	U [b] (μg/L)	Cr [b] (μg/L)	$NO_3/^{99}Tc$ (μg/pCi)	NO_3/SO_4
North of BY Tank Farm									
E33-13	356,500	2,609	98,025	59.2	3,000	29.8	28.6	137	3.6
E33-38	384,000	10,595	138,500	152.8	6,715	186	21.4	36	2.8
E33-7	628,500	8,440	119,750	263.5	7,708	4.0	28.8	74	5.2
E33-26	323,750	6,235	124,500	56.0	14,350	151	15.1	52	2.6
North of B Tank Farm									
E33-15	395,500	367	77,300	2.1	2,690	3.4	33.5	1,078	5.1
E33-16	640,325	4,619	109,750	2.3	6,233	16.6	71.5	139	5.8
E33-17	247,500	84	46,525	1.9	2,268	5.1	23.5	2,964	5.3
E33-18	143,500	1,696	50,825	3.2	3,363	113	42.4	85	2.8
E33-20	314,500	300	65,650	2.1	2,673	3.8	19.6	1,048	4.8
E33-39	37,275	72	96,200	2.2	689	2.9	9.6	517	0.4
Waste Management Area B-BX-BY									
E33-31	236,750	3,028	83,275	11.8	3,265	67.8	10.8	78	2.8
E33-42	99,275	2,188	46,125	2.5	2,285	26.9	8.6	45	2.2
E33-32	87,025	1,087	57,925	3.4	12,363	3.5	6.2	80	1.5
E33-43	23,388	172	59,000	2.8	15,000	3.0	3.3	136	0.4
E33-44	214,250	6,370	101,600	8.3	8,068	412.8	20.7	34	2.1
E33-41	41,375	947	41,900	3.8	1,973	21.2	9.4	44	1.0
E33-9	133,500	3,690	119,500	10.2	4,763	477.5	14.8	36	1.1
E33-45	57,500	2,410	43,200	21.5	2,410	10.8	7	24	1.3
E33-339	22,350	68	64,000	2.5	16,350	3.7	3.5	329	0.3
E33-335	19,475	56	52,475	2.5	11,090	2.9	3.7	347	0.4
E33-334	20,675	51	56,100	3.5	13,675	2.8	3.8	405	0.4
E33-337	17,233	76	52,900	4.6	11,040	3.2	3.5	228	0.3
E33-338	6,790	16	32,133	2.5	1,693	2.7	2.8	434	0.2
E33-46	16,400	1,680	33,700	2.5	2,810	2.9	7	10	0.5
Low-Level Waste Management Area 1 and Vicinity									
E33-21	19,400	111	55,825	2.1	9,335	2.8	4.2	174	0.3
E33-34	420,750	7,945	124,000	184.9	13,325	51.9	18.9	53	3.4
E33-35	104,325	2,233	43,100	2.3	2,333	3.3	5.4	47	2.4
E33-28	25,100	153	51,900	6.3	8,955	2.9	4.9	164	0.5
E33-29	23,225	43	53,325	3.2	8,828	5.1	3.6	534	0.4
E28-27	32,100	17	66,075	5.0	17,475	10.4	4.9	1,879	0.5

[a] Well prefix 299 omitted.

[b] Average concentration calculated using most recent four measurements except for wells 299-E33-337 and 299-E33-338 (three measurements) and except for 299-E33-45 and 299-E33-46 (one measurement). Average concentrations are rounded to the nearest integer.

Figure C.40. Areal Distribution of Nitrate/Technetium-99 Ratios for Fiscal Year 2001

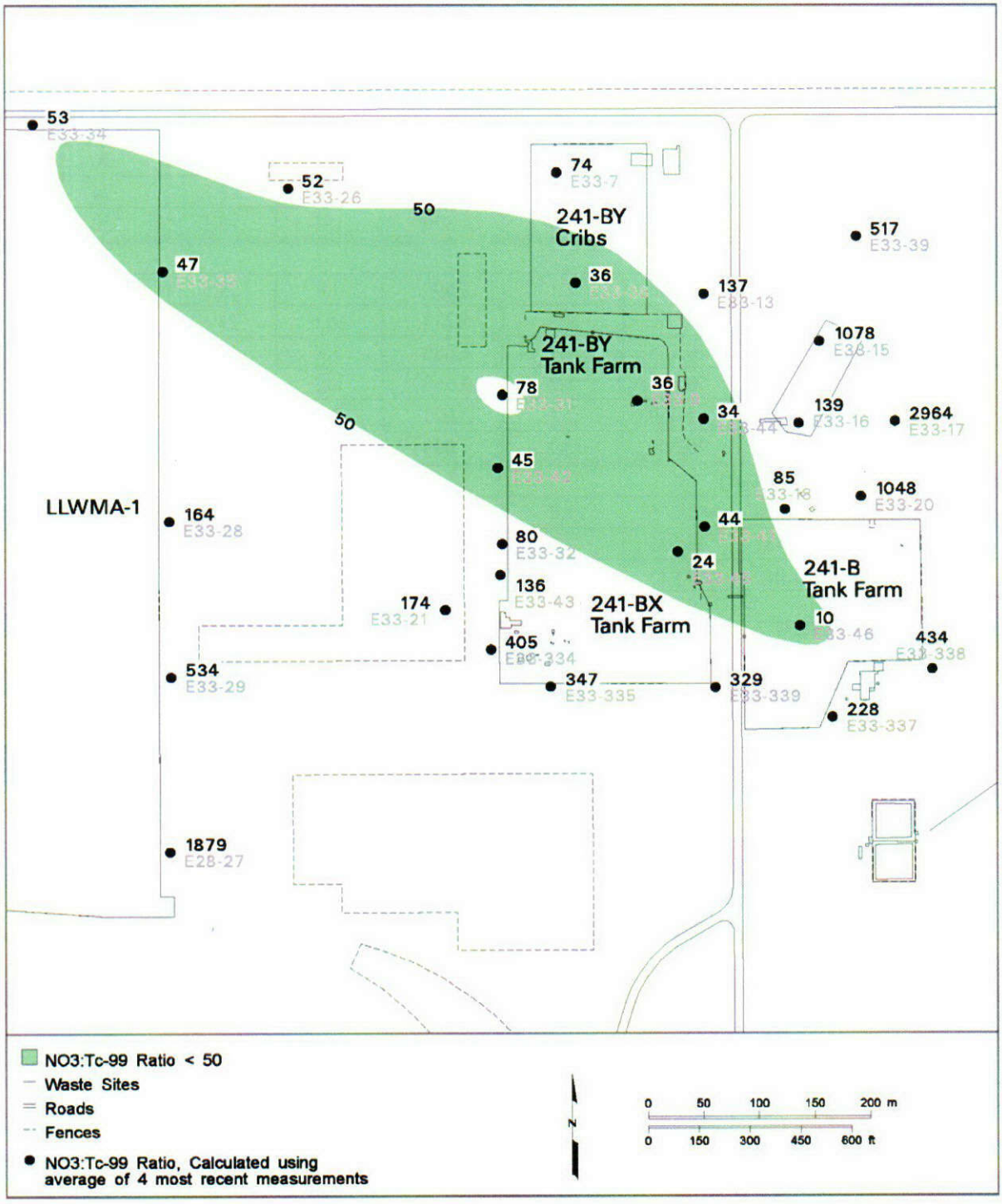

Figure C.41. Concentration Contours of Major Mobile Contaminants in the Vicinity of Waste Management Area B-BX-BY Based on Fiscal Year 2001 Averages from Table C.12

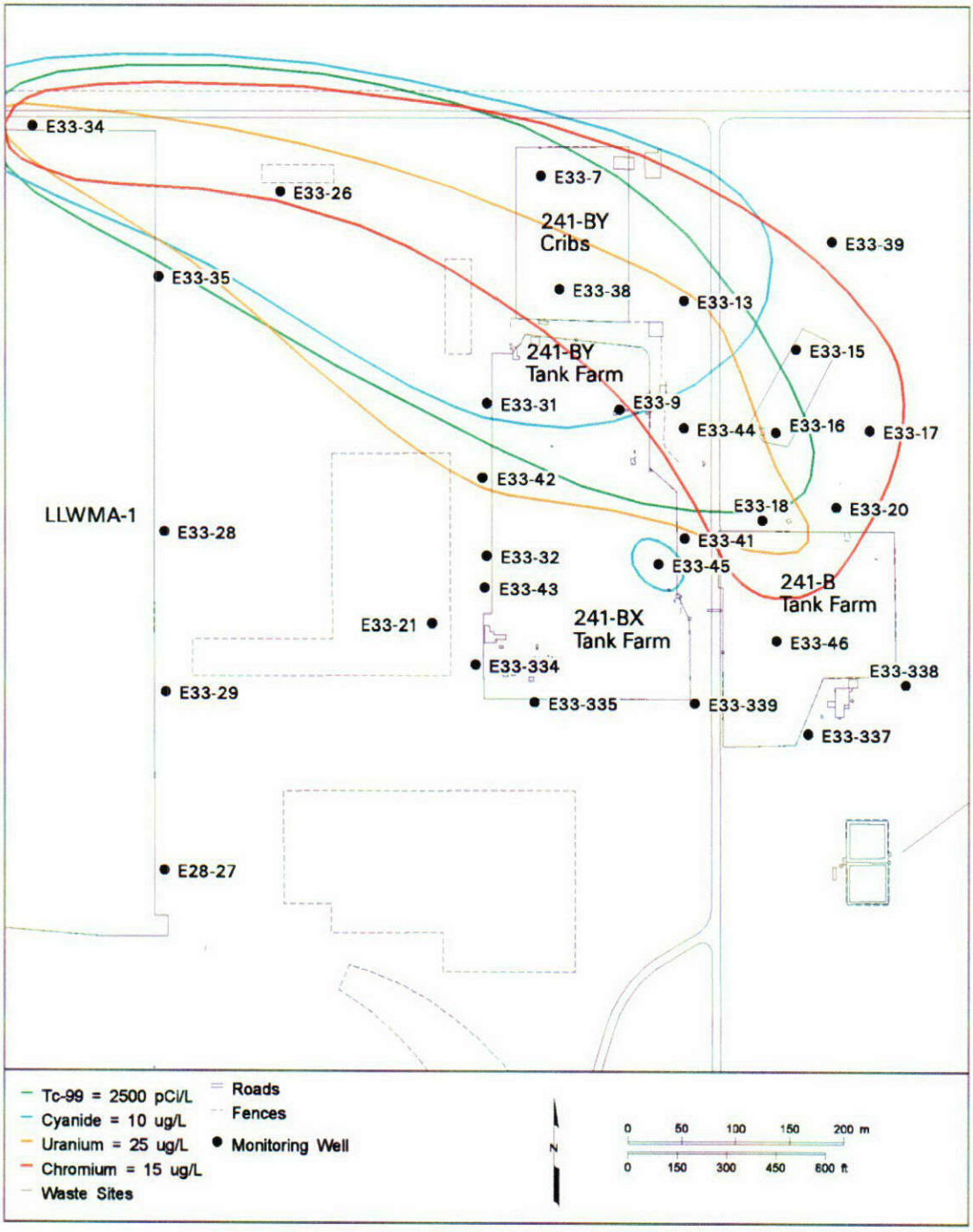

C.6.5.2.1 Nitrate/Technetium-99 Ratios. The ratio of nitrate to technetium-99 is one diagnostic tool used to identify different contaminant plumes with different sources in the groundwater. Tank related sources based on fission yield and process flow sheet estimates are expected to have low ratios because of the high concentrations of fission-produced technetium-99 with respect to nitrate.

The nitrate/technetium-99 ratios in Table C.13 (averages of most recent four sampling events) are shown together with well locations in Figure C.40. There appears to be a central zone in the vicinity of the BY cribs and the BY tank farms area with ratios that are in general similar to the soil ratios for the BY cribs (Table C.13). Wells with a ratio of less than 50 are shown within the shaded area. Beyond this zone, higher ratios are found, suggesting mixing of a BY crib type source with an ambient background containing elevated nitrate but lower concentrations of technetium-99. Very high ratios east of BY cribs and the BY tank farm are consistent with inventory based (Simpson et al. 2001) ratios for the 216-B-8 crib and tile field.

The largest volume of tank waste related discharges to the ground in the past, as previously noted, was the BY cribs (approximately 10 million gallons). Groundwater nitrate/technetium-99 ratios for wells north of the BY cribs (e.g., well 699-53-50) are similar to the BY crib core data (Table C.12) and the average ratio of 44 is based on inventory estimates for discharges to the BY cribs (Simpson et al. 2001; and Appendix B). It has previously been assumed that the high technetium-99 that appeared in well 699-53-50 (up to 30,000 pCi/L) was from the BY cribs. This assumption is supported by the nitrate/technetium-99 ratio data for BY crib core samples (Table C.13) and the inventory based estimate.

Table C.13. Nitrate/Technetium-99 Ratios in Soil and Groundwater Waste Management Area B-BX-BY and Vicinity

NO_3/Tc-99 (μg/pCi)					
Location	**Medium**	**Mean**	**Range**	**Standard Deviation**	**Number of Data Points**
299-E33-45[a]	Soil	13.8	[8.4, 25.4]	5.9	10
BY Cribs[b]	Soil	26.7	[16.1, 40.4]	9.0	7
699-50-53A[c]	Groundwater	27.7	[18.1, 43.7]	12.4	7
699-49-57A[d]	Groundwater	58.7	[34.6, 141.0]	28.2	17

[a] Only results above the perched water zone were used. Core samples collected in 2000.
[b] Core samples collected in 1991. Only 216-B-43 and 216-B-49 had useable data.
[c] Based on highest technetium-99 concentrations that occurred between 8/26/1987 and 4/28/1995. Technetium-99 concentrations ranged from 8,640 pCi/L to 32,700 pCi/L.
[d] Data used are from 2/9/1988 to 11/20/2000. Technetium-99 concentrations ranged from 610 to 3,200 pCi/L.

It is also noteworthy that the soil column nitrate/technetium-99 ratios near tank BX-102 (well 299-E33-45) are lower than for the BY crib soil cores (Table C.12). As noted by Narbutovskih in Hartman et al. (2002), these differences may allow distinction between tank sources and residual contamination remaining from the BY crib releases in the past. For example, the lowest observed groundwater ratios occur in the southeast portion of the WMA (exploratory boreholes 299-E33-45 and 299-E33-46). The ratios for these wells are similar to those observed for the vadose zone at the BX-102 (299-E33-45) site (Table C.13). Also, the groundwater ratios for wells 299-E33-44 and 299-E33-41 located nearby have been consistently lower (below 30 and as low as 14 in 299-E33-41) than for wells in the surrounding area. This more limited area of low ratios is most likely related to the spill site east of tank BX-102.

C.6.5.2.2 Contaminant Concentration Contours. Concentration contours of the major mobile tank waste and related constituents (i.e., technetium-99, uranium, cyanide, and chromium) are shown in Figure C.41. The general northwest-southeast trend is similar to the nitrate/technetium-99 ratio plot, reflecting the dominating northwesterly groundwater flow direction until the more recent flow reversal. The apparent northwest-southeast orientation of the plume distribution maps may also be influenced by a paleochannel oriented in the same direction.

In addition to the above, there are some differences in the individual constituent plots that point to possible source areas that are not evident from the nitrate/technetium-99 ratio plot. For example, uranium, cyanide, and technetium-99 all appear to be more closely related to the BY cribs and BY tank farm area. The uranium plume appears to be shifted more to the south than cyanide and technetium-99, possibly reflecting a uranium-rich tank waste spill in the BY tank farm area. However, no other evidence (e.g., spectral gamma data) points to a BY tank farm vadose zone source.

The chromium contour (area greater than 15 ug/L) is extended more to the east than the technetium-99, uranium, and cyanide plumes. This is consistent with the waste composition discharged to the 216-B-8 crib and tile field (second cycle waste that would have been depleted in uranium and technetium-99 with no cyanide but with hexavalent chromium used in the oxidation-reduction purification step). In addition to the above, uranium appears to be displaced further to the south than the cyanide and technetium-99.

The cyanide contour is centered more around the BY cribs and to the northwest, most likely reflecting the waste type in the BY cribs and immediate area. There is one cyanide anomaly at well 299-E33-45 (vadose exploratory borehole).

In addition to the above, the concentration contours or 'halos' do not suggest that the BX trenches (216-B-35 through 216-B-42 are major contributors to the existing plume distribution patterns in the WMA and vicinity. This inference is also consistent with the nitrate/technetium-99 ratios for wells in that area (Figure C.40).

In summary, the areal distribution plots indicate impacts on groundwater at and in the vicinity of the WMA from at least three different source types: 1) the BY crib area and adjacent unplanned release, 2) the 216-B-8 crib and tile field (north of the B tank farm), and 3) localized sources within the BX-BY portions of the WMA. The contaminants from these sources co-mingle and

show a general northwest to southeast trend that reflects recent past direction and an old stream channel oriented in the same general direction.

C.6.6 DISCUSSION

Contemporary groundwater contamination in the vicinity of B-BX-BY includes remnants of nuclear fuel reprocessing wastewater discharges that occurred over a relatively short time period 40 to 50 years ago. Since groundwater flow rates were on the order of 1 m/day or greater, more than sufficient time has passed for this contamination to leave the area. For example, at 1 m/day or 365 m/yr, groundwater contamination from a short-term release event should have migrated nearly 4 km away from the area in only 10 years and in less time at higher flow rates. Thus the persistent presence of residual waste constituents in groundwater must be due to either a combination of flow reversals or transport of residual waste in the soil column beneath the spill and discharge sites to groundwater. Distinguishing between these two possibilities is important for purposes of identifying further interim corrective measures. If the residual groundwater contamination is due to flow reversal, then there is no action that can be taken to attenuate the groundwater contamination. However, if it is due to infiltration from either precipitation events or leaking water lines, then the feasibility of additional corrective action may need to be considered. Data and observations presented in the foregoing sections can be used to evaluate these alternative explanations for the persistent presence of contaminants in groundwater 40 to 50 years after discharges ceased.

C.6.6.1 Flow Reversal Hypothesis

The large release of tank type waste occurred between 1954 and 1955. Based on the flow analysis presented in Section C.6.3, the inferred flow direction at this time was to the north until about June 1959. The inferred flow rate at this time was about 5 m/day in the area just north of the BY cribs (Section C.6.3). Based on gross beta levels in nearby wells, the groundwater concentrations dropped by 6 orders of magnitude within a year following termination of discharge to the BY cribs. The inferred flow rate of 5 m/day would theoretically transport the trailing edge of the 1954 through 1955 BY crib release nearly 2 km to the north by the end of 1957. This would position the trailing edge of the plume near a location beneath Gable Mountain Pond. With the rapid increase in discharge to the pond beginning in 1958, the mound created would have driven most of the 1954 through 1955 release northward through the gap. Only the trailing edge of the plume, which would have been at much lower concentrations than during the 1954 through 1955 release period, would theoretically have been in the right position to be transported back in the southerly direction. Unless the inferred flow rate was much lower than the 5 m/day estimate for the 1955 through 1959 time frame, it seems unlikely that much of the original release would have been susceptible to transport back in the southerly direction.

C.6.6.2 Episodic Transport

If the above considerations are correct, then some other source or release mechanism must account for the persistent presence of tank waste constituents that still exist in groundwater in the vicinity of WMA B-BX-BY today. One possibility is a release that occurred in the 1970s time frame. This was characterized by highly variable but persistently high nitrate and gross beta concentrations over about a 10-year period as indicated in well 299-E33-26 located west of the

BY cribs (Figure C.30). Operational history of cribs during this time does not suggest release of a high nitrate waste with beta activity. However, the 216-B-50 crib received large volumes of evaporator overheads between 1965 and 1974. Narrative provided in the WIDS noted concern in the early 1970s about the proximity of the evaporator discharge site and adjacent cribs that received large volumes of supernatant waste from the in-tank scavenging process. This type of soil column source contained high concentrations of mobile constituents such as nitrate, cobalt-60, cyanide, and other contaminants. The concern was that the tritium-bearing wastewater from the evaporator discharge site (216-B-50) could mobilize the residual high salt waste in the adjacent soil column beneath cribs 216-B-46 and 216-B-49. The occurrence of silt stringers in the Hanford formation in this area could have facilitated lateral spreading and allowed the 216-B-50 wastewater to come in contact with residual waste from the 216-B-46 and 216-B-49 cribs.

The timing for the observation in the nearby monitoring well (299-E33-26) and the release history of evaporator waste to 216-B-50 however, do not coincide well. For example, the crib operated from 1965 through 1974 but well 299-E33-26 shows a response from about 1971 to 1981 or 1982. The average discharge rate to the crib was about 10 L/min. Perhaps the infiltration rate was slow enough to account for the 6-year off set in timing. But even if the vadose transport delay occurred, a westerly flow direction (Table C.9) does not appear until about 1973. Thus, it is difficult to reconcile this source with an arrival time of 1971 in well 299-E33-26.

One other alternative is the simpler idea of episodic transport from the major soil column sources (i.e., BY cribs and spills within the WMA and vicinity). For example, large snowmelt events have occurred periodically over time. In recent years, the largest snowfalls on record occurred in 1993 and in 1996 to 1997. A rapid snowmelt scenario would involve a relatively short-term occurrence of groundwater contamination transport near the source areas.

As discussed in Section C.6.5.1, recent time series plots of contaminants in the WMA and vicinity suggest release events that were short-term in nature (contaminant concentrations that increase rapidly and then decline over a period of months). One problem with this scenario, at least for the BY cribs, is that a plastic, soil, and cheat grass cover was placed over the BY cribs area in the mid-1970s. It is thus unlikely that residual soil column contamination from this source is susceptible to transient natural infiltration events since the 1970s. However, there is an adjacent spill site located immediately east of the BY cribs. This area may still be subject to episodic soil washdown events that result in a groundwater contaminant signature characteristic of BY crib type waste. Other uncovered source areas (e.g., 216-B-8 crib and tile field) would be subject to the same release and transport process. If this is the case, then control of surface water run-on, water line leaks, and natural infiltration becomes a more important *Comprehensive Environmental Restoration, Compensation, and Liability Act* (CERCLA) as well as RCRA issue. Work is progressing toward this end as part of the interim corrective measures in the tank farm areas.

C.6.7 SUMMARY AND CONCLUSIONS

Historical discharges and spills of liquid waste to the ground within and in the vicinity of WMA B-BX-BY resulted in complex patterns of groundwater contamination resulting from:

- Historical changes in flow direction
- Co-mingling or mixing of multiple plumes from different sources
- Mobilization of residual vadose zone sources from infiltration events and/or leaking water lines.

The highest groundwater concentrations of technetium-99 are in the vicinity of the BY cribs and are attributed primarily to residual soil column sources from discharges in the mid-1950s. The technetium-99 in the BY crib area is associated with high concentrations of nitrate and cyanide with some cobalt-60. The areal contaminant distribution and concentration history are consistent with a reversal in flow direction from a northerly to a southerly direction in the late 1990s. Elevated uranium is found locally in the vicinity of the BY tank farm while a small tritium plume has been found along the southern margin of the waste management area.

The agreement between nitrate/technetium-99 ratios in groundwater and in the soil column near tank BX-102 where spills occurred in the past suggest this area is a localized source of groundwater contamination that was intersected by the two new borehole characterization wells drilled for this investigation. A direct link between the tank BX-102 spill source and the underlying soil and groundwater contamination cannot be made due to the discrepancy between predicted tank contents (contaminant ratios) and subsurface observations. Sludge sample analyses of the tank contents would help eliminate this uncertainty.

C.7.0 SUMMARY OF GEOCHEMICAL PROPERTIES OF SELECTED RADIONUCLIDES

A literature survey was initiated to evaluate the variety of gamma-emitting radionuclides encountered in WMA B-BX-BY. In developing the WMA S-SX field investigation report, cesium-137 was the only gamma emitting radionuclide of concern (Knepp 2002). However, in WMA B-BX-BY, the spectral gamma logging data identify seven gamma emitting radionuclides, cesium-137, antimony-125, europium-152, europium-154, cobalt-60, uranium-235, and uranium-238 (DOE-GJPO 1998). The geochemical properties of a number of these isotopes, such as antimony-125 and the two europium isotopes, have not been extensively investigated at Hanford. This task was initiated to assure that understanding of the geochemical properties of these isotopes reflects the current state of knowledge. A literature review was conducted to assess the important oxidation/reduction, aqueous speciation, solubility, and adsorption processes affecting the environmental behavior of antimony, cobalt, europium, technetium, and uranium in vadose zone sediments with low-organic matter content, in semi-arid environments such as those at the Hanford Site (Krupka and Serne 2002). All references supporting the summary statements given below are listed in *Geochemical Factors Affecting the Behavior of Antimony, Cobalt, Europium, Technetium, and Uranium in Vadose Zone Sediments* (Krupka and Serne 2002). Technetium-99 was included in this task because of its importance in the long-term risk calculations.

C.7.1 ANTIMONY

Compared to most elements, little is known about the environmental behavior of antimony, especially with respect to its mobility in sediments and soils. Antimony can exist in several oxidation states, including -3, 0, +3, and +5. Under natural environmental conditions, Sb(V) and Sb(III) are the stable oxidation states under oxidizing and reducing conditions, respectively, based on equilibrium thermodynamic considerations. Limited thermodynamic data for antimony aqueous species and solids preclude quantitative aqueous speciation and solubility calculations for Sb(V) and Sb(III) over the entire Eh-pH range germane to the Hanford vadose zone. However, most geochemists consider antimony to be relatively mobile in the environment, especially under oxic conditions.

Contrary to thermodynamic predictions, Sb(V) and Sb(III) have been found coexisting in a wide range of natural aqueous systems. Researchers have suggested that the metastability of Sb(III) under oxic conditions may have resulted from biotic processes and/or a slow rate of Sb(III) oxidation. Proposed explanations for observed metastability of Sb(V) in otherwise reducing environments include the transport of Sb(V) on sinking detritus from oxic waters, formation of Sb(V) thiocomplexes, or advection of oxic waters containing high Sb(V) concentrations, all coupled with a slow rate of Sb(V) reduction.

Thermodynamic data for the aqueous species and solids of Sb(V) and Sb(III) are limited. Under oxic conditions, the hydrolytic species $Sb(OH)_6^-$ is calculated to be the dominant antimony aqueous species at pH values greater than approximately 2.5 under oxidizing to slightly reducing conditions. At moderately reducing conditions, the speciation is dominated by the Sb(III) hydrolytic species $Sb(OH)_3^\circ$ (aq) at pH values from 2 to 12, and by $Sb(OH)_4^-$ at pH values greater 12. Antimony, especially under oxic conditions, is very soluble. The concentrations of

antimony in most soils are not likely limited by solubility considerations. Under reducing conditions, antimony concentrations may be limited by the solubility of antimony sulfides, such as stibnite (Sb_2S_3).

The concentrations of antimony in soils and sediments are likely controlled by adsorption reactions. However, very little is known about the adsorption/desorption behavior of Sb(V) or Sb(III). Because dissolved Sb(V) is present primarily as the anionic hydrolytic species $Sb(OH)_6^-$ over almost the entire pH range, the adsorption of Sb(V) to hydroxide and oxide mineral surfaces should be limited to negligible as pH increases from circumneutral to highly basic pH values. Under these conditions, antimony should be highly mobile in the geochemical environment. However, the adsorption of Sb(V) to mineral surfaces may be significant at acidic pH conditions. Only one adsorption study of antimony onto sediment from the Hanford Site was identified during the course of this review. The results of this study indicated that the adsorption of antimony is very low in Hanford soils contacting high-salt, high pH solutions (i.e., simulated SST liquors).

C.7.2 COBALT

Cobalt can exist in the +2 and +3 oxidation states. Under most geochemical conditions, Co(II) is the stable valence state in water. Cobalt(III) is a strong oxidizing agent, is not thermodynamically stable, and decomposes under Eh-pH conditions common for most natural waters. Some complexing ligands, such as EDTA and NH_3, can stabilize the Co(III) valence state and allow it to persist in aqueous solutions wherein Co(III) would normally readily reduce to Co(II) species.

Under oxidizing and moderately reducing conditions, the uncomplexed ion Co^{2+} is the dominant cobalt aqueous species at pH values less than 9.5. At pH values from 9.5 and 13.5, the hydrolytic species $Co(OH)_2^\circ$ (aq) becomes dominant. Under very reducing conditions in the presence of dissolved sulfide, Co(II) bisulfide species, such as $Co(HS)_2^\circ$ (aq), likely dominate the aqueous speciation. Cobalt does not appear to form any important complexes with dissolved chloride, nitrate, sulfate, and carbonate. Cobalt may form strong complexes with natural and synthetic organic ligands, such as EDTA.

No discrete cobalt minerals have been identified in surface sediment and soil systems. Cobalt is often found in solid solution with other elements, such as Fe(II), Fe(III), Mn(III), Cu(II), Mg(II), Cr(III), and Sn(IV), and in minerals rich with such elements. Thermodynamic calculations indicate that, at a total concentration of $10^{-14.8}$ mol/L dissolved cobalt, the mineral cattierite ($Co^{II}S_2$) may precipitate under very reducing conditions over a wide pH range. Increasing the total concentration of dissolved cobalt to $10^{-12.0}$ mol/L, Co_3O_4 ($Co^{II}Co_2^{III}O_4$) calculates to be oversaturated at pH values greater than 9 under highly oxidizing conditions. However, for most environmental conditions relevant to the Hanford vadose zone, pure cobalt-bearing minerals such as these are not expected to act as solubility controls.

The adsorption of cobalt has been studied on a variety of minerals, sediments, soils, and crushed rock materials. The adsorption of cobalt in sediments and soils is closely linked to its oxidation state, and is largely controlled by the presence of iron and manganese oxides and clay minerals. In the absence of organic complexants, cobalt is moderately-to-highly adsorbed on minerals, and

cobalt K_d values commonly reported in the literature range from 10^3 to 10^5 mL/g. Recent studies indicate that at high surface loadings, surface-mediated precipitation processes may be responsible for the high adsorption (i.e., large K_d values) observed for cobalt. At high pH values and at high surface loadings of cobalt, Co(II) adsorption results in the precipitation of a $Co^{II}(OH)_2$-like phase on mineral surfaces. On aluminum-containing adsorbents, the surface precipitate was found to have a hydrotalcite-like structure containing aluminum ions. The solution pH has a significant effect on the adsorption of cobalt. Cobalt in the absence of organic complexants exhibits cation adsorption behavior. As such, the adsorption of cobalt is zero to minimal at acidic conditions, then increases in the pH range of 4 to 7 with increasing pH, and continues to be high at basic pH conditions. The presence of some inorganic ligands, such as cyanide and possibly nitrite, and other dissolved cations, such as the alkali and alkaline earth ions, can decrease cobalt adsorption. The diminished adsorption effects of the anions cyanide and nitrite are believed to be caused by the formation of anionic complexes that form with the uncomplexed cobalt cations. The anionic aqueous complexes are electrostatically repelled by most soil surfaces, which have an inherent negative charge at high pH conditions. The diminished adsorption effects caused by alkali and alkaline earth cations are due to competitive cation exchange processes.

Complexation of cobalt by organic ligands, such as EDTA, significantly reduces cobalt adsorption at near neutral and basic pH values. Co-EDTA complexation has been identified as the cause for the enhanced ^{60}Co mobility observed at several nuclear waste disposal sites. This decrease in cobalt adsorption is typically caused by the formation of anionic cobalt complexes, which do not readily adsorb on mineral surfaces at basic pH values. Cobalt(II) is initially complexed to form the anionic complex $Co^{II}EDTA^{2-}$. This complex however, is then dissociated via a complex series of reactions that result in the oxidation of Co(II) to Co(III) and formation of $Co^{III}EDTA^-$. The reaction process initially involves the adsorption of $Co^{II}EDTA^{2-}$ to surface sites on the iron and aluminum oxides in the sediments, which in turn leads to the dissolution of these oxides. The dissociation of $Co^{II}EDTA^{2-}$ is promoted by the solubilized Fe(III) and Al(III). The dissolution-exchange reaction generates a suite of adsorbates Co^{2+}, $Co^{II}EDTA^{2-}$, FeEDTA, and $AlEDTA^-$ that compete for the EDTA aqueous ligand and the surface adsorption sites. Dependent upon the concentrations of each of the aqueous species, number of surface adsorption sites, and pH of the system, the distribution of the total mass of cobalt between the solution and solid phases is complicated but may be estimated using computer modeling methods.

Several studies of the adsorption of Co(II) on sediments from the Hanford Site have been completed. Based on a compilation of Kd values reported in Co(II) adsorption studies using Hanford Site sediments, it can be concluded that cobalt is highly immobile (i.e., Kd > 10^3 mL/g) for natural groundwater conditions at the Hanford Site in the absence of organic chelating agents, such as EDTA. However, Co-60 is known to be mobile in both the vadose zone and groundwater in some waste types leaked from tanks or intentionally discharged to cribs and specific retention trenches. Specifically, the waste streams coming from the uranium recovery process carry an unidentified mobile Co-60 species. In addition, a number of the waste streams coming from the B Plant isotope recovery processes carry an unidentified mobile Co-60 species. In the case of the B Plant waste streams, the Co-60 species is likely to involve organic chelating agents used in the isotope recovery processes. Little is known about the speciation of the mobile Co-60 associated with the uranium recovery waste streams.

C.7.3 EUROPIUM

Europium is a member of the lanthanide series of transition metals, which includes the element group known as the rare earth elements. Considerable attention has been given to the geochemical behavior of europium and the other rare earth elements. Because of the unique chemical behavior of this series of elements, the rare earth elements have been used extensively as tracers by geochemists in the study of the origin and formation of rocks. In addition, the use of europium and the other rare earth elements as analogues in the study of the geochemical behavior of trivalent actinide elements, such as Am(III) and Cm(III), is well accepted.

The most stable oxidation state for europium and the other elements in the lanthanide series is +3. For a few lanthanide series elements, such as europium, other oxidation states are known, but these are less stable. Europium is the only lanthanide for which the +2 oxidation state is sufficiently stable under natural conditions to affect its mineralogy and aqueous chemistry. Thermodynamic calculations indicate that the stability of Eu(II) is restricted to circumneutral pH values at extremely reducing conditions. Essentially no information is available for the aqueous geochemistry and environmental behavior of Eu(II). Given the similarities in their ionic radii, the Eu^{+2} ion will likely have a geochemical behavior similar to Sr^{+2}, and substitute for Ca^{+2} in minerals.

Europium(III) readily forms complexes with dissolved ligands present in natural waters. In the absence of dissolved sulfate, the uncomplexed ion Eu^{+3} is the dominant Eu(III) aqueous species predicted at acidic pH conditions from thermodynamic data. With the addition of dissolved sulfate, the Eu(III) sulfate complex $EuSO_4^+$ will replace Eu^{+3} as the dominant Eu(III) aqueous species at acidic pH conditions. However, at pH values from 6 to greater than 13, thermodynamic calculations indicate that the aqueous speciation of Eu(III) will be dominated by the formation of carbonate complexes. In carbonate-containing waters, the dominant Eu(III) species are predicted to be the neutral species $Eu(OH)_2CO_3^\circ$ (aq) from approximately pH 6 to 9, and the anionic species $Eu(OH)_2CO_3^-$ from pH 9 to greater than 13. It should be noted that the formation of strong carbonate-complexes, especially $Eu(OH)_2CO_3^-$, is inconsistent with the observed low-solubility and high adsorption properties observed by researchers who have studied the geochemistry of Eu(III) at basic pH conditions.

Europium(III) is considered sparingly soluble in environmental systems. Its low solubility may be a contributing factor to the large partition (distribution) coefficient, K_d, values that have been experimentally determined for europium. Europium(III) may exist as a primary component in several solid oxides, hydroxides, halides, hydroxyhalides, oxyhalides, sulfides, phosphates, carbonates, sulfates, and nitrates present in tank sludges and contaminated vadose zone sediments, but thermodynamic constants for such solids are limited. Solubility calculations based on currently available thermodynamic data suggest that the concentrations of dissolved Eu(III) will be limited to a total concentration of about 10^{-6} mol/L dissolved europium by the solubility of $Eu_2(CO_3)_3 \cdot 2H_2O$ in pH range from 5 to 8 for Hanford groundwater conditions. Similar calculations by others and the result of a limited solubility study indicate that dissolved Eu(III) may be controlled by solid $Eu(OH)_3$. The precipitation of $Eu(OH)_3$ is rapid and a likely solubility control for dissolved europium in slightly acidic to alkaline solutions.

The adsorption behavior of europium is similar to the other rare earth elements and trivalent actinides, such as Am(III) and Cm(III). Trivalent elements are considered to be highly sorbed in sediments (i.e., exhibit high K_d values) and thus immobile in most environments. The mobility of trivalent elements in the environment however increases at acidic pH values and in high ionic strength solutions. Few studies were identified for europium adsorption on sediment samples from the Hanford Site. Based on a published geochemical data package compiled to support the performance assessment studies of immobilized low-activity tank wastes at the Hanford Site, a range of K_d values from 100 to 1,500 ml/g was recommended for the radionuclide group "Ac, Am, Ce, Cm, Eu" for the "chemically impacted far field in sand sequence" environment where the pH is in the range from 8 to 11.

Because trivalent elements strongly adsorb to sediment particles, there is potential for colloid-facilitated transport of europium and other trivalent elements in vadose zone and groundwater systems. The reader is cautioned however that the importance of colloid-facilitated migration, especially in environmental systems that do not involve fracture flow of porewater or groundwater, is still the subject of debate.

C.7.4 TECHNETIUM

Technetium exists in oxidation states from +7 to -1. In natural environments, the most stable oxidation states of technetium are +7 and +4 under oxidizing and reducing conditions, respectively. Other oxidation states are encountered chiefly in complex compounds. The environmental behavior of technetium under oxic conditions has been studied extensively. Dissolved technetium is present in oxic environmental systems as the aqueous technetium(VII) oxyanion species TcO_4^- over the complete pH range of natural waters. The TcO_4^- anion is essentially nonadsorptive (i.e., K_d values are ≈0 ml/g) at circumneutral and basic pH values, and is also highly soluble. The concentration of technetium(VII) in the vadose zone and groundwater will therefore not be limited by adsorption or solubility processes, and thus will be highly mobile in oxic environments, such as the Hanford vadose zone. Under reducing conditions, technetium(IV) is sparingly soluble and highly sorbed. Technetium(IV) is therefore considered to be essentially immobile in reducing subsurface environments. However, studies of technetium under reducing conditions are limited compared to the number of technetium studies conducted under oxic conditions.

Under reducing conditions, technetium aqueous speciation is dominated at pH values greater than 2 by the neutral technetium(IV) species $TcO(OH)_2^\circ$ (aq) in the absence of dissolved carbonate. In carbonate-containing waters, technetium(IV) carbonate complexes, such as $TcCO_3(OH)_2^\circ$ (aq) and $TcCO_3(OH)_3^-$, may become important aqueous complexes of technetium. Thermodynamic calculations suggest the possible formation of Tc^{3+} at pH values less than 2 under extremely reducing conditions. Although the thermodynamic stability of TcO_4^- is well established, thermodynamic data for other aqueous complexes and solids containing technetium in its various valence states are extremely limited. The absence of such data precludes the use of thermodynamic calculations to evaluate the environmental behavior of reduced species of dissolved technetium with respect to pH, Eh, and the presence of important dissolved complexing ligands such as dissolved phosphate, sulfate, chloride, and others.

Technetium(VII) as TcO_4^- is highly soluble, and does not form solubility-controlling phases in geochemical systems. Technetium(VII) can be reduced to technetium(IV) by biotic and abiotic processes. This reduction results in a decrease in the dissolved concentrations of technetium due to the precipitation of the sparingly soluble solid $TcO_2 \cdot nH_2O$. Under reducing conditions, concentrations of total dissolved technetium will be limited to approximately 10^{-7} mg/L at pH values greater than 5 by the solubility of $TcO_2 \cdot 1.6H_2O$ (am) based on thermodynamic considerations. In reduced iron-sulfide systems, technetium(VII) can be reduced to technetium(IV) with coprecipitation with FeS solid (mackinawite).

Numerous studies on the sorption of technetium on sediments, soils, pure minerals, oxide phases, and crushed rock materials have been conducted. These studies consist primarily of measurements of K_d values for technetium(VII). The adsorption of technetium(VII) oxyanion TcO_4^- is expected to very low to zero at circumneutral and basic pH conditions, and to increase with when pH values decrease to less than 5. Technetium(IV) is considered to be essentially immobile, because it readily precipitates as sparingly soluble hydrous oxides and forms strong complexes with surface sites on iron and aluminum oxides and clays.

Several technetium K_d studies have been completed using Hanford sediments. A recent compilation of K_d values measured for Hanford sediments indicates that the adsorption of technetium(VII), as pertechnetate (TcO_4^-), is low for nearly all of the geochemical conditions associated with the vadose zone and upper unconfined aquifer at the Hanford Site. The compiled technetium(VII) K_d values typically ranged from 0.0 to 0.1 ml/g, and values from a few studies were as large as approximately 1 ml/g.

It is generally assumed that technetium is released to and present in the vadose zone and groundwater at the Hanford Site as oxidized technetium(VII). The results of recent studies of waste samples from certain underground storage tanks at the Hanford Site indicate that a significant fraction of the technetium in the waste is present in the +4 oxidation. Based on these results, the conceptual model for the release of technetium from the Hanford underground storage tanks may need to consider the potential mobility of technetium(IV) in the near-field, vadose sediments and potential interactions of organics present in the tanks with respect to complexing and stabilizing technetium(IV) and possibly other intermediate valence states of dissolved technetium.

C.7.5 URANIUM

The geochemical behavior of uranium has received extensive study due to the importance of uranium as an energy source and as a geochronology indicator. Uranium can exist in the +3, +4, +5, and +6 oxidation states in aqueous environments. Uranium(VI) (i.e., uranyl, UO_2^{2+}) and U(IV) are the most common oxidation states of uranium in natural environments. Uranium will exist in the +6 oxidation state under oxidizing to mildly reducing environments. Uranium(IV) is stable under reducing conditions, and is considered relatively immobile, because U(IV) forms sparingly soluble minerals, such as uraninite (UO_2). Dissolved U(III) easily oxidizes to U(IV) under most reducing conditions found in nature. The U(V) aqueous species (UO_2^+) readily disproportionates to U(IV) and U(VI).

The aqueous speciation of U(VI) in carbonate-containing waters at near neutral and basic higher pH values is dominated by a series of strong anionic aqueous carbonate complexes [e.g., $UO_2CO_3^\circ$ (aq), $UO_2(CO_3)_2^{2-}$, and $UO_2(CO_3)_3^{4-}$]. Because anions do not readily adsorb to mineral surfaces at basic pH conditions, the formation of anionic U(VI) carbonate complexes at pH values greater than 6 result in an increase in U(VI) solubility, decreased U(VI) adsorption, and thus increased mobility of uranium. The Hanford vadose zone and upper unconfined aquifer environments contain adequate carbonate concentrations to have these uranyl carbonate complexes dominate the aqueous speciation of uranium. In fact, direct verification for the uranyl carbonate dominance in vadose zone porewaters from borehole 299-E33-45 is presented in Appendix D. Under reducing conditions, the speciation of U(IV) is dominated by the neutral aqueous species $U(OH)_4^\circ$ (aq) at pH values greater than 2.

Under reducing conditions or near a uranium source where elevated concentrations of uranium may exist, uranium mineral dissolution, precipitation, and coprecipitation processes become increasingly important and several uranium (co)precipitates may form depending on the environmental conditions. Uranium(IV) is considered relatively immobile under reducing conditions, because U(IV) readily precipitates as sparingly soluble minerals, such as uraninite (UO_2). Near sources of uranium release, solubility processes are particularly important for U(VI) in those sediments that become partially saturated with water or completely dry between periods of recharge, such as the surface soils and vadose zone sediments. Under these conditions, the concentration of uranium in the residue pore fluids may exceed the solubility limits for U(VI)-containing minerals and/or coprecipitates with other minerals, such as iron oxides. Characterization studies at several Department of Energy sites, including two recent studies of uranium-contaminated sediments from the Hanford Site, indicate that sediments and soils contaminated from disposal or spills of uranium-containing liquid wastes at these sites can contain uranium minerals or coprecipitates. Detailed sediment characterization studies of contaminated sediments from borehole 299-E33-45 near tank BX-102 (Appendix D) and the 300 Area at the Hanford Site suggest the possible presence of U(VI) minerals such as clarkeite, uranophane, soddyite, boltwoodite, weeksite, uranyl phosphate, and meta-autunite.

Under oxidizing conditions in the far field away from input sources of uranium contamination, U(VI) concentrations in sediments and soils will likely be controlled by surface adsorption processes. Uranium(VI) adsorbs onto a variety of minerals and related phases, including clays, oxides, silicates, and natural organic material. Important environmental parameters affecting uranium adsorption include oxidation/reduction conditions, pH, concentrations of complexing ligands such as dissolved carbonate, ionic strength, and mineralogy. As with the adsorption of most dissolved metals, aqueous pH has a significant effect on U(VI) adsorption due to the consequence of pH on U(VI) aqueous speciation and the number of exchange sites on variable charged surfaces of solids such as iron-, aluminum-oxides, and natural organic matter. The measured adsorption of U(VI) by sediments and single-mineral phases in carbonate-containing aqueous solutions is low at pH values less than 3, increases rapidly with increasing pH from pH 3 to 5, reaches a maximum in adsorption in the pH range from pH 5 to 7 to 8, and then decreases with increasing pH at pH values greater than 7 to 8, dependent on adsorbent. The observed increase in U(VI) adsorption onto sediments from acidic to near neutral pH values is due to the dominant U(VI) aqueous species being cationic and neutral over this pH range. However, the subsequent decrease in U(VI) adsorption with increasing basic pH values results from the dominant U(VI) aqueous species being anionic U(VI) carbonate complexes.

The published uranium Kd values when compiled for all sites typically exhibit two to three (or more at higher pH) orders of magnitude of scatter at any pH value. A significant amount of this variation in Kd values at a given pH value is related to heterogeneity in the mineralogy of the soils and is an important factor relative to the adsorption behavior of U(VI). Soils containing larger percentages of iron oxide minerals and mineral coatings and/or clay minerals will exhibit higher sorption characteristics than soils dominated by quartz and feldspar minerals, such as found in Hanford Site sediments. Several studies of the adsorption of U(VI) on sediments from the Hanford Site have been completed. A recent review indicated that uranium adsorption is relatively low for natural groundwater conditions at the Hanford Site and recommended a range of Kd values from 0.2 to 4 mL/g as appropriate for these conditions.

Numerous laboratory and modeling studies have been conducted using the surface complexation of uranium onto single mineral phases. Electrostatic surface complexation models were developed to provide a mechanistic description of the adsorption of metals onto mineral surfaces, and have been incorporated into several geochemical modeling/reaction codes. The current state of knowledge and availability of constants for using electrostatic surface complexation models to calculate the adsorption of uranium onto important soil minerals is probably as advanced as those for any other trace metal. The results of a recently published study indicated that this modeling approach could be used to qualitatively predict the main characteristics of the pH-dependent adsorption of U(VI) on the sediments in carbonate-containing systems, such as those at the Hanford Site. The authors of that study proposed that electrostatic surface complexation models could be used to assess the relative mobility of U(VI) in geochemical systems by indicating whether U(VI) was weakly or strongly adsorbed onto the geologic materials.

C.8.0 REFERENCES

40 CFR 141, "National Primary Drinking Water Regulations," *Code of Federal Regulations*, as amended.

Agnew, S. F., 1997, *Hanford Tank Chemical and Radionuclide Inventories: HDW Model Rev. 4*, LA-UR-96-3860, Los Alamos National Laboratory, Los Alamos, New Mexico.

Agnew, S. F., R. A. Corbin, T. B. Duran, K. A. Jurgensen, T. P. Ortiz, and B. L. Young, 1997, *Waste Status and Transfer Summary (WSTRS Rev. 4)*, LA-UR-97-311, Los Alamos National Laboratory, Los Alamos, New Mexico.

ASTM, 2002, Standard Test Method for Measurement of Soil Potential (Suction) Using Filter Paper, D-5298-94, *Annual Book of ASTM Standards*, Volume 0408:1123-1128. American Society for Testing and Materials International, West Conshohocken, Pennsylvania.

Anderson, J. D., 1990, *A History of the 200 Area Tank Farms*, WHC-MR-0132, Westinghouse Hanford Company, Richland, Washington.

Barney, G. S., 1976, *Vapor-Liquid-Solid Phase Equilibra of Radioactive Sodium Salt Wastes at Hanford*, ARH-ST-133, Atlantic Richfield Hanford Company, Richland, Washington

Buckingham, J. S., 1967, *Waste Management Technical Manual,* ISO-100, Isochem Inc, Richland, Washington.

Deka, R. N., M. Wairiu, P. W. Mtakwa, C. E. Mullins, E. M. Veenendaal, and J. Towend, 1995, "Use and accuracy of the filter paper method for measuring soil matric potential," *European J. of Soil Sci.* 46:233-238.

DOE-GJPO, 1997, *Vadose Zone Characterization Project at the Hanford Tank Farms: BY Tank Farm Report*, GJO-96-2-TAR, GJO-HAN-6, U.S. Department of Energy, Grand Junction Project Office, Grand Junction, Colorado.

DOE-GJPO, 1998, *Hanford Tank Farms Vadose Zone: BX Tank Farm Report*, GJO-98-40-TAR, GJO-HAN-19, U.S. Department of Energy, Grand Junction Project Office, Grand Junction, Colorado.

DOE-GJPO, 1999, *Vadose Zone Characterization Project at the Hanford Tank Farms: Tank Summary Data Report for Tank B-110*, GJ-HAN-131, prepared by U.S. Department of Energy Grand Junction Office for U.S. Department of Energy Office of River Protection, Richland, Washington.

DOE-GJPO, 2000a, *Hanford Tank Farms Vadose Zone: B Tank Farm Report*, GJO-99-113-TAR, GJO-HAN-28, U.S. Department of Energy, Grand Junction Project Office, Grand Junction, Colorado.

DOE-GJPO, 2000b, *Hanford Tank Farms Vadose Zone: Addendum to the BY Tank Farm Report*, GJO-96-2-TARA, GJO-HAN-6, U.S. Department of Energy, Grand Junction Project Office, Grand Junction, Colorado.

DOE-GJPO, 2000c, *Hanford Tank Farms Vadose Zone: Addendum to the BX Tank Farm Report*, GJO-98-40-TARA, GJO-HAN-19, U.S. Department of Energy, Grand Junction Project Office, Grand Junction, Colorado.

DOE-GJPO, 2000d, *Hanford Tank Farms Vadose Zone: Addendum to the B Tank Farm Report*, GJO-99-113-TARA, GJO-HAN-28, U.S. Department of Energy, Grand Junction Project Office, Grand Junction, Colorado.

DOE-RL, 2000, *Review of Generation and Flow of Recycled Uranium at Hanford*, DOE/RL-2000-43, U.S. Department of Energy, Richland Operations Office, Richland, Washington.

Gasper, K. A., 1989, *By-Product Recovery from High-Level Wastes*, Westinghouse Hanford Company, Richland, Washington

GE, 1944, Hanford Technical Manual Sections A, B, and C, HW-10475 ABC, General Electric Hanford Atomic Products Operation, Richland, Washington.

Gee, G. W., 1987, *Recharge at the Hanford Site: Status Report.* PNL-6403. Pacific Northwest Laboratory, Richland, Washington.

Gee, G. W., M. J. Fayer, M. L. Rockhold, and M. D. Campbell, 1992, "Variations in Recharge at the Hanford Site," *NW Sci.* 66:237-250.

Gee, G.. W., A. L. Ward, J. C. Ritter, J. B. Sisson, J. M. Hubbell, and H. A. Sydnor, 2001, *Installation of a Hydrologic Characterization Network for Vadose Zone Monitoring of a Single-Shell Tank Farm at the U. S. Department of Energy Hanford Site,* PNNL-13712, Pacific Northwest National Laboratory, Richland, Washington.

Godfrey, W. L., 1971, Inventory of Rhodium, Palladium, and Technetium Stored Hanford Wastes, ARH-1979, Atlantic Richfield Hanford Company, Richland, Washington.

Hanlon, B. M., 2002, *Waste Tank Summary Report for Month Ending January 31, 2002*, HNF-EP-0182, Rev. 166, CH2M HILL Hanford Group, Inc., Richland, Washington.

Hartman, M. J., L. F. Morasch, and W. D. Webber, editors, 2001, *Hanford Site Groundwater Monitoring for Fiscal Year 2000*, PNNL-13404, Pacific Northwest National Laboratory, Richland, Washington.

Hartman, M. J., L. F. Morasch, and W. D. Webber, editors, 2002, *Hanford Site Groundwater Monitoring for Fiscal Year 2001,* PNNL-13788, Pacific Northwest National Laboratory, Richland, Washington.

Hubbell, J. M., and J. B. Sisson, 1996, "Portable tensiometer for use in deep boreholes". *Soil Sci.* 161:376-381.

Hubbell, J. M, and J. B. Sisson, 1998. "Advanced tensiometer for shallow or deep capillary pressure measurements", *Soil Sci.* 163: 271-277.

Jensen, H. F., 1972, "Leak Investigation - 101-BX", Letter 092572 to L. W. Roddy, September 25, Atlantic Richfield Hanford Company, Richland, Washington.

Jones, T. E., R. Khaleel, D. A. Myers, J. W. Shade, and M. I. Wood, 1998, *A Summary and Evaluation of Hanford Site Tank Farm Subsurface Contamination*, HNF-2603, Rev. 0, Lockheed Martin Hanford Corporation, Richland, Washington.

Jones, T. E., B. C. Simpson, M. I. Wood, and R. A. Corbin, 2001, *Preliminary Inventory Estimate for Single-Shell Tank Leaks in B, BX, and BY Tank Farms*, RPP-7389, Rev. 0, CH2M HILL Hanford Group, Inc., Richland, Washington.

Jones, T. E., 2002, *Tc-99 and other Selected Radionuclide Inventories in Irradiated Hanford Fuel*, Letter Report, RPP-13495, CH2M HILL Hanford Group, Inc.,, Richland, Washington

Knepp, A. J., 2002, *Field Investigation Report for Waste Management Area S-SX*, RPP-7884, CH2M HILL Hanford Group, Inc., Richland, Washington.

Krupka, K. M., and R. J. Serne, 2002, *Geochemical Factors Affecting the Behavior of Antimony, Cobalt, Europium, Technetium, and Uranium in Vadose Zone Sediments*, PNNL-14126, Draft, Pacific Northwest National Laboratory, Richland, Washington.

Kupfer, M. J., A. L. Boldt, K. M. Hodgson, L. W. Shelton, B. C. Simpson, R. A. Watrous, B. A. Higley, R. M. Orme, M. D. LeClair, G. L. Borsheim, R. T. Winward, N. G. Colton, S. L. Lambert, D. E. Place, and W. W. Schulz, *Standard Inventories of Chemicals and Radionuclides in Hanford Site Tank Wastes*, HNF-SD-WM-TI-740, Rev. 0C, Lockheed Martin Hanford Corporation, Richland, Washington.

Larson, D. E., 1967, *B-Plant Phase III Flowsheets*, ISO-986, Isochem, Inc., Richland, Washington.

Larson, D. E., 1968, *B-Plant Recovery of Cesium from Current Acid Wastes by Phosphotungstate Precipitation*, ARH-564, Atlantic Richfield Hanford Company, Richland, Washington.

Lindsey, K. A., B. N. Bjornstad, J. W. Lindberg, and K. M. Hoffmann, 1992, *Geologic Setting of the 200 East Area: An Update*, WHC-SD-EN-TI-012, Westinghouse Hanford Company, Richland, Washington.

Mann, F. M., K. C. Burgard, W. R. Root, P. E. Lamont, R. J. Puigh, S. H. Finfrock, R. Khaleel, D. H. Bacon, E. J. Freeman, B. P. McGrail, and S. K. Wurstner, 2001, *Hanford Immobilized Low-Activity Waste Performance Assessment: 2001 Version*, DOE/ORP-2000-24, Rev. 0, Office of River Protection, Richland, Washington.

McCain, R. G., and C. J. Koizumi, *Correlation of Spectral Gamma Log Response and Sr-90 Concentrations for a Steel-Cased Borehole,* 2002, GJO-2002-322-TAR, MACTEC-ERS, Grand Junction, Colorado.

Metz, W. P. and G. L. Borsheim, "Additions of Diatomite to TK-102-BX", 1971, Letter 091071, to L. W. Roddy, September 10, Atlantic Richfield Hanford Company, Richland, Washington

Narbutovskih, S. M., 2000, *Groundwater Quality Assessment Plan for Single-Shell Waste Management Area B-BX-BY at the Hanford Site,* PNNL-13022, Pacific Northwest National Laboratory, Richland, Washington.

Resource Conservation and Recovery Act of 1976, 42 USC 6901, et seq.

Roberts, F. P., 1971, *Summary of Research on Tc, Rh and Pd By Battelle-Northwest*, BNWL-B-49, Battelle-Northwest, Richland, Washington.

Roberts, F. P., F. M. Smith, and E. J. Wheelwright, 1962, *Recovery and Purification of Technetium-99 From Neutralized PUREX Wastes*, HW 73121, Hanford Atomic Products Operation, Richland, Washington.

Rogers, P. M., and A. J. Knepp, 2000, *Site-Specific SST Phase 1 RFI/CMS Work Plan Addendum for WMA B-BX-BY*, RPP-6072, Rev. 1, CH2M HILL Hanford Group, Inc., Richland, Washington.

Serne, R. J., H. T. Schaef, B. N. Bjornstad, D. C. Lanigan, G. W. Gee, C. W. Lindenmeier, R. E. Clayton, V. L. LeGore, R. D. Orr, M. J. O'Hara, C. F. Brown, G. V. Last, I. V. Kutnyakov, D. S. Burke, T. C. Wilson, and B. A. Williams, 2002a, *Characterization of Vadose Zone Sediment: Borehole 299-W23-19 [SX-115] in the S-SX Waste Management Area,* PNNL-13757-2, Pacific Northwest National Laboratory, Richland, Washington.

Serne, R. J., G. V. Last, H. T. Schaef, D. C. Lanigan, C. W. Lindenmeier, C. C. Ainsworth, R. E. Clayton, V. L. LeGore, M. J. O'Hara, C. F. Brown, R. D. Orr, I. V. Kutnyakov, T. C. Wilson, K. B. Wagnon, B. A. Williams, and D. S. Burke, 2002b, *Characterization of Vadose Zone Sediment: Borehole 41-09-39 in the S-SX Waste Management Area.* PNNL-13757-3, Pacific Northwest National Laboratory, Richland, Washington.

Shuh, D. K., *Final Report - Research Program to Investigate the Fundamental Chemistry of Technetium,* 2000, LBNL-47194, Lawrence Berkeley National Laboratory, Berkeley, California.

Simpson B. C., R. A. Corbin, S. F. Agnew, 2001, *Hanford Soil Inventory Model*, BHI-01496, Rev. 0, Bechtel Hanford Inc., Richland, Washington.

Sisson, J. B, and J. M . Hubbell, 1999, "Water Potential to Depths of 30 meters in Fractured Basalt and Sedimentary Interbeds", pp.855-865. In M .Th. van Genuchten, F. J. Leij, and L. Wu (eds.). *Proceedings of the International Workshop on Characterization and Measurement of the Hydraulic Properties of Unsaturated Porous Media.* Oct 22-24, 1997, Riverside, California, University of California, Riverside Press.

Smith, P. W., and R. E. Tomlinson, 1967, *Hanford High Level Waste Management Reevaluation Study,* ISO-981, Isochem, Inc., Richland, Washington.

Spane, F. A., 1999, *Effects of Barometric Fluctuations on Well Water-Level Measurements and Aquifer Test Data*, PNNL-13078, Pacific Northwest National Laboratory, Richland, Washington.

Spane, F. A., P. D. Thorne, and D. R. Newcomer, 2001, *Results of Detailed Hydrologic Characterization Tests - Fiscal Year 2000,* PNNL-13514, Pacific Northwest National Laboratory, Richland, Washington.

Waite, J. L., 1991, *Tank Wastes Discharged Directly to the Soil at the Hanford Site,* WHC-MR-0227, Westinghouse Hanford Company, Richland, Washington.

Williams, J. C., 1999, *Historical Vadose Zone Contamination from B, BX, and BY Tank Farm Operations*, HNF-5231, Rev. 0, Lockheed Martin Hanford Corporation, Richland, Washington.

Williams, B. A., B. N. Bjornstad, R. Schalla, and W. D. Webber, 2000, *Revised Hydrogeology of the Suprabasalt Aquifer System, 200-East Area and Vicinity, Hanford Site, Washington,* PNNL-12261, Pacific Northwest National Laboratory, Richland, Washington.

Womack, J. C., and D. J. Larkin, 1971, *Investigation and Evaluation of 102-BX Tank Leak,* ARH-2035, Atlantic Richfield Hanford Company, Richland, Washington.

Wood M. I, T. E. Jones, R. Schalla, B. N. Bjornstad, and S. M. Narbuovskih, 2000, *Subsurface Conditions Description of the B-BX-BY Waste Management Area*, HNF-5507, Rev. 0, CH2M HILL Hanford Group, Inc., Richland, Washington.

This page intentionally left blank.